EVALUATION OF THE EFFECT OF CRUMB RUBBER ASPHALT MODIFICATION VARIABLES ON THE ASPHALT BINDER PERFORMANCE

A THESIS SUBMITTED TO
THE GRADUATE SCHOOL OF NATURAL AND APPLIED SCIENCES
OF
MIDDLE EAST TECHNICAL UNIVERSITY

BY

MEHMET ÖZÇİLOĞLU

IN PARTIAL FULFILLMENT OF THE REQUIREMENTS
FOR
THE DEGREE OF MASTER OF SCIENCE
IN
CIVIL ENGINEERING

JANUARY 2023

Approval of the thesis:

EVALUATION OF THE EFFECT OF CRUMB RUBBER ASPHALT MODIFICATION VARIABLES ON THE ASPHALT BINDER PERFORMANCE

submitted by **MEHMET ÖZÇİLOĞLU** in partial fulfillment of the requirements for the degree of **Master of Science** i**n Civil Engineering, Middle East Technical University** by,

Prof. Dr. Halil Kalıpçılar
Dean, Graduate School of **Natural and Applied Sciences** _____

Prof. Dr. Erdem Canbay
Head of the Department, **Civil Engineering** _____

Assoc. Prof. Dr. Hande Işık Öztürk
Supervisor, **Civil Engineering, METU** _____

Examining Committee Members:

Prof. Dr. Murat Güler
Civil Engineering, METU _____

Assoc. Prof. Dr. Hande Işık Öztürk
Civil Engineering, METU _____

Prof. Dr. İsmail Özgür Yaman
Civil Engineering, METU _____

Prof. Dr. Mustafa Şahmaran
Civil Engineering, Hacettepe University _____

Asst. Prof. Dr. Güzide Atasoy Özcan
Civil Engineering, METU _____

Date: 27.01.2023

I hereby declare that all information in this document has been obtained and presented in accordance with academic rules and ethical conduct. I also declare that, as required by these rules and conduct, I have fully cited and referenced all material and results that are not original to this work.

Name Last name : Mehmet Özçiloğlu

Signature :

ABSTRACT

EVALUATION OF THE EFFECT OF CRUMB RUBBER ASPHALT MODIFICATION VARIABLES ON THE ASPHALT BINDER PERFORMANCE

Özçiloğlu, Mehmet
Master of Science, Civil Engineering
Supervisor : Assoc. Prof. Dr. Hande Işık Öztürk

January 2023, 140 pages

Crumb rubber (CR) has long been used in pavement production as it enhances the pavement performance and contributes to recycling scrap tires. However, the performance of CR modified asphalt (CRMA) prepared through the wet process is affected by the modification variables, i.e., CR ratio, CR and asphalt properties, mixing parameters (temperature, duration and rate), and mixing procedure. On the other hand, CRMA preparation procedure is still not standardized yet. This experimental study aims to contribute to the literature and standardization process by thoroughly investigating the effect of two CR modification essential variables, mixing duration and mixing rate, on the intermediate and high temperature performance of modified asphalt. Since the effects of the other variables are mainly known, these variables were kept constant with optimum values based on the previous studies. In order to simulate the current industry and research experiences, CRMA samples were prepared by using a broad range of mixing rate and mixing duration levels. Overall, 24 different CRMA samples were prepared in the laboratory environment either using a low shear mixer or high shear mixer. These asphalt samples were analyzed based on the conventional asphalt tests (Brookfield viscosity

test, penetration test, softening point test and resilience test) and performance tests (dynamic shear rheometer [DSR] test). In addition to that, the potential of the use of image-based technologies to characterize modified asphalt behavior is analyzed. For that reason, the sample images (unaged and aged) are captured by fluorescence microscopy and analyzed. Accordingly, it is concluded that modifying asphalt with CR improves the intermediate and high temperature performance such as rutting, fatigue-cracking and aging-resistance. In addition, the effect of mixing rate was observed mainly in the high shearing and lower shearing levels and only in the viscosity and high temperature true grade results. Any significant difference was not observed within the low shear mixing levels. Furthermore, 30 minutes of the mixing duration was not sufficient particularly according to resilience test results. For the rest of mixing durations, the effect of mixing duration on the intermediate and high temperature performance of CRMA was very limited. Therefore, it is suggested to utilize lower levels of low shear mixing if high shear mixing is not particularly demanded and not extensive mixing durations for the CRMA preparation process. Consequently, energy consumption during the CRMA production can be reduced.

Keywords: Crumb Rubber Modified Asphalt, Mixing Time, Mixing Duration, Rheology, Fluorescence Microscopy

ÖZ

KAUÇUK MODİFİYE ASFALT MODİFİKASYON DEĞİŞKENLERİNİN ASFALT PERFORMANSI ÜZERİNDEKİ ETKİSİNİN BELİRLENMESİ

Özçiloğlu, Mehmet
Yüksek Lisans, İnşaat Mühendisliği
Tez Yöneticisi: Doç. Dr. Hande Işık Öztürk

Ocak 2023, 140 sayfa

Öğütülmüş kauçuk hem asfalt kaplama performansını arttırdığı hem de ömrünü tamamlamış lastiklerin geri dönüşümüne katkı sağladığı için yol kaplamalarında uzun süredir kullanılmaktadır. Fakat ıslak prosesle hazırlanan kauçuk modifiye asfalt bağlayıcıların performansları öğütülmüş kauçuk oranı, asfalt ve kauçuğun karakteristikleri, karışım parametreleri (sıcaklık, süre ve hız) ve karışım prosedürleri gibi değişkenlerden etkilenmektedir. Bununla birlikte kauçuk modifiye asfalt hazırlama prosedürü hala standartlaştırılamamıştır. Bu deneysel çalışma, iki temel kauçuk modifikasyon değişkeninin (karışım hızı ve karışım süresi) modifiye asfalt performansı üzerinde etkilerini detaylı bir şekilde inceleyerek literatüre ve standartlaştırma sürecine katkı sağlamayı amaçlamaktadır. Diğer değişkenlerin etkileri büyük ölçüde bilindiğinden dolayı bu değerler daha önce yapılan çalışmalar baz alınarak optimum seviyelerde sabit tutulmuştur. Bu doğrultuda güncel endüstriyel ve bilimsel araştırma deneyimlerini simule etmek için karışım süresi ve karışım hızı seviyeleri geniş aralıkta alınarak kauçuk modifiye asfalt numuneleri hazırlanmıştır. Laboratuvar ortamında düşük ve yüksek parçalayıcı karıştırıcılar kullanılarak toplamda 24 farklı kombinasyona sahip kauçuk modifiye asfalt numuneler hazırlanmıştır. Bu asfalt numuneler konveksiyonel asfalt testleri (Brookfield viskozite testi, penetrasyon testi, yumuşama noktası testi ve elastik

dirençlilik testi) ve performans testleri (dinamik kesme reometresi [DSR]) kullanılarak analiz edilmiştir. Ek olarak asfaltın karekterizasyonunda görüntü tabanlı teknolojilerin kullanım potansiyeli değerlendirilmiştir. Bu doğrultuda floresan mikroskop kullanılarak numunelerin (orijinal ve yaşlandırılmış) görüntüleri alınıp analiz edilmiştir. Test sonuçları öğütülmüş kauçuk ile modifiyenin edilmesi asfaltın tekerlek izi, yorulma çatlağı ve yaşlanma dayanımı gibi orta ve yüksek sıcaklık performansını arttırdığını göstermiştir. Bununla birlikte karıştırma hızının etkisi genel olarak düşük ve yüksek parçalayıcı karıştırma seviyeleri arasında ve sadece viskozite ile yüksek sıcaklık gerçek performans sınıfı testlerinin sonuçlarında gözlemlenmiştir. Düşük parçalayıcı karıştırma seviyeleri arasında herhangi önemli bir etki görülmemiştir. Karıştırma süresi için ise özellikle elastik dirençlilik testi 30 dakikanın yeterli olmadığını göstermiştir. Diğer karışım sürelerinin asfaltın orta ve yüksek sıcaklık performansı üzerindeki etkisinin önemli derecede olmadığı görülmüştür. Böylelikle kauçuk modifiye asfalt hazırlama prosedüründe kullanılmak üzere özellikle yüksek parçalayıcı karıştırıcılar gerekmediği sürece düşük parçalayıcı karışım hızlarının düşük seviyelerinin kullanılması ayrıca karışım süresi için uzun karışım süreleri kullanılmaması tavsiye edilmektedir. Bu sayede kauçuk modifiye asfalt üretiminde kullanılan enerji tüketimi azaltılabilir.

Anahtar Kelimeler: Kauçuk Modifiye Asfalt, Karışım Hızı, Karışım Süresi,
Reoloji, Floresan Mikroskop

To My Family

ACKNOWLEDGMENTS

I would like to state that there are a number of people whose guidance, support and encouragement made this study possible and quite an experience.

First and foremost, I would like to express my deepest gratitude to my supervisor assoc. Prof. Dr. Hande Işık Öztürk for her guidance, support and patience throughout the study in a friendly manner.

I also want to present my appreciation and respect to my committee members Prof. Dr. Murat Güler, Prof. Dr. İsmail Özgür Yaman, Prof. Dr. Mustafa Şahmaran, and Asst. Prof. Dr. Güzide Atasoy Özcan for their valuable comments and advices.

My special appreciation goes to Dr. Yalçın Karakaya and Dr. Reza Shabani for sharing their experiences in the laboratory and Duygu Demirtürk and Uhde Yıldırım for making the Transportation Laboratory a fun place. In addition, to the laboratory technician, Ahmet Sağlam, who never hesitated to offer his help.

Furthermore, I would like to thank the Office of Scientific Research Projects Coordination at Middle East Technical University for supporting this thesis with financial assistance (TEZ-YL-303-2022-10842).

Finally, I am more than thankful to my family who helped me, encouraged me and supported my decisions throughout my life.

TABLE OF CONTENTS

LIST OF TABLES

TABLES

LIST OF FIGURES

FIGURES

LIST OF ABBREVIATIONS

ANOVA: Analysis of Variance

AR: Asphalt Rubber

ASTM: American Society for Testing and Materials

CalTrans: California Transportation Department

CMAI: Complex Modulus Aging Index

CR: Crumb Rubber

CRMA: Crumb Rubber Modified Asphalt

DSR: Dynamic Shear Rheometer

EEA: European Economic Area

ELT: End of Life Tire

ETRMA: European Tire and Rubber Manufacturers Association

FHWA: Federal Highway Administration

FM: Fluorescence Microscope

FTIR: Fourier-Transform Infrared Spectroscopy

HMA: Hot Mix Asphalt

METU: Middle East Technical University

MSCRT: Multiple Stress Creep Recovery Test

PG: Performance Grade

RTFOT: Rotating Thin Film Oven Test

RUMAC: Rubber Modified Asphalt Concrete

SBS: Styrene-Butadiene-Styrene

SEM: Scanning Electron Microscope

SBR: Styrene-Butadiene Rubber

TFOT: Thin Film Oven Test

USTMA: United States Tire Manufacturers Association

CHAPTER 1

INTRODUCTION

1.1 Research Objectives and Scope

Asphalt is a bituminous material obtained from refining crude oil or natural deposits. This material offers desirable characteristics, such as good binding, durability, water resistance, and flexibility. Thus, it is widely used in road constructions as binder. However, the increasing number of traffic loads and severe environmental conditions necessitate the improvement of asphalt binder since the physical performance of asphalt is limited. There are a few technics to improve the characteristics of asphalt, and one of them is modifying asphalt with polymeric materials. In this regard, either polymers produced for such reasons or recycled polymers are utilized. However, employing the recycled polymers is a better option in terms of transportation and environment sustainability, and cost. Crumb rubber (CR) is one of these recycled polymers used in the modification of asphalt and mostly generated from scrap tires.

Millions of tires complete their life every year and stored in large volumes. These scrap tires pose a threat to environment. This concern gave rise to the various ideas to recycle the scrap tires. One of them came out as using CR in asphalt mixtures by either replacing fine aggregates with CR (dry process) or directly introducing CR to asphalt as a modifier (wet process). The resultant product of wet process is called CR modified asphalt (CRMA) or asphalt rubber (AR). However, the CR modification of asphalt has not been standardized yet. In terms of wet process, it is still investigated how CR affects the asphalt properties, and what kind of interaction mechanism between CR and asphalt takes place. The resultant product of the CR modification is affected by material (asphalt and CR) properties and preparation

variables (CR ratio, mixing temperature, mixing duration, mixing rate). Therefore, the studies focus on these factors to obtain the combinations providing the most desirable results in terms of asphalt binder performance. Previous researches utilized different mixing rates and durations while investigating CRMA performance. Therefore, this study aimed to understand the effect of mixing time and duration on the intermediate and high temperature performance of CRMA by taking into broad range of these variables in one study. Mixing durations and rates were selected as 30, 60, 90, 120, 150, 180 minutes and 700, 1000, 1200, 6800 rpm, respectively, considering the applications in the industry and literature. Thus, a design matrix consisting 24 different modified asphalt binders was prepared. While evaluating the intermediate and high temperature performance of binders prepared with each combination, conventional and advance performance-based tests were utilized on these samples. Moreover, this study attempts to utilize image-based methods to further investigate the CR modified asphalt samples. It was revealed that fluorescence microcopy is a better alternative to Scanning Electron Microscopy (SEM). Thus, fluorescence microcopy was used to analyze the differences in CR particle morphologies and the interaction between CR and asphalt induced by changing mixing rate and duration levels in this study.

1.2 Motivation and Steps of the Study

As briefly mentioned in the previous section, in the process of modifying base asphalt with crumb rubber through the wet process, material properties and the modifying variables (CR ratio, mixing temperature, mixing rate, mixing duration) are the significant factors determining the performance of final product, CRMA. Moreover, it is essential to understand the interaction mechanism between the CR particles and asphalt. However, the CRMA preparation procedure hasn’t been standardized yet. In the framework of this study, the effect of two mixing variables (mixing duration and mixing rate) on the intermediate and high temperature performance of CRMA is investigated by selecting a wide range of levels for these

two variables. Furthermore, fluorescence microscopy is employed to understand the changes in CR particle morphology and asphalt matrix phase as a result of changing modification levels. Therefore, this study aims to contribute to the literature and standardization process with its findings obtained through the analysis.

The major steps of this study were given as follows:

a) The literature is reviewed on the wet process CRMA binders to determine the common asphalt and CR properties, CR ratio, mixing temperatures, durations and rates since these variables have not been standardized. The effect of the variables, CR and asphalt properties, CR ratio and mixing temperature, on CRMA are mainly revealed. Therefore, these variables are fixed at the optimum values based on the previous practices and studies.
b) Experimental matrix of this study is built on the 6 different mixing durations and 4 different rates. Performance and physical tests are carried out on these 24 different CRMAs.
c) The effect of these variables on the intermediate and high temperature performance and physical properties of binders were analyzed.
d) According to the findings of the experiments, the sample size is reduced and further analyzes are performed on the images captured by fluorescence microcopy.

1.3 Outline of the Research

Chapter 2 covers the detailed literature review about CRMA. The chapter mainly includes how CR contributes to the environment and improvement of asphalt, details about CR and asphalt properties, CR production processes, CRMA production methods, variables affecting the intermediate and high temperature performance of CRMA and methods used to evaluate CRMA by the researchers.

In Chapter 3, details about the raw materials (CR and asphalt) used in this study were given. In addition, the experiment program, the procedure followed by during the preparation of samples, and the methods utilized to evaluate samples are explained.

In Chapter 4, the tests results obtained through the conventional tests, performance tests and the fluorescence microscopy analysis were discussed for the different combinations of mixing rates and durations.

Chapter 5 presents the outcomes of the study based on the test results and analysis discussed in Chapter 4 and offers future work for the further research.

CHAPTER 2

LITERATURE REVIEW

2.1 Introduction

Crumb rubber modified asphalt (CRMA) has been studied by researchers for decades to improve its production technologies and evaluation methods. The main motivation behind these studies is that this modified material enhances pavement performance and contributes to environmental sustainability. In this chapter, details about CRMA are investigated based on the knowledge provided by the literature.

2.2 The Background of Crumb Rubber Modified Asphalt

2.2.1 Problems Related to Asphalt Pavement Performance

Asphalt pavement structures generally comprise layers of asphalt-bounded, unbounded granular materials and natural soil, which are named as wearing layer, base layer, and subbase layer. The loads applied on the top layer are spread and transferred to the underlying layers in a decreasing manner. For that reason, the top layer is designed to have the highest load-spreading capacity whereas the bottom layer has the lowest load-spreading capacity (Wang, 2015). A pavement is designed to function for its projected time; however, it often requires maintenance before the anticipated time due to some factors, which are mainly heavy traffic loads, adverse climatic conditions, poor road construction, and weak subgrade. Among those factors, heavy traffic loads are the main reason causing major pavement failures (Pais et al., 2013). Furthermore, the increasing number of people and expanding

industrialization leads to more transportation network requirements (Pereira et al., 2008). In order to overcome performance-related problems of the surface layer, various solutions are developed to enhance asphalt binders such as rejuvenator agents which reverse the aging of recycled asphalt binders, methods to vary the asphalt chemical composition (saturates, aromatics, resin, asphaltene), polymer additives which improve the elastic properties of asphalt binders and crumb rubber modification and etc. (Glover et al., 2000). Upon these methods, crumb rubber stands out not only because of the improvement in pavement performance but also because of the environmental concerns.

2.2.2 Environmental Problems Related to Scrap Tires

The increasing rate of population and industrialization causes waste products at undesirable levels. One of these waste products is scrap tires (also called "end-of-life tires" (ELT)) (Pereira et al., 2008; Presti, 2013). Every year, approximately 17 million scrap tires are generated across the world and the annual growth rate of this number is estimated as 2% (Zhang, 2016). The amount of scrap tires produced in the U.S. is 4,658,302 tons in 2019 (USTMA, 2019). This figure is 257,000 tons for Turkey and 3,450,053 tons for Europe (twenty-eight member countries of the European Union plus Turkey, Norway, Serbia, and Switzerland) (ETRMA, 2021). Scrap tires are seen as one of the most concerning waste products as they are manufactured in large volumes and don't decompose easily (Presti, 2013). They are either stockpiled/landfilled or utilized as fuel, new recycled products, and recycled tire production (Akbas, 2021). The life cycle of a tire can be seen in Figure 2.1. Improper management of disposed scrap tires may pose environmental and health risks such as fire hazards and a place to breed for rodents and pests like mosquitos (Presti, 2013). Figure 2.2a shows the world's largest scrap tire disposal area with 50 million tires in Kuwait (Mukhtar, 2021) and a fire broke out in this area in April 2021 (Figure 2.2b). Some countries are taking measures to prevent such risks. For instance, European Union banned the disposal of scrap tires (EEA, 2003). Since the

scrap tire disposal ratio decreases worldwide, other utilization options to recover these tires gain more importance. One of these options is to use them as a fuel source since they provide energy at the level of good quality coals. Another approach is to process scrap tires chemically, i.e., thermolysis, pyrolysis, and gasification. Finally, scrap tires are utilized in ground form after the steel and fabric components of these tires are separated. In the civil engineering area, crumb rubber (ground tire rubber) is used for different purposes such as rubberized asphalt pavements, flooring for playgrounds and stadiums, shock-absorbing mats, paving blocks, roofing material, and more (Presti, 2013).

Figure 2.1. Life cycle of a tire (Akbas, 2021).

(a) (b)

Figure 2.2 (a) Kuwait scrap tire disposal area (Mukhtar, 2021), (b) fire breakout in this area (Pure Energy Circle, 2021).

2.2.3 Utilizing Crumb Rubber Modified Asphalt

As a solution to pavement performance-related problems, modifying asphalt binders with pure polymers is explicitly preferred in practice (Navarro et al., 2007). However, employing these materials in asphalt binders is costly and increases the cost of the resulting binder. As a solution, recycled polymers such as recycled rubber are considered as a good option in terms of engineering, economy, and environment since they exist in large quantities and present low cost (Zaman et al., 1995). Scrap tire rubber is introduced into asphalt mixes in granular form, i.e., crumb rubber (CR) (Medina et al., 2020). USTMA (2019) presents 17% of the reclaimed CR (approximately 170 thousand tons) is utilized in asphalt-related areas in 2019 in the United States. Crumb rubber modified asphalt (CRMA, also called as rubberized asphalt or asphalt rubber) is used for various applications, such as hot mixtures, surface treatments, and joint and crack sealants (FHWA, 1997). However, the design of CRMA is an important issue and it must be handled with care. When required, the resulting binder must satisfy the requirements of specifications and also show sufficient performance under the anticipated climate and traffic conditions. In this regard, research programs are still carried on to enhance technologies in this field to provide CRMA with better quality (Presti et al., 2014).

2.3 Effect of Crumb Rubber on Asphalt Binders and Flexible Pavements

The addition of CR in asphalt changes the characteristic properties of the base asphalt. It increases the viscosity so that pavements with thicker asphalt binder film can be constructed by preventing bleeding or draining down. It also improves the, softening point, resilience, elasticity, and resilience of the base bitumen at high temperatures. In addition, CRMA shows better anti-aging performance. Consequently, pavements constructed with CRMA show better resistance to major failures, rutting (permanent deformation), fatigue cracking, thermal cracking, and reflective cracking. Improved durability extends the pavement life, and lowers the

maintenance costs. Furthermore, it provides a more comfortable ride, lower traffic noise, decreased construction durations due to thinner lifts, and increased safety as the carbon black component of rubber maintains the black color of pavement longer, thus more distinguishable road markings (contrast). Such advantages related to CRMA and eliminating scrap tires from being a waste in the environment make this method considered as green engineering (Caltrans, 2003; FHWA, 1997; Wang et al., 2013a; Fini et al., 2013; Santagata et al., 2007; Chiu et al., 2008).

2.4 Raw Materials

In this section, information from the literature about two raw materials, CR and base asphalt, used in the production of CRMA, is presented.

2.4.1 Base Asphalt

ASTM D8 (2022) defines asphalt as the residue, in dark brown to black color, acquired from the refining process of crude petroleum, natural sources, or both combined, and it shows binding properties. This material has been utilized mainly for paving and water-proofing applications due to its impermeable, adhesive and flexible nature throughout history. The source and the production process of the crude oil strongly affect the chemical composition and the mechanical properties of the asphalt (Stangl et al., 2007). In addition, asphalt's rheological properties are controlled by the physical and chemical interactions between its components and highly affected by temperature (Loeber et al., 1998).

Asphalt is graded into four different categories based on mechanical and rheological properties of asphalt: penetration (e.g., Pen 40/50), viscosity (e.g., AC-2.5), viscosity of aged asphalt (e.g., AR-2000) and Superpave performance (e.g., PG-64). The most widely used grading system is the Superpave performance grading which determines the pavement temperature range in which asphalt is suitable to use (Papagiannakis and Masad, 2008).

Asphalt comprises hydrocarbons (mainly), sulfur, nitrogen, oxygen, and low content of some metals. These components form a wide variety of molecules which are grouped under two fractions: maltenes and asphaltenes. Maltenes also can be divided into saturates, aromatics, and resins. Consequently, asphalt has four chemical fractions: saturates, aromatics, resins, and asphaltenes (SARA) (Read and Whiteoak, 2003). Asphaltenes are complex materials. Both asphaltenes and resins show high polar characteristics. The high polarity forms the high adhesive properties of resins (Cong et al., 2013; Rahman, 2004). The molecular weight of asphaltene changes between 1000 and 100,000 whereas it is between 500 and 50,000 for resins (Cong et al., 2013). Asphaltenes exist as aggregated micelle structures in asphalt and resins peptize these structures while decreasing their size at the same time, which reduces the consistency of the asphalt (Cong et al., 2013; Handle et al., 2016). Increasing the amount of asphaltene leads to harder asphalt with higher viscosity. Aromatics consist of a viscous liquid phase where asphaltenes, surrounded by resins, are dispersed (Figure 2.3). Of all the fractions of asphalt, aromatics possess the lowest molecular weight ranging between 300 and 200, furthermore, they show significantly low polar characteristics. Saturates are defined as linear branch chain aliphatic hydrocarbons and their molecular weight changes between 300 and 20,000. The degree of interaction between CR and asphalt changes depending on the chemical composition of asphalt. For that reason, the chemical composition of asphalt becomes one of the significant factors which should be considered in the design of CRMA (Cong et al., 2013; Rahman, 2004).

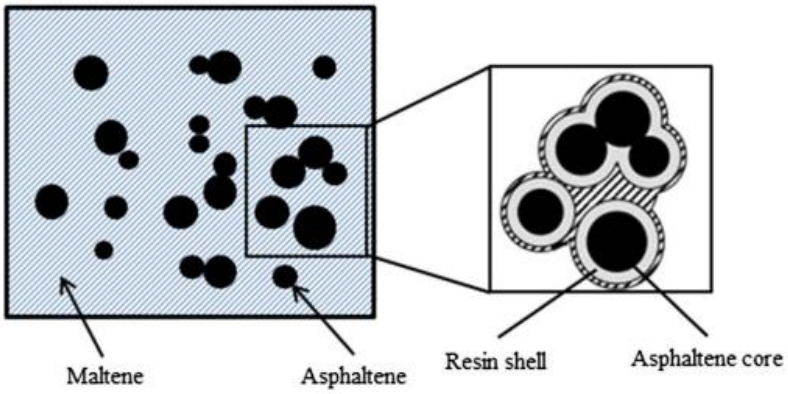

Figure 2.3. Schematic representation of the colloidal structure of asphalt (Pan et al., 2017)

2.4.2 Crumb Rubber

Crumb rubber (CR) is defined as fine rubber particles obtained from scrap tires and utilized to modify asphalt paving materials (Caltrans, 2003). In literature, CR is also called by different terms, such as ground tire rubber, scrap tire rubber, rubber granulate, rubber powder, size-reduced rubber, particulate tire rubber, and pulverized rubber (Karger-Kocsis et al., 2013). The size of CR particles may change between 0.015 mm and 2 mm (Thives, 2013). Some of the commonly used CR gradation ranges for the wet process are presented in Table 2.1. It should be highlighted that there has no established standard yet.

Table 2.1 Commonly used CR gradations (Data from Way et al., 2012)

Sieve Size (mm)	Caltrans	Texas DOT			Arizona DOT		Florida DOT		
% Passing	Scrap Tire	Grade A	Grade B	Grade C	Type A	Type B	Type A	Type B	Type C
2.36	100	100	-	-	100	-	-		-
2	98-100	95-100	100	-	95-100	100	-		-
1.18	45-75	-	70-100	100	0-10	65-100	-		100
0.6	2-20	-	25-60	90-100	-	20-100	-	100	70-100
0.425	-	-	-	45-100	-	-	-		-
0.3	0-6	0-10	-	-	-	0-45	100	40-60	20-40
0.15	0-2	-	-	-	-	-	50-80	-	-
0.075	0	-	0-5	-	-	0-5	-	-	-

2.4.2.1 Scrap Tire Composition

The tire is a complex product. Steel, fabric, and rubber are the main components comprising the body of a tire. While steel and fabric work as the skeleton, rubber forms the “flesh” around this skeleton in the tread, sidewall, apexes, liner, and shoulder. (Rahman, 2004). A typical structure of a tire can be seen in Figure 2.4. Of all these components, rubber holds the highest percentage with approximately 60% by weight (Thodesen et al., 2009).

Tire rubber consists of natural rubber, synthetic rubber, carbon black, anti-oxidants, fillers, and oils with an extender nature soluble in hot asphalt (Caltrans, 2003). The ratio of natural rubber to synthetic rubber changes depending on the size and purpose of the tire. The tire size and durability requirement increase leads to an increase in the ratio (Rahman, 2004). In this regard, truck tires typically contain more natural rubber than car tires (Hicks et al., 1995).

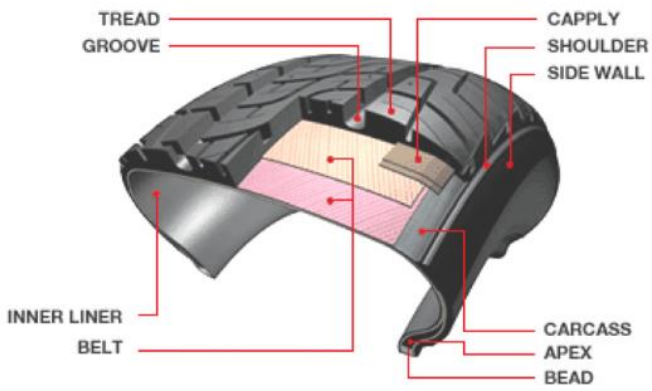

Figure 2.4. Components of a tire (Lee and Kim, 2008)

Raw natural rubber is normally brittle at low temperatures and sticky at high temperatures (Jain, 2016). In addition, its initial shape doesn't recover after it is largely strained (Mark et al., 2013). This inelastic nature of raw rubber is explained by its structure consisting of long polymer chains whose motions can be independent relative to each other. For that reason, this material is processed to enhance its properties (Presti, 2013). This can be achieved by the vulcanization process. In this process, a vulcanizing agent (mainly sulfur) is added to raw rubber and heated under pressure. Sulfur atoms (or a single atom) bond long polymer chains to each other by forming cross-links amongst them (Figure 2.5). Cross-linking consequently enhances the retractile force and elasticity, therefore, vulcanized rubber can regain its initial shape after the release of the deforming stress (Mark et al., 2013).

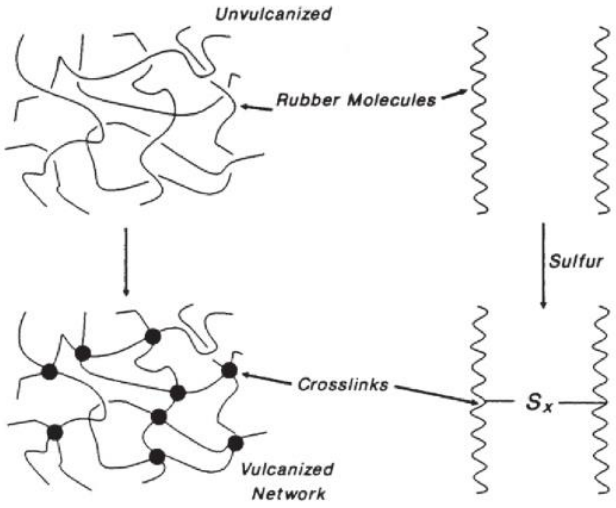

Figure 2.5. Cross-linking through vulcanization process (Mark et al., 2013)

Moreover, another product, synthetic rubber is obtained from crude oil products and some other minerals. It is generated in two steps. Initially, monomers (long molecules formed by large number of small units) are formed, and the next, polymerization takes place to constitute rubber. Synthetic rubber has several types, such as styrene-butadiene rubber (SBR), silicone rubbers, fluorocarbon rubbers, and epichlorohydrin rubber. SBR is the type employed in bitumen and tires (Rahman, 2004).

2.4.2.2 Crumb Rubber Production

Crumb rubber can be produced through two processes: ambient grinding and cryogenic grinding (Klingensmith and Baranwal, 1998).

The first method is ambient grinding. This method is a mechanical process of grinding scrap tires or rubber at ambient temperature in order to reduce particle sizes (Thieves et al., 2013; Presti, 2013). The grinding process is conducted by tearing and crushing the material with the help of rotating sharp faces/edges (Presti, 2013; Neto et al., 2006b). The ambient ground CR can be obtained through three methods. The first one is the cracker mill process in which revolving corrugated drums grind the

rubber passing between them, to the sizes ranging between 5 mm and 0.5 mm. The resultant particles have irregular geometry and relatively high surface area. The other CR ambient grinding method is the granulator process. In this method, rubber is ground by the means of rotating blades producing rubber particles whose sizes range between 9.5 mm and 0.5 mm. The last one is the micro-mill process which grinds rubber very finely that the size of resultant CR particles ranges between 0.5 mm to 0.075 mm. Of all the methods, the most widely employed one is the cracker mill process (Chesner et al., 2002).

The ambient grinding process (Figure 2.6) starts with the shredding of scrap tires into chips with the size of 50 mm. The chips are transferred to a granulator and ground to smaller sizes under 10 mm while the most of steel and fiber are separated from the material. In the next step, the remaining steel is removed by means of magnetization, and the remaining fiber is removed by using shaking screens and wind shifters. Additional grinding steps can follow the process depending on the requirement of CR particle size (Reschner, 2008).

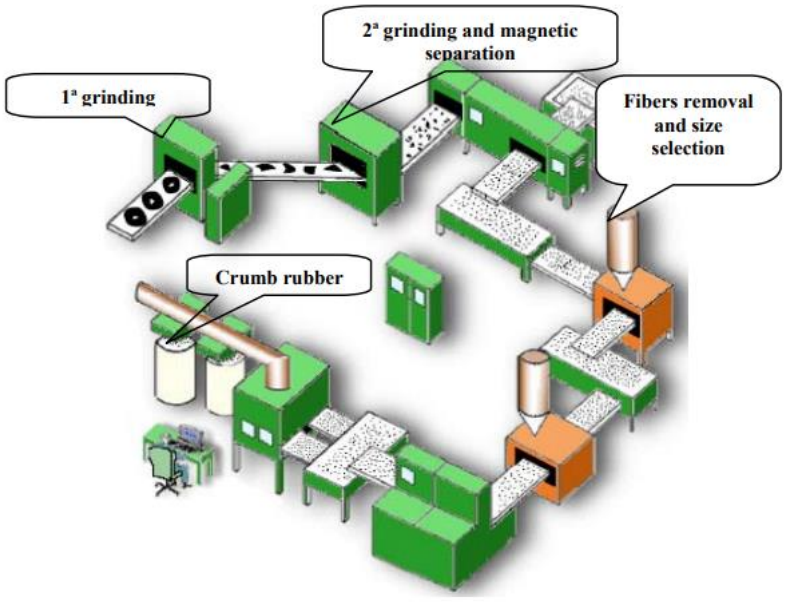

Figure 2.6. An example of ambient grinding plant (Neto et al., 2006)

The second method is cryogenic grinding. Cryogenic grinding is a process in which the temperature of tires or rubber chips is decreased to a level between -87 and -198 °C by using nitrogen. This range of temperature is below the glass transition temperature for rubber, thus the rubber chips become brittle. Frozen rubber chips are crushed into smaller particles by means of a hammer mill. In the following step, steel and fiber are removed from the material. Since the material leaving the hammer mill is still cold, drying is applied to the material. Finally, the resultant rubber particles are classified based on their sizes. By this method, smooth CR particles are obtained (Reschner. 2008; Presti, 2013). Figure 2.7 demonstrates the cryogenic grinding process schematically.

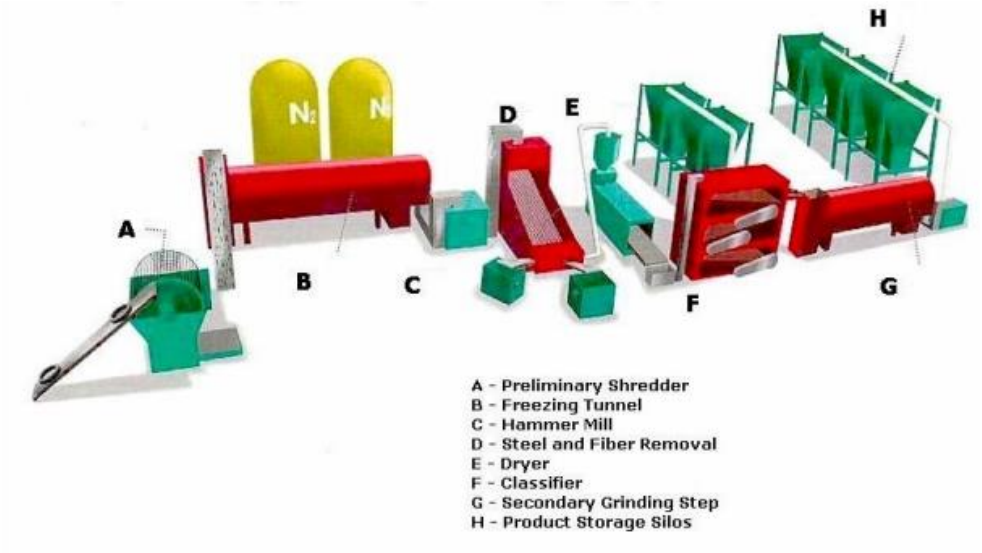

Figure 2.7. An example of cryogenic grinding plant (RTI Cryogenics Inc., Canada)

Cryogenic grinding requires fewer machinery pieces and consumes less energy compared to ambient grinding. In addition, the removal of fiber and steel is quite easier, therefore cleaner final product is obtained. However, the cost of nitrogen is a disadvantage for cryogenic grinding (Reschner, 2008). Thus, ambient grinding is a more cost-effective method for CR production (Presti, 2013).

The morphology of the CR particles produced by both methods is studied by some researchers. Thives et al., (2013) examine CR particles from both methods by employing scanning electron microscopy (SEM) and find the ambient particles appear spongy (Figure 2.8a), while cryogenic particles have a smooth texture and angular corners (Figure 2.8b). In another study, Thodesen et al. (2009) obtained similar results that ambient particles present rough morphology while cryogenic particles present smooth texture and fractured edges. As a result of having a smooth surface and regular shape, cryogenic particles have less surface area compared to ambient particles.

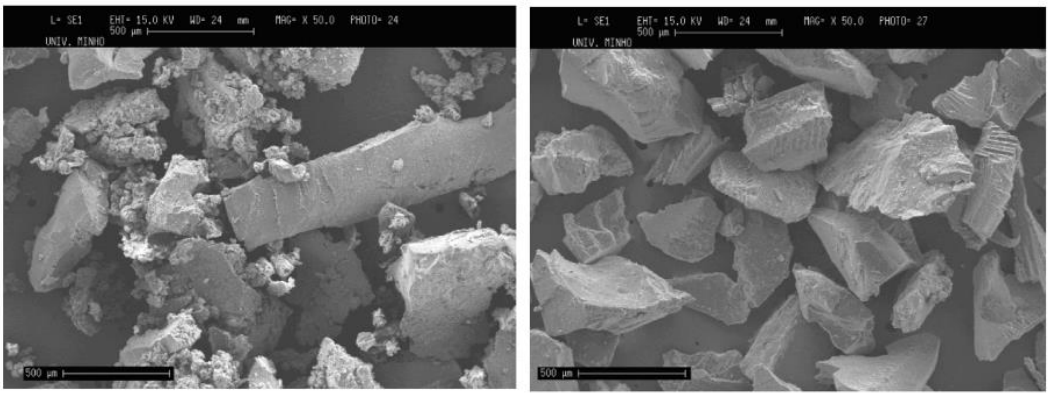

(a) (b)

Figure 2.8. SEM images: (a) ambient particles (b) cryogenic particles (Thives et al., 2013)

Overall, ambient grinding is the most widely employed method in obtaining CR particles (Presti, 2013).

2.5 Crumb Rubber Modification Methods of Asphalt Mixtures

Utilization of CR in asphalt mixtures is conducted through three main methods: wet process, dry process, and terminal process (Picado et al., 2020). However, the terminal process is mostly studied under the wet process since the production method

is based on the wet process. Details about these methods will be discussed briefly in the following sections.

2.5.1 Wet Process

The wet process was first developed by Charles McDonald, a material engineer in the City of Phoenix Arizona in the 1960s, by reacting CR with base asphalt for 45-60 mins. He consequently developed a patching material in order to maintain failing pavements. He called the resulting material as “Asphalt Rubber” and the asphalt rubber patch as “Band-Aids” (Figure 2.9). In the 1970s, the application was extended to utilize asphalt rubber on larger surface areas as a slurry seal and cheap seal. Later on, by the 1975s, asphalt rubber was integrated into asphalt mixtures, mainly gap-graded and open-graded mixtures (Way et al., 2012; Caltrans, 2003; Presti, 2013).

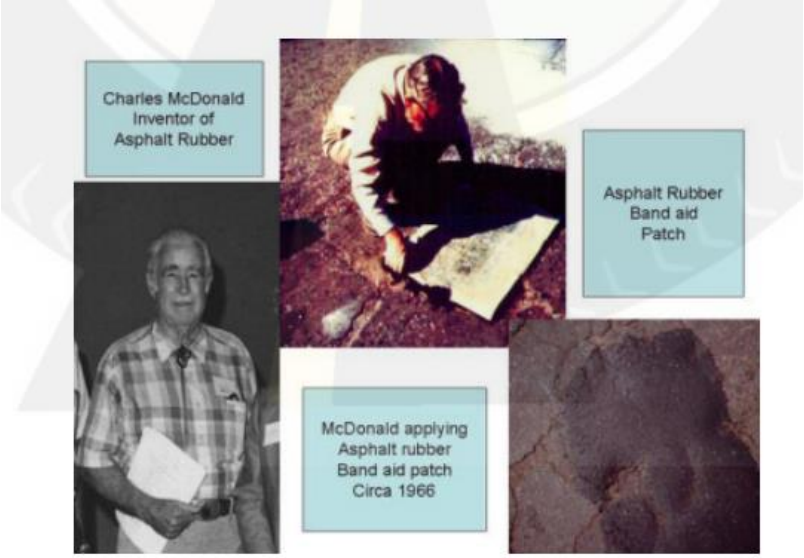

Figure 2.9. C. McDonald and his applied asphalt rubber product (Way et al., 2012).

The wet process is called any procedure in which CR is added to base asphalt before the asphalt binder is mixed with aggregates or other applications (Heitzman, 1992). The CR ratio used in the blend ranges from 5% to 25% by the weight of the base

asphalt binder (sometimes it is given as by the weight of the total blend) depending on the purpose of the final product (Presti, 2013), and the mixing/blending temperature generally ranges between 160 and 205 °C (Hicks and Epps, 2000). Figure 2.10 demonstrates an example of the production of CRMA through the wet process. The term, crumb rubber modified asphalt, is regarded as the product of the wet method (Lo Presti and Airey, 2013). In the literature, "asphalt rubber" is also associated with the wet process product. American Society for Testing and Materials (ASTM) D8 (2022) defines asphalt rubber as a blend of asphalt binder with crumb rubber, comprising a minimum of 15% CR of the total blend weight, and some additives prepared at a temperature allowing rubber particles to swell. These additives can be exampled as aromatic oils and even kerosene which have lighter weight and are used to thin the asphalt rubber in case it is too thick (Williams et al., 2015). However, Glover et al. (2000) criticize this definition as it quite narrows the term to a low-cured product with high rubber content. In addition, it doesn't include any explanation about the properties of the resulting product.

Figure 2.10. CRMA preparation process (Fernández-Ruiz et al., 2020).

The wet process is applied through two production methods: continuous blend and terminal blend (Williams et al., 2015).

2.5.1.1 Continuous Blend

The continuous blending method was derived from the original wet process which was founded by Charles McDonald. In the original method, CR and base asphalt are mixed for a few minutes in a blending tank and transferred to tanks with circulation systems where CR and bitumen are allowed to react for the required time. In the continuous blending method, CR and base asphalt are reacted continuously in a unit equipped with agitators (Presti, 2013; Heitzman, 1992). With the help of this method, reaction tanks are eliminated (Kandhal, 1992). Also, another approach in the continuous blending method was to accelerate the reaction between CR and the base asphalt by using smaller-sized CR particles. Because the reaction time was an issue in McDonald's method. For that reason, CR particles having 118 μm (No.80) in diameter were utilized in the preparation of CRMA. This method was initially proposed by Rouse Rubber Industries and it was first experimentally implemented in Florida in 1990 (Heitzman, 1992).

2.5.1.2 Terminal Blend

In this method, CRMA is produced by reacting CR and asphalt at the refinery or at a terminal prior to being transferred to the asphalt mix plant or field. In the early applications, a lower amount of CR (typically 10% by the weight of total weight) with some additives were used. That means lower viscosity values and lower performance compared to CRMA prepared with the continuous blend method. However, this content can be changed up to 15% with new adaptations (Caltrans, 2003). In the production of terminal blended CRMA, typically CR particles with 600 μm (No.30) diameter or smaller, are used in order to break down these rubber particles in a shorter time and ensure their stable distribution through the normal circulation without the requirement of agitation equipment such as augers or paddles (Han et al., 2016). The resulting product generally has a solubility value higher than 97.5% (The Magazine of Asphalt Institute, 2008).

The Magazine of Asphalt Institute (2008) excludes the terminal blend method from the wet process based on the production place. The same source states that the terminal blended CRMA is manufactured at a terminal or refinery, whereas the wet process product is manufactured in the field. In addition, CalRecycle (2010) emphasizes that subsequent agitation is not essential for uniform dispersion of the CR particles in the asphalt during the terminal blend process. However, CRMA can be produced without agitation also in the field. For this reason, more researchers use the terminology “wet process-no agitation” instead of “terminal blend” to prevent confusion about the production concept (Han et al., 2016).

2.5.2 Dry Process

The dry process defines the technology in which some of the fine and coarse aggregates are replaced with crumb rubber particles before mixing with hot asphalt binder (Figure 2.11) (Heitzman, 1992). Final products manufactured with the dry process are sometimes called as rubber modified asphalt concrete (RUMAC) and aggregate-rubber (FHWA, 1997; Neto et al., 2006).

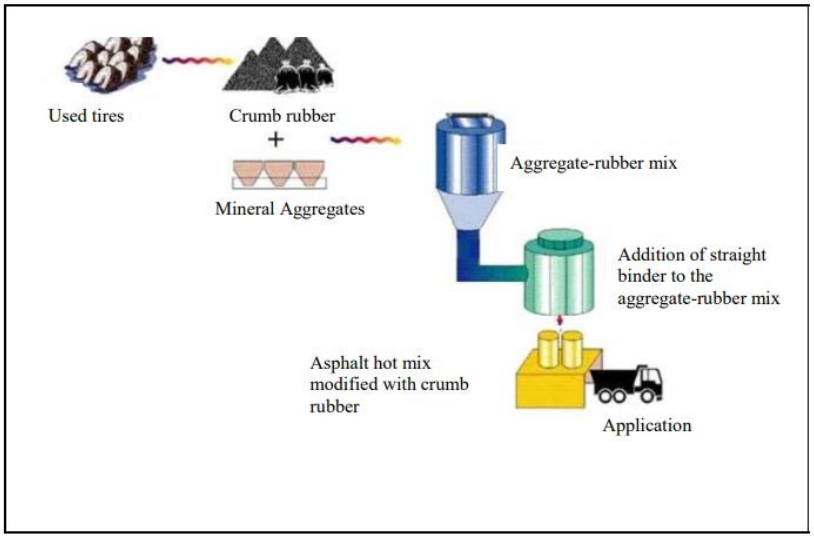

Figure 2.11. Schematic representation for the dry process (Neto et al., 2006).

Dry process technologies started to arise in the 1960s. One of them was developed by two Swedish companies, Skega AB and ABVaegfoerbaetringar (ABC). They introduced their dry process method under the name of PlusRide, and patented it in the USA (Takallou and Takallou, 1991). This method uses gap-graded asphalt mixtures (Figure 2.12) and the mixture is not designed based on standard Marshall or Hveem procedure (Takallou and Hicks, 1988). The only parameter to calculate asphalt content in the mix design is the percent air voids, ranging between 2 and 4%. The gradation of aggregate and CR and the CR ratio are specified by the patent which keeps these parameters constant. The CR ratio is determined as 3% by the weight of the total mixture. Based on these parameters, asphalt content changes between 7.5 and 9% (Heitzman, 1992).

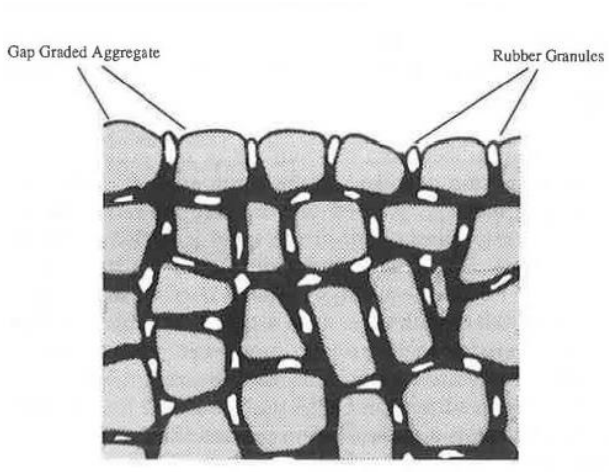

Figure 2.12. CR particles in gap-graded rubber modified asphalt concrete (Takallou and Takallou, 1991).

In 1989, another method “generic dry process” was developed by H. Barry Takallou. This method was initiated with the idea of RUMAC production with dense or gap gradations unlike the PlusRide method limiting the dry process only to gap gradation. The design standards of this approach are similar to the conventional asphalt mix. CR ratio changes in the range of 1 and 3% by the weight of the total mix. Compared to the PlusRide method, a better binder modification can be obtained with the generic method considering this method allows the usage of finer CR particles and CR

particles react with the asphalt binder before placement and compaction of the mix (Heitzman, 1992; Takallou and Takallou, 1991).

Although the dry process provides superiority against the wet process in some aspects, such as cost and the amount of CR consumed, irregular performance outcomes obtained from the experimental applications constructed with the dry process led the studies to mainly focus on the wet process (Santagata, 2007).

2.6 Interaction Between Crumb Rubber and Asphalt

2.6.1 Interaction Mechanism Between Crumb Rubber and Asphalt

CRMA, produced by mixing CR with asphalt at high temperatures (160 to 200 °C), shows different features than the base asphalt because of the interaction taking place between CR and base asphalt (Jensen and Abdelrahman, 2006). This interaction is a physical phenomenon and the CR particles don't melt in the asphalt (RAF; Heitzman, 1992). Also, Liu et al., (2014) support this approach by conducting FTIR spectrum analysis on a CRMA sample. It is concluded that the asphalt properties are altered physically by the CR.

The interaction between CR and asphalt takes place in two mechanisms: particle swelling and degradation (devulcanization and depolymerization) in case of excessive mixing conditions (Abdelrahman and Carpenter, 1999). Swelling is the process induced by the penetration of liquid into the internal structure of the polymer (Shen and Amirkhanian, 2005). In the case of CR and asphalt interaction, swelling of the CR particles happens by absorbing the light and more volatile fractions of the asphalt, namely maltenes (saturates, aromatics, and resins) (Rahman, 2004). At the same time, carbon black is released to the asphalt from the CR particles (Xiang et al., 2009). The reduction of the light fractions in the asphalt matrix, by CR particles, decreases the interparticle distance, which rises the viscosity of the continuous phase

of the asphalt (Jensen and Abdelrahman, 2006). The interaction between asphalt and CR generates a gel-like material, having an elasticity lower than rubber (López-Moro et al., 2013). CR particles can swell two to four times of their original volume mainly depending on the asphalt composition and CR content. On the other hand, CR gradation has little influence on the swelling ratio. (Ould-Henia and Dumont, 2006). Swelling of CR particles continues until a point. However, if the mixing conditions are excessive, such as keeping temperature at elevated levels or for a long time, vulcanization (breakings in crosslinks) and depolymerization of CR particles will start to take place (Figure 2.13a) (Jensen and Abdelrahman, 2006). Once the CR particles disintegrate, they will free the absorbed fractions of the asphalt back to the asphalt matrix, which will result in the decrease in viscosity (Figure 2.13b) (Ghavibazoo and Abdelrahman, 2013).

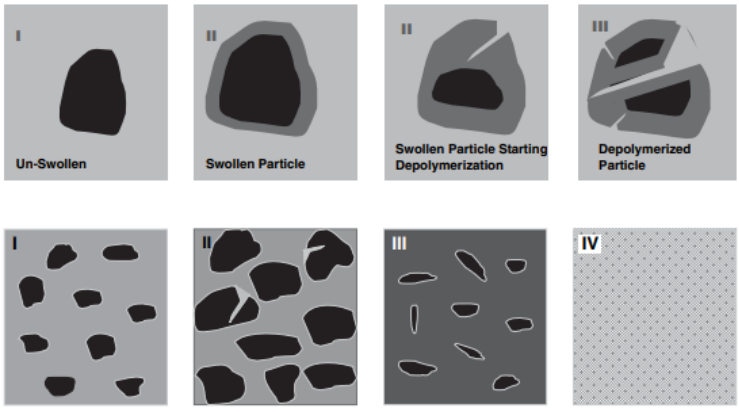

(a)

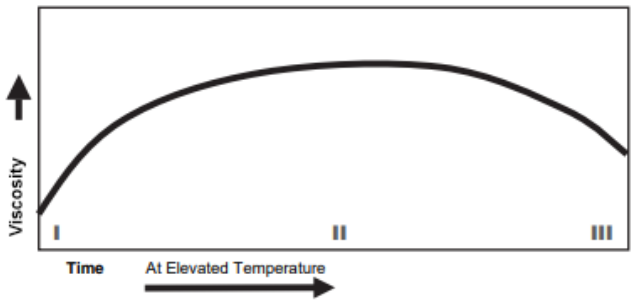

(b)

Figure 2.13. CR – asphalt interaction over time at excessive conditions: (a) CR particle changes and their distribution in the asphalt matrix (b) viscosity changes (Abdelrahman, 2006).

2.6.2 Factors Affecting the CR-asphalt Interaction and CRMA Properties

CR-asphalt interaction and CRMA properties are mainly affected by some factors which are asphalt properties (chemical composition), CR properties (chemical composition, size, shape, and surface area), CR content, mixing temperature, mixing duration, and mixer rate and type (Heitzman, 1992; Lee et al., 2008). In this section, these factors are discussed in detail.

2.6.2.1 Asphalt Properties

The chemical composition of asphalt plays an important role in the interaction between CR and asphalt (Ould-Henia and Dumont, 2006). These chemical fractions differ depending on the origin and grade of the asphalt (Artamendi et al., 2006). Thodesen et al. (2009) conducted an experiment by producing CRMA binders using asphalt from two different sources and reported that the origin of asphalt significantly affects the CRMA properties. Since the CR particles swell by absorbing the light fractions of asphalt, it is suggested to choose asphalt with high aromatic fractions for better CR- asphalt compatibility (Ould-Henia and Dumont, 2006). Asphalts containing high asphaltene fraction exhibit poor ability to swell CR particles and have lower adhesion (Artamendi et al., 2006; Huff and Vallerga, 1979). In such cases, CRMA can be improved by adding a light fraction, such as kerosene, however, aromatic oil is more desirable (Glover et al., 2000).

2.6.2.2 Crumb Rubber Ratio and Properties

CR ratio of CRMA and CR properties are other important factors that affect the interaction between CR and asphalt and thus the final properties of CRMA (Lee et al., 2008). Of all the factors, the CR ratio has the most significant effect on the CRMA performance (Jensen and Abdelrahman, 2006) and it varies from 5% to 25%

by weight of the binder in the literature. There are a number of studies investigating the effect of the CR ratio. Pereira et al. (2008) and Cong et al. (2013) indicated that increasing amount of CR ratio increases the viscosity of the modified asphalt and makes it stiffer. However, the elasticity of the modified asphalt increases with increasing CR content. Thodesen et al. (2009) measured the viscosity of CRMA samples prepared with four different CR ratios (5%, 10%, 15% and 20%), two different asphalt origins, and four different CR types. It was reported that the effect of the other factors (asphalt origin and CR types) was not significant for the CRMA with 5% CR, while a significant difference was observed for the CRMA with 20% CR.

The swelling mechanism of CR particles is governed by the particle size through the interaction time. While it takes some time to swell for coarse particles, finer particles may swell instantly when introduced to base asphalt (Jensen and Abdelrahman, 2006). It is because finer particles have larger surface area. Therefore, the diffusion of the light components of the asphalt into the CR particles is accelerated (Neto et al., 2006). The time required for particles with #80 mesh size, to interact with AC-30 asphalt at 163 °C is around one minute. However, depolymerization will take place earlier for finer particles since the finer particles reach to their maximum swelling level more quickly during production and storage (Jensen and Abdelrahman, 2006; Fontes et al., 2006).

The studies in the literature show that CR morphology can differ depending on the production method of CR. Thives et al. (2013) studied the morphology of two different CR particles produced by the ambient grinding process and the cryogenic grinding process. The results of the study show that the CR particles produced by the ambient grinding process have a larger surface area than those produced by the cryogenic grinding process. This is due to the fact that CR particles from ambient grinding exhibit porous surfaces with irregular shapes, while the particles prepared by cryogenic grinding have smooth surfaces with beveled corners. Oliver (1981)

reported that the elastic recovery of the modified asphalt is significantly related to the CR production method, and increases with decreasing CR particle size. In addition, Thodesen et al. (2009) found that CRMAs produced with ambient ground CR have higher viscosity values than those produced with cryogenic ground CR.

In the literature, there are also various types of CR obtained from truck tires, car tires, sole tires, agriculture tires, tread rubber, hose and ball, which are investigated. However, these studies mainly focus on truck and car tire CRs. Cao and Bai (2008) conducted a test on the truck and car tire CRs and found that CRMA with truck tire CR is stiffer at high temperatures based on the G*.sinδ and G*/sinδ parameters and less stiff at low temperatures than the CRMA with car tire CR based on the elastic recovery and the S value. It was concluded the CRMA with truck tire CR has better high and low-temperature performance than the CRMA with car tire CR. Artamendi et al. (2006) presented that the truck tire CR absorbs more amount of asphalt fractions with a higher absorption rate compared to the car tire CR due to the higher natural rubber content of truck tires.

2.6.2.3 Mixing Temperature

How temperature affects the interaction between CR and asphalt, was investigated by various researchers. Green and Tolonen (1977) stated that temperature has two effects on asphalt-CR interaction: the rate of swelling of CR particles and the extent of swelling of CR particles. Temperature increase (an increase of free energy in the system) leads to a significant increase in the rate of swelling. This phenomenon decreases the entropy as the energy in the system is increased by stretching CR particles. In order to compensate for the entropy change, the CR particles become stiffer, thus the extent of swelling decreases. Lo Presti and Airey (2013) stated employing high temperatures accelerates the reaction between asphalt and CR. Li et al. (2018) tested different CRMA prepared by using temperatures, varying from 140 to 195°C, based on their viscosities. The authors reported that increasing mixing

temperature increases the viscosity of CRMA, however too high temperatures degrade the CR particles, and viscosity decreases back.

2.6.2.4 Mixing Duration

The effect of mixing duration on CR-Asphalt interaction is mainly investigated in conjunction with mixing temperature. CR particles can swell, by absorbing the light fractions of asphalt, until they reach equilibrium swelling during the interaction process (Rahman, 2004; Jensen and Abdelrahman, 2006). After this point, if the mixing duration is kept long at elevated temperatures, the swelling is replaced with the degradation of CR particles and loss of modification (Jensen and Abdelrahman, 2006). Subhy et al. (2016) studied CRMAs prepared by employing different mixing temperatures and durations. The authors concluded that 140 min of mixing durations is desirable for a mixing temperature of 180 °C, while it is 15, 25 and 60 min for 200 °C. The results of the experiment show the mixing duration is shortened for the increasing mixing temperatures. Pereira et al. (2008) conducted an experiment on CRMA samples produced with mixing durations, from 40 to 90 mins. Based on the conventional tests, it was concluded that the mixing duration in this range doesn't have a significant effect on the final product. In addition, based on the viscosity values, it was observed for 21% CR ratio, the depolymerization starts after 150 min for 200°C, whereas it is 210 min for 190 °C. Mashaan and Karim (2013) also investigated the effect of mixing duration on the final product properties through the rheological tests and the softening point test. The researchers selected the mixing duration levels as 30 min and 60 min and found there was minor differences in results. Furthermore, the Analysis of Variance (ANOVA) outputs presented the mixing duration factor for those two levels as insignificant. It was also suggested that it is necessary to examine the effect of mixing duration in a wider range of time.

2.6.2.5 Mixing Rate

The elastomeric property of the CRMA, a determinant factor for the CRMA performance, is in relation to the CR-asphalt interaction. A sufficient dispersion of the CR particles in the asphalt is essential for better interaction through building a homogeneous rubber network in the asphalt (Oliver, 1982; Pereira et al., 2008; Hicks and Epps, 2000). The mixing rate ranges applied in the field and laboratory studies varied in a wide range from low to high (Hicks and Epps, 2000). It is possible to see this range between 200 rpm and 14000 rpm in the literature. Low-speed mixing rate help CR particles evenly disperse and prevent the settlement, whereas high-speed mixing rate (shearing) may bring about decaying CR particles to smaller pieces during the dispersion process (Hicks and Epps, 2000; Jensen and Abdelrahman, 2006). Sienkiewicz et al. (2017) compared a high-shear mixer with a stirrer mixer usage based on the CRMA test results. The authors reported stirring performs better in terms of high-temperature storage stability of CRMA, while high shear mixing results in better CR particle dispersion for CRMA with a 10-15 CR ratio. In another study, Aflaki and Memarzadeh (2011) pointed out the low-temperature performance is enhanced more via high-shear mixing compared to low-shear mixing, whereas the intermediate and high-temperature performance is more improved via low shear mixing based on the DSR (rheological properties) test results. Celauro et al. (2012) stated high shear mixing can reduce mixing time to one-third of that required to obtain the same results using low shear mixing. These results can be related to the decreasing particle size by high shear mixing, thus faster interaction between CR and asphalt as Jensen and Abdelrahman (2006) explained.

2.7 Methods to Evaluate CRMA Performance and Interaction

The resultant product of asphalt and CR mixing, CRMA, is evaluated by employing the conventional asphalt tests, dynamic shear rheometer (DSR), and alternative methods such as microscopy (fluorescence, light, atomic force, etc.), differential

scanning calorimeter (DSC), FTIR, etc. Within this section, the methods, employed to evaluate CRMA samples in this thesis, will be discussed.

2.7.1 Conventional Asphalt Test Methods

In the literature, penetration test, softening point test, resilience test, flash and fire point test, and rotational viscosity tests (Brookfield and handheld viscometers (Haanke, Rion, etc.)) are the most common conventional tests employed in order to evaluate physical properties of CRMA. In addition, some researchers rarely utilize the ductility test. Rodríguez-Alloza et al. (2013) stated that the non-homogeneous distribution of CR particles in asphalt prevents modified asphalt from forming homogeneous thin thread during elongation, resulting in early breaking. For this reason, ductility is not a reliable factor to asses CRMA performance. ASTM D6114/6114M (2019) suggests the conventional tests and limits as in Table 2.2.

Table 2.2 Conventional tests and limitations for CRMA, suggested by ASTM D6114/6114M (2019)

Binder Designation		Type I (Hot Climate Areas)	Type II (Moderate Climate Areas)	Type III (Cold Climate Areas)
Apparent Viscosity, 175 °C (Pa.s)	min	1.5	1.5	1.5
	max	5.0	5.0	5.0
Penetration, 25 °C, 100 g, 5 s (1/10 mm)	min	25	50	50
	max	75	100	100
Penetration, 4 °C, 100 g, 5 s (1/10 mm)	min	10	15	25
Softening Point, °C	min	57	54	52
Resilience, 25°C, %	min	25	20	10
Flash Point, °C	min	232	232	232

The penetration test determines the consistency of asphaltic materials. It is conducted by applying a needle into the material surface vertically under specific conditions (time, temperature, and load) and measuring the distance, the needle penetrated, in tenths of a millimeter, Figure 2.14, (ASTM D5/D5M, 2020). The softening point test measures the temperature an asphaltic material reaches a certain softness by heating two asphalt samples, poured in rings, under the specific weight of a metal ball on each and observing the temperature that the sample's contact with the plate placed under them (ASTM D36/D36M, 2020). The resilience test measures the recovery amount of asphaltic material in percent after a metal ball is forced into the surface (ASTM D5329, 2020). Viscosity is defined as the resistance of a fluid to flow and is formulated as the ratio of shear stress to shear rate (Gresham, 2008; ASTM D4402/D4402M, 2022). Viscosity is a significant property in order to determine the consistency of asphalt at elevated temperatures (Papagiannakis and Masad, 2008). In addition, it is an important factor in controlling the pumpability of asphalt and the workability and compaction of asphalt mixtures (Subhy et al., 2016). Asphalt shows Newtonian behavior at high temperatures, such as at mixing temperatures, (independent of shear rate), and non-Newtonian behavior at lower temperatures, such as 60°C, (dependent on shear rate) (Papagiannakis and Masad, 2008). Because of the CR particles, most of the conventional viscosity measurement methods are not applicable to CRMA. For this reason, the Brookfield viscometer is employed for CRMA viscosity determinations at high temperatures (Neto et al., 2006b). Brookfield viscometer measures the viscosity through the torque necessary to keep the rotation of a spindle, immersed in the asphalt, at a constant speed under a constant temperature, Figure 2.14, (Papagiannakis and Masad, 2008).

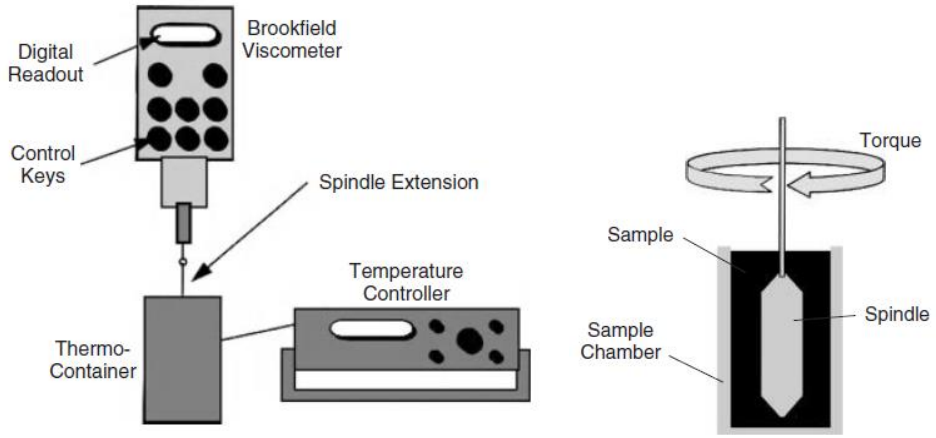

Figure 2.14. Brookfield viscometer (Mamlouk and Zaniewski, 1999)

The effect of CR modification of asphalt on the conventional test results, obtained by a number of researchers (Cong et al., 2013; Wulandari and Tjandra, 2017; Liu et al., 2014; Sienkiewicz et al., (2017)), show consistency. Based on these studies, the addition of CR increases softening point, resilience, and viscosity values while it decreases penetration values. In the literature, some researchers benefited from the conventional tests while they were trying to find the combination of CRMA mixing variables presenting the most desirable physical properties. Of all the conventional tests, Pereira et al. (2008) decided to choose their optimum CRMA design based on the viscosity test results as the viscosity of asphalt is a critical factor for the pumpability of asphalt binder and the workability and compaction of asphalt-aggregate mixtures. Subhy et al. (2016) developed a modified impeller, namely Dual Helical Impeller, for Brookfield viscometer with the aim of maintaining the homogeneity of CRMA during viscosity measurements. However, Presti et al. (2017) indicated that conventional tests are designed for base asphalt; therefore, alternative test methods must be considered for complex heterogeneous materials such as CRMA.

2.7.2 Dynamic Shear Rheometer (DSR)

Dynamic shear rheometer (DSR) is utilized to characterize the viscoelastic properties of asphalt binders which are complex shear modulus (G*) and phase angel (δ). The test is conducted by applying shear stress or strain dynamically through two parallel plates as presented in Figure 2.15 (ASTM D7175, 2015; Papagiannakis and Masad, 2008). The complex shear modulus is the ratio of maximum shear stress to maximum strain and represents the stiffness or the resistance of asphalt binder to deformation under shear stress. It comprises two components: the storage modulus (G′) and the loss modulus (G′′) which are the elastic and the viscous components, respectively. The phase angle is the time lag between the application of the shear stress and the response of shear strain (Airey and Rahimzadeh, 2004). While the phase angle is 90° for viscous materials, it is 0° for elastic solid materials (Papagiannakis and Masad, 2008).

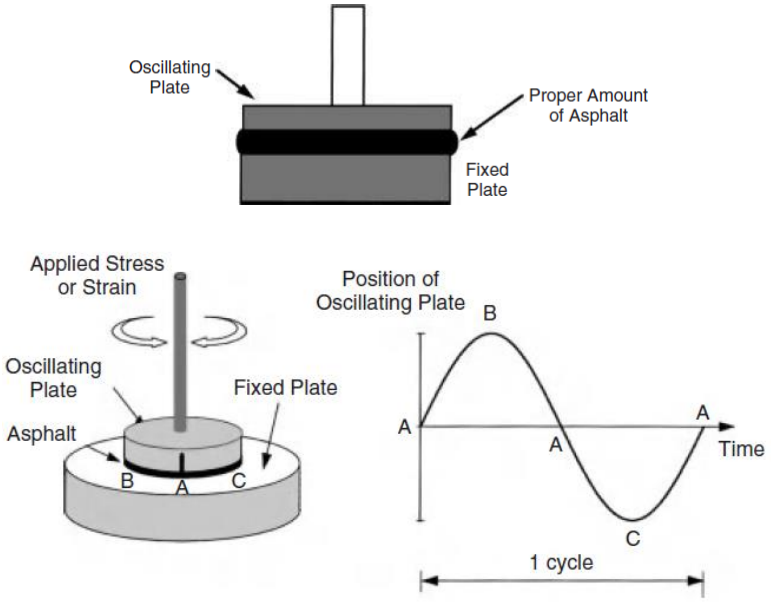

Figure 2.15. Dynamic shear rheometer (Mamlouk and Zaniewski, 1999)

Viscoelastic (rheological) parameters (G* and δ) are determined in a number of modes of DSR test, such as amplitude sweep test, frequency sweep test, temperature sweep test, and multiple stress creep recovery test (MSCRT). For the amplitude sweep test, a single frequency and multiple stress or strain values are employed. It is generally conducted to determine the linear viscoelastic region where the complex shear modulus is not in relation to shear strain. Therefore, this linear viscoelastic region can be used for the frequency sweep test. Changing frequency levels can represent how the asphalt binders react under changing traffic loads and temperatures. For this reason, the frequency sweep test is conducted at multiple frequency levels (Duan et al., 2021; Navarro et al., 2007). Temperature sweep test is also conducted at multiple temperatures for different purposes, such as determining the performance grade of asphalt (maximum and minimum service temperature), rutting resistance (G*/sin(δ)) at intermediate and high temperatures, and fatigue resistance (G*Sin(δ)) at low temperatures (Lv et al., 2021a; Ma et al., 2020). Furthermore, in MSCRT mode, the asphalt binder sample is statically loaded and allowed to recover for specific durations repeatedly. In ASTM D7405 (2020), the loading and recovering times are given as 1 and 9 seconds, respectively. The test is conducted at different stress levels. Consequently, the obtained nonrecoverable creep compliance is utilized to evaluate the behavior and the permanent deformation of asphalt binders at various stress levels (Southern, 2015; Amirkhanian, 2020).

Since DSR offers variety of measurement modes, the researchers employed different testing modes in the assessment of the rheological properties of CRMA. The temperature sweep test conducted by Zhang et al. (2002) demonstrated that the CR addition increases the high-temperature performance grade of asphalt. Liang et al. (2015a) conducted temperature and frequency sweep tests to investigate how the addition of CR affects the rheological properties of asphalt and found that CRMA shows improved viscoelastic properties. Duan et al. (2021) presented a detailed study about DSR modes while comparing CR modification with SBS modification. One of the findings in the study is that CRMA has a wider viscoelastic region. Some of the

researchers, such as Subhy et al. (2016), rather constructed master curves and black diagrams, by employing temperature and frequency sweep tests, in order to evaluate the CRMA in terms of the rheological properties and viscoelasticity-stiffness relationship, respectively. DSR also allows researchers to evaluate the low-temperature performance of asphaltic materials when it is operated with plates having a diameter of 4 mm. Chang et al. (2020) constructed master curves with the frequency sweep test results obtained at -18°C and -28°C by utilizing 4 mm plates in their study.

2.7.3 Fluorescence Microscopy

Fluorescence microscope (FM) provides a technology that monitors the structure and morphology of samples that are excited with shortwave light to generate fluorescence (Dallas, 2020; Lv et al., 2021a). FM excites samples either by transmitting the light through the sample (diascopic fluorescence) or reflecting the light from the sample surface (episcopic fluorescence) (Bagnell, 2012). Since the first method is applicable to transparent samples, the episcopic fluorescence is appropriate for thick and opaque samples, such as polymer-modified asphalt (Bagnell, 2012; Hao and Wang, 2021). In episcopic FM, light produced by the source initially travels through an excitation filter to separate a specific wavelength of light. This high-energy light follows the path through the objective lenses and illuminates the sample for excitation. The excited sample emits a lower energy light with a longer wavelength (fluorescence). Finally, the fluorescence travels through the emission filter to prevent the remaining radiations from reaching the detector (Figure 2.16) (Rise, 2021). With FM, two-dimensional (2D) and three-dimensional images (3D) images can be obtained. 2D images are mainly produced by scanning a fixed excited thickness; therefore, the image doesn't only contain information from the surface but a part of the underlaying layer (Hao and Wang, 2021).

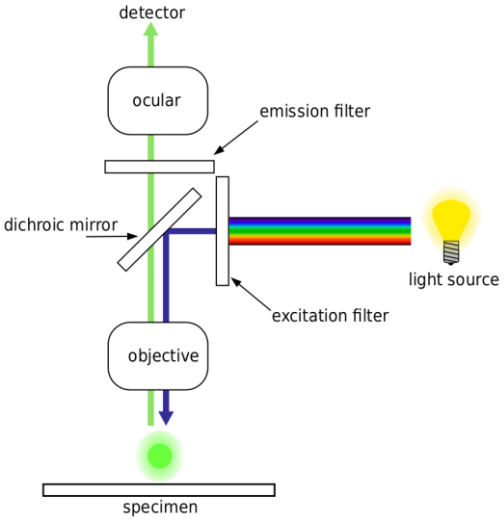

Figure 2.16. The working principle of a fluorescence microscope. By derivative work: Henry Mühlpfordt (talk)

FM is benefitted in asphalt and modified asphalt studies for different purposes. Handle et al. (2016) investigated the fluoresce sources in the chemical components of asphalt, SARA. It was revealed that the asphaltene fraction barely emits fluorescence, whereas the aromatics fraction is the strongest fluorescence source followed by the resins fraction. Saturates don't have a structure that is able to emit fluorescence. In addition, polymers are also one of the materials that can produce fluorescence (Zhou et al., 2020). Hao and Wang (2021) reconstructed a 3D image of a polymer (SBS)-modified asphalt sample using 2D images taken at different depths of the sample in order to analyze particle morphology (Figure 2.17a). López-Moro et al. (2013) employed FM to monitor the interaction between asphalt and CR particles, and the researchers were able to observe the maltenes intensified around the rubber particle and the carbon black released into the asphalt matrix (Figure 2.17b). Some researchers, such as Lv et al. (2021a) and Zhou et al. (2020), studied the dispersion of CR particles in the asphalt matrix as an indicator of compatibility between CR and asphalt through FM images (Figure 2.17c).

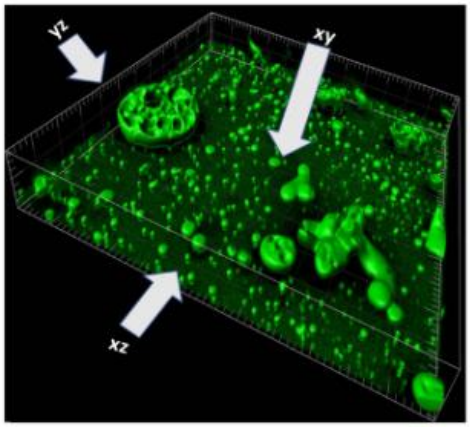

(a)

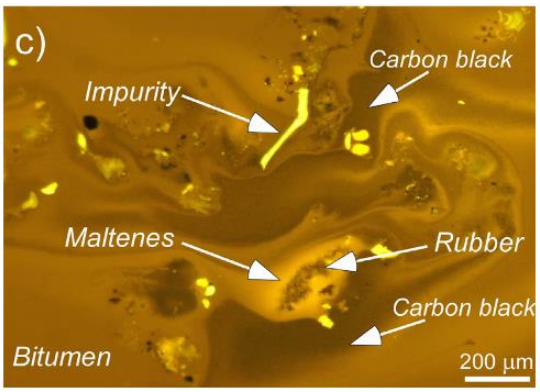

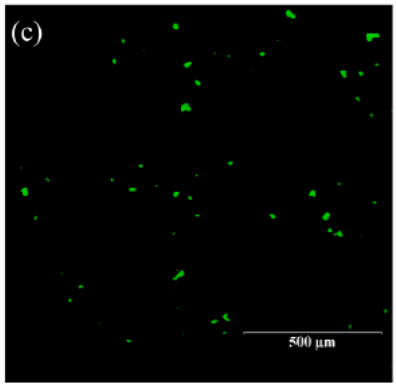

(b) (c)

Figure 2.17. Fluorescence images: (a) 3D image of a polymer modified asphalt (Hao and Wang, 2021), (b) component exchange between asphalt and CR (López-Moro et al., 2013), (c) CR distribution in asphalt matrix (Lv et al., 2021a)

2.8 Gaps in the Literature

In the previous studies, the effect of the modification variables, material properties, mixing temperature, CR ratio on the intermediate and high temperature performance of CRMA was thoroughly investigated, the effects of the variables were mainly revealed. However, the effect of the mixing duration and rate are still in question. Furthermore, the effect of these variables has not been thoroughly investigated by employing a wide range of modification levels, testing methods and analyzing through florescence microscopy yet.

CHAPTER 3

METHODOLOGY

3.1 Introduction

This chapter includes the details of the studied modification variables of crumb rubber modified asphalt (CRMA), properties of raw materials, and sample preparation methods. In addition, the methods employed to evaluate the modification performance, (i.e., conventional and nonconventional asphalt test methods, statistical analysis methods, and imaging methods) are also discussed in detail. All the tests were performed in the Transportation Laboratory of the Civil Engineering Department and the Central Laboratory of Middle East Technical University based on ASTM standards, AASHTO standards, and Turkish General Directorate of Highway specifications, further referenced in related sections. The flow chart of the experimental program is presented in Figure 3.1.

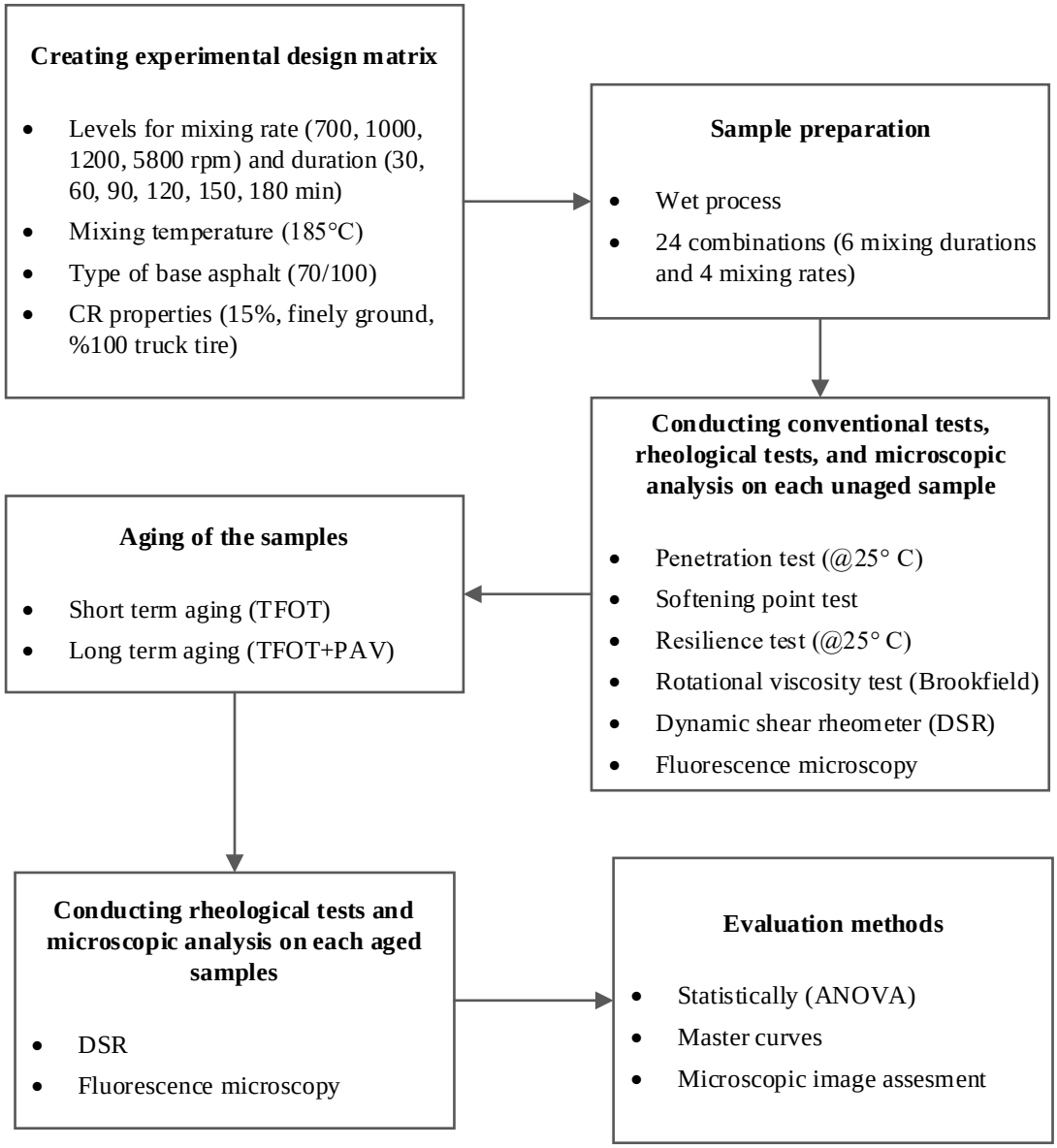

Figure 3.1. The flow of the experimental program

3.2 Selection of Levels for CRMA Modification Variables

Within the scope of the study, the effect of two crumb rubber (CR) modification variables, mixing rate and duration, on the intermediate and high temperature performance of the modified asphalt was investigated. For this reason, the experimental matrix was designed by selecting mixing rate and duration in different levels, whereas the rest of the variables (asphalt type, CR content, CR gradation, and mixing temperature) were kept constant (i.e., one level is selected for each one). In order to determine these levels, a hundred relevant papers were gone through and the variable levels in those papers were tabulated as in Table A.1. Moreover, the constant variables were determined by considering the conclusions and suggestions of these papers. For the mixing rate and duration levels, the values used in the literature were selected by keeping the range as wide as possible in order to study the effect of these variables in a broader range. As a result, six levels (30, 60, 90, 120, 150, 180 min) for mixing duration and four levels (700, 1000, 1200, 6000 rotation per minute (rpm)) for mixing rate were selected. CR content, mixing temperature, and asphalt type were determined as %15 by the weight of the base binder, 185°C and 70/100, respectively. More details about the raw materials will be discussed in the following section.

3.3 Materials

Details about the raw materials, CR and base asphalt, used in the experimental design are presented in this section. Since the focus of the study is to investigate the effect of mixing rate and duration, only one type of asphalt and CR were employed in the design.

3.3.1 Base Asphalt

Referring to the fact that CR particles absorb the lightweight fractions of asphalt and consequently decrease the viscosity, a relatively softer asphalt type, 70/100, was selected for the study. Because a softer asphalt generally embodies a higher percent of lightweight fractions. The base asphalt used in this study was produced at the Kırıkkale Refinery located in Kırıkkale, Turkey. The characteristic properties of the base asphalt are given in Table 3.1.

Table 3.1 Characteristic properties of the base asphalt

Physical tests	Test value	Specifications
Penetration @ 25°C (0.1 mm)	72.33	ASTM D5
Softening point (°C)	46	ASTM D36
Ductility @ 25°C (cm)	150+	ASTM D113
Viscosity @ 135 °C (Pa.s)	0.337	ASTM D4402
Specific gravity	1.038	ASTM D70
High temp. true grade (°C)	64.60	AASHTO T315
Intermediate temp. true grade (°C)	21.30	AASHTO T315

3.3.2 Crumb Rubber

In order to obtain a good interaction between base asphalt and CR particles, a finely graded (i.e., higher surface area) crumb rubber was utilized in the study (Figure 3.2). The particle size distribution of the CR can be seen in Table 3.2. In addition, the comparison of the CR gradation used in this study with respect to the gradations used in the literature is presented in Figure 3.3. It should be highlighted that the majority of gradations from the literature centers in the region where the CR gradation used in this study lies. The gradations in the literature focus on the same region to provide

better interaction between CR and base asphalt. In addition, the limits determined by the Arizona Department of Transportation (ADOT) is presented, which many researchers adopted these limits to their study. It should be noted that in this study, CR was obtained from truck tires by ambient grinding process and provided by a local producer in Ankara. In order to obtain the morphological characteristics of the CR particles, scanning electron microscope (SEM) was employed. Figure 3.4 presents the SEM images of the CR particles magnified 100x, 1000x, and 2500x. As seen in the images, CR particles have irregular shapes with slightly rounded corners. Furthermore, the particle surfaces have a spongy texture which provides larger surface area; thus, more contact with asphalt. These morphological properties of the CR particles show similarity with that of the ambient ground CR particles used in the study by Thives et al. (2013).

Figure 3.2. Crumb rubber used in the study.

Table 3.2 Gradation of the crumb rubber used in the study and the limits by ADOT

CR used in the study		ADOT (type B)	
Sieve size		% Passing	
(mm)	% Passing	min.	max.
2.0	100	100	100
1.18	100	65	100
0.60	91.13	20	100
0.30	38.56	0	45
0.15	7.14	-	-
0.075	0.67	0	5

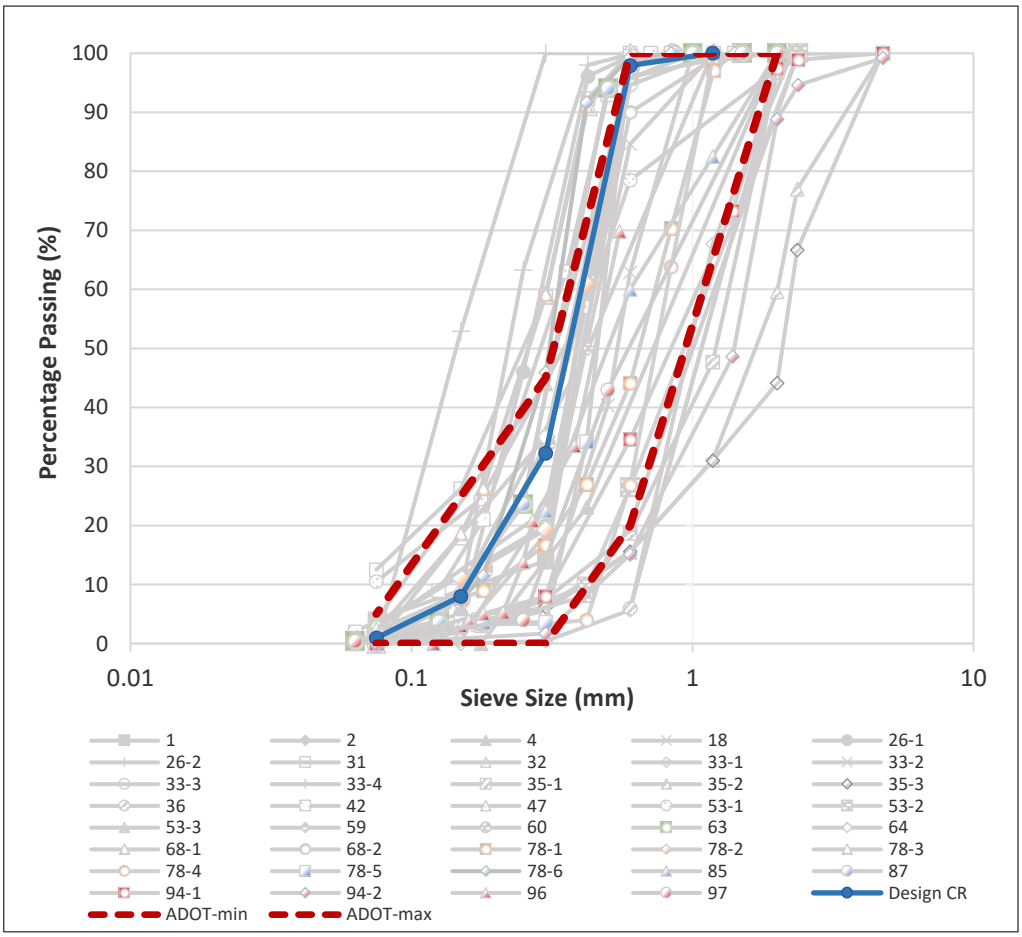

Figure 3.3. Gradations of the crumb rubber used in the study and in the literature (The IDs in the legend represent the paper numbers given in Table A.1).

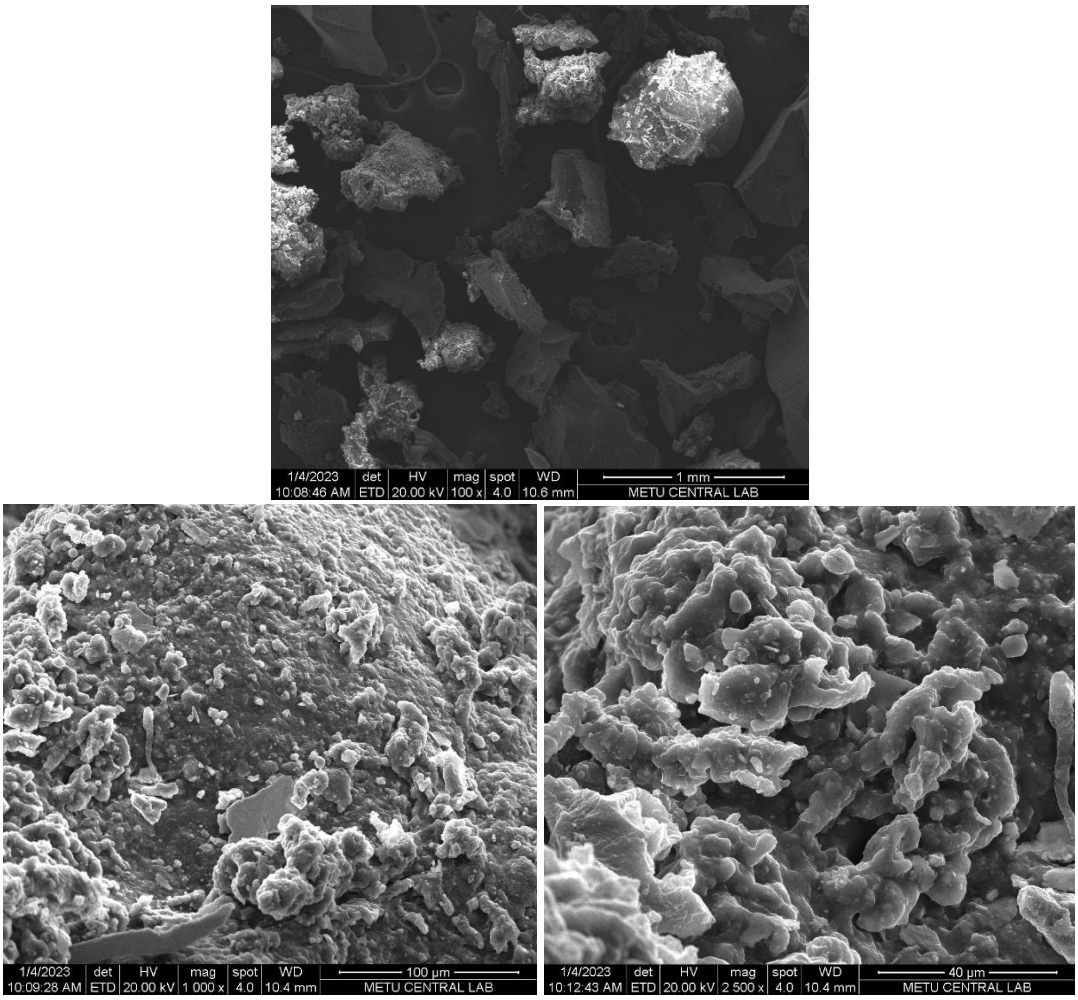

Figure 3.4. SEM images of the CR particles used in this study

3.4 Preparation of CR Modified Asphalt

CR modified asphalt mixtures were prepared by using the wet process method, in which CR is directly added to base asphalt. Mixture preparation of CR and base bitumen was conducted by utilizing mechanical mixers. For the mixing rates of 700, 1000, 1200 rpm, a mixer with a dissolver stirrer (Figure 3.4a) and for 6000 rpm, a high shear mixer (Figure 3.4b) was used. In order to ensure effective and homogenous mixing, proper containers are chosen as a glass beaker of 600 ml for the first type of mixer and a glass balloon of 250 ml for the high shear mixer.

(a) (b)

Figure 3.5. Mixers; (a) mixer with dissolver stirrer, (b) high shear mixer.

Samples were prepared as follows:

- The base asphalt was heated up to the mixing temperature, 185°C, by constant stirring to ensure even temperature distribution within the mixing container.
- CR, %15 by weight of base asphalt, was poured into the mixing container slowly and gradually. In order to prevent the agglomeration of CR particles, a cone with a small opening at the bottom, providing a slow flow of CR, was used. This step was completed within 5 minutes.
- Duration of mixing time started after the whole CR was added (Figure 3.6).
- As soon as the mixing process was completed, the mixture was poured into test containers before any settling or floating of CR particles took place.

Since the experiment matrix consists of six mixing duration levels and four mixing rate levels, CRMA mixtures were prepared in 24 combinations. The whole process

was conducted under a laboratory fume hood to prevent any possible hazardous fume and odor released by hot CRMA.

Unaged, short-term aged and long-term aged samples were, respectively, denoted as CR-mixing duration-mixing rate, T-CR-mixing duration-mixing rate, P-CR-mixing duration-mixing rate.

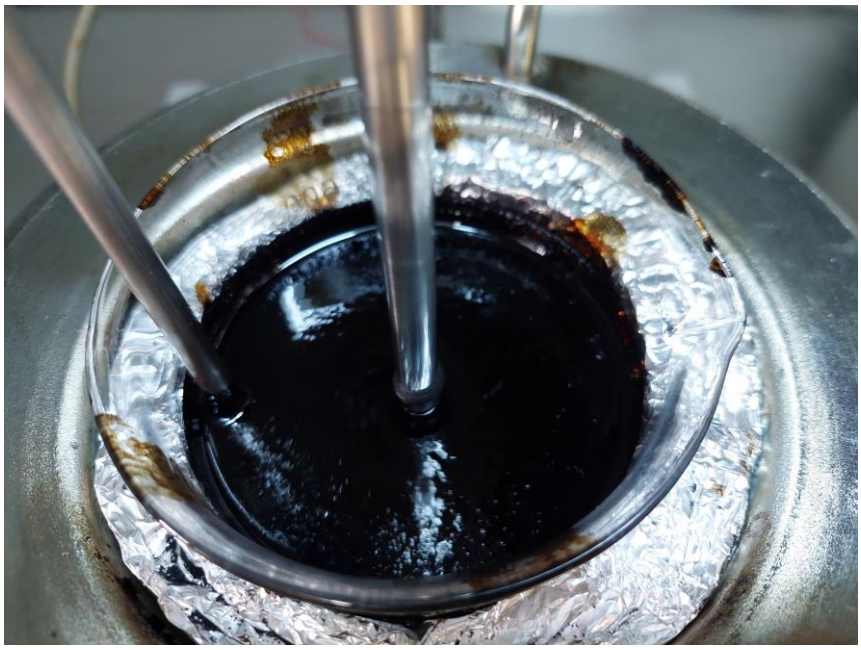

Figure 3.6. Mixing process of the base asphalt and CR.

3.5 Methods to Evaluate the Effect of CR Modification on Asphalt

In this section, the methods used to evaluate the intermediate and high temperature performance of CRMA with different mixing time and duration levels are presented. The framework of these methods includes conventional asphalt performance tests, dynamic shear rheometer (DSR) test, fluorescence microscopy, and statistical analysis.

3.5.1 Conventional Performance Tests

Conventional performance tests were conducted to measure the physical properties of the base asphalt and CRMAs. These tests were selected based on ASTM D6114 "Standard Specification for Asphalt-Rubber Binder" which consists of the penetration test, softening point test, resilience test, and rotational viscosity test.

3.5.1.1 Penetration Test

Penetration test was performed in accordance with ASTM D5/D5M "Standard Test Method for Penetration of Bituminous Materials." First, in the case of base asphalt, the liquefied sample was poured into a flat-bottomed glass container with dimensions of 35 x 50 mm (in relation to the range of expected penetration values) (Figure 3.6a). As for CRMA, this step was applied as soon as mixture preparation was completed before any settlement or floating of CR particles took place. The sample was left to cool at an air temperature between 15 and 30°C for 60 to 90 mins. Following the air cooling, the sample was conditioned in a water bath of 25°C for another 60 to 90 mins. Then, the sample container in a transfer dish was placed on the level penetrometer stand (Figure 3.6b). The penetrometer dial was set to zero and the needle was descended until the tip of the needle touches the sample surface. Next, the needle loaded with a weight of 100 g, was released for 5 seconds and the vertical displacement of the needle tip was measured in tenths of millimeters with the help of the penetrometer dial. This measurement was conducted on three different spots of the sample surface and the spots were at least 10 mm apart from the side of the container and each other. The mean of three measurements was taken as the penetration value of the sample. With this test, consistency (hardness) for the base asphalt and each CRMA sample with different modification levels was obtained.

(a) (b)

Figure 3.7. (a) A penetration test sample, (b) a penetrometer.

3.5.1.2 Softening Point Test

Asphalt is a thermoplastic material, and thus its behavior is affected by temperature changes. Softening point test is used as one of the methods to evaluate characteristics of asphalt at elevated temperatures. In this study, softening point test was conducted according to ASTM D36/D36M "Standard Test Method for Softening Point of Bitumen (Ring-and-Ball Apparatus)." Two brass rings, 19 mm in diameter, were heated to sample temperature and placed on a flat and smooth brass plate covered with a thin layer of release agent (petroleum jelly). The rings were filled with the hot sample by forming excess material on top and left to cool at ambient temperature for 30 mins (Figure 3.7a). Meanwhile, a glass beaker, 10 mm in diameter and 140 mm in depth, was filled with water at 5°C. Also, two steel balls, each having 3.5 g in weight and 9 mm in diameter, and the brass ring holder assembled with two ball centering guides and a thermometer were submerged in the water. Once the samples cooled after 30 mins, excess material was trimmed, and the rings containing the samples were placed on the ring holder in the water. The water temperature was

maintained at 5°C for 15 mins to equilibrate the specimen temperature to water temperature. After 15 mins, steel balls were positioned on the samples with the help of ball centering guides, and the water was heated at a rate of 5°C/min (Figure 3.7b). Once each ball, surrounded with the sample, contacts the bottom plate, the temperature value is recorded. The mean of these two temperatures was taken as the softening point of the sample, providing that these two values didn't differentiate more than 1°C.

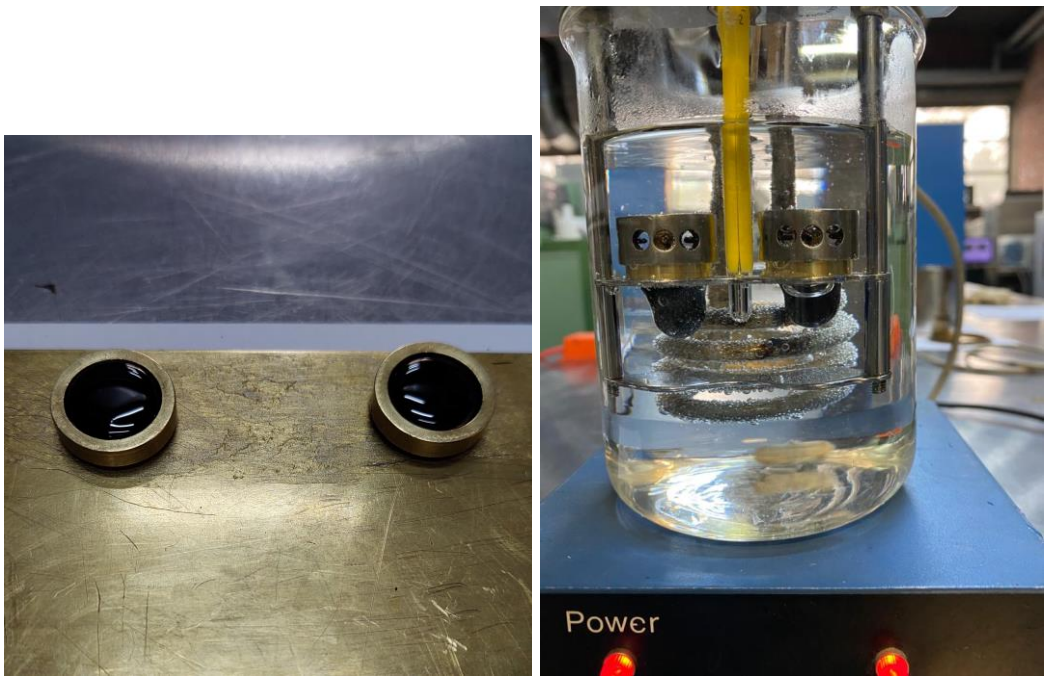

(a) (b)

Figure 3.8. (a) Softening point test samples, (b) test setup during test.

3.5.1.3 Resilience Test

Rubber can be deformed in large amounts, yet it has the ability to recover completely in a quick manner. Thus, rubber has a high elasticity. Since resilience is a good criterion to measure the elasticity of a material, it is utilized to evaluate the elasticity of CRMA based on different mixing variables. In this study, the resilience test was performed in accordance with ASTM D5329 "Standard Test Methods for Sealant

and Fillers, Hot Applied, for Joints and Cracks in Asphalt Pavements and Portland Cement Concrete Pavements." This test is similar to a penetration test. Instead of a needle, a standard steel ball of 27.5 g in weight, is used (Figure 3.8). First, the hot sample was poured into a flat-bottomed cylindrical container having a diameter of 60 to 75 mm and depth of 45 to 55 mm and allowed to cool at ambient temperature for 90 to 120 mins. In addition, the sample was maintained in a water bath at 25°C, for 120 mins. Following the conditioning period, the sample was removed from the water bath. Its surface was dried and covered with talc, an excess of which was blown off. Talc is used to prevent the sticking of the steel ball to the sample surface. The sample container was placed on the level penetrometer stand. The penetrometer dial was set to zero and the ball was lowered until the tip of it contacted the sample surface. The ball, loaded with the weight of 75 g (including the ball's weight), was released for 5 seconds and its vertical movement was read on the penetrometer dial. This reading was recorded as *P*. Additional 100 unit (10 mm) was forced on the sample surface at a uniform rate of 10 seconds. The ball was maintained at this point for 5 seconds and released for the next 20 seconds to let the specimen recover. At the end of 20 seconds, the final reading was recorded as *F*. This measurement was made three times on three different points of the same sample surface equally apart from each other and at least 13 mm from the edge of the container. Resilience for each point was calculated by using Equation 3.1 and the mean of resilience values of the three points was taken as the resilience of the sample.

$$\text{Recovery, \%} = P + 100 - F \tag{3.1}$$

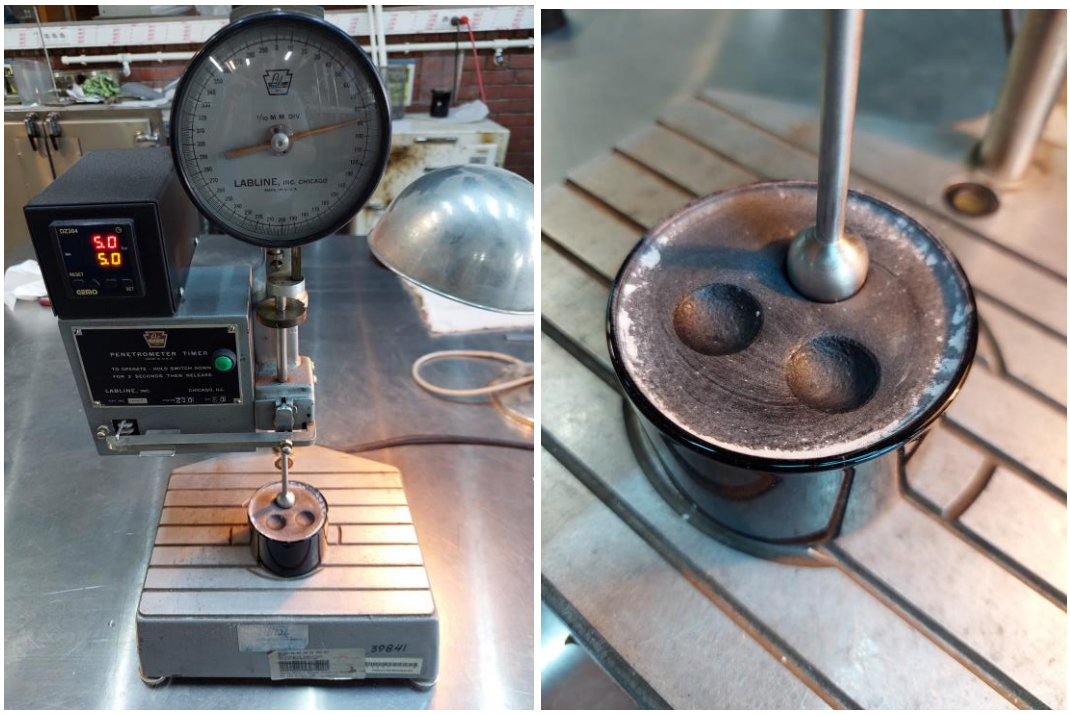

Figure 3.9. Resilience test.

3.5.1.4 Rotational Viscosity Test

Viscosity is one of the significant factors to evaluate base and CRMA binders, as it governs the workability of binder and mixing and compaction temperatures of hot mix asphalt. In this study, high-temperature rotational viscosity tests were conducted using a Brookfield RVDV-II+PRO viscometer (Figure 3.9a). The procedure is based on ASTM 4402. The measurement geometry and rotation rate were chosen as the spindle of #27 and 20 rpm, respectively based on studies in the literature (Xu et al., 2017; Li et al., 2019).

As the first step, the spindle, sample chamber (Figure 3.9b), and thermal chamber heater were preheated to a temperature a little higher than the test temperature considering temperature drops while transferring and pouring the sample. Then, the sample chamber was filled with approximately 10.5 g of sample and placed in the thermal chamber heater. The spindle was hung on the viscometer and lowered to

submerge in the sample. The temperature was allowed to stabilize to the test temperature and maintained for more than 10 mins. Following the temperature stabilization, viscosity measurement was started. The viscosity values were measured at 10 °C intervals between 130 °C and 180 °C. Finally, temperature-viscosity graphs were plotted using the data.

(a) (b)

Figure 3.10. (a) Brookfield viscometer, (b) sample chamber and spindle

3.5.2 Dynamic Shear Rheometer (DSR) Test

Compared to conventional test methods, DSR is a more advanced technique to evaluate the performance of asphaltic materials through rheological properties. In this study, rheological measurements of the samples were made by using Malvern Kinexus KNX2210 dynamic shear rheometer (Figure 3.10a). The plate diameter – gap values were adopted as 25 mm - 1 mm, 25 mm – 1 mm, and 8 mm – 2 mm for the measurement of unaged, short-term aged, and long-term aged CRMA binders, respectively, based on studies in the literature (Duan et al., 2021; Mashaan and Karim, 2013; Chen et al., 2019a). DSR samples were prepared by pouring the modified and unmodified asphalt binders into silicone molds (Figure 3.10b). Then,

the sample was loaded between preheated plates, and the excess material was trimmed (Figure 3.10c). When the system was ready, a temperature sweep test was carried out for each sample to determine the true grade temperatures. Temperatures providing the closest values to the limits in Equation 3.2, Equation 3.3, and Equation 3.4 define the true grade values.

$G^*/\sin\delta \geq 1.0$ kPa (unaged binder) (3.2)

$G^*/\sin\delta \geq 2.2$ kPa (short-term aged binder) (3.3)

$G^*\sin\delta \leq 5000$ kPa (long-term aged binder) (3.4)

→ High temp. true grade

→ Intermediate temp. true grade

Furthermore, a frequency sweep test was conducted using 21 frequency levels between 0.1 Hz and 10 Hz for each sample. It was repeated for 5 different temperatures (40 °C, 52 °C, 64 °C, 76 °C, 88 °C). Consequently, 105 complex shear modulus (G*) and phase angle (δ) values were obtained.

(a)

(b)

(c)

Figure 3.11. (a) The DSR used in this study, (b) a molded DSR sample, (c) a loaded and trimmed sample between plates of 25 mm.

3.5.3 Aging of Materials

In this study, the modified and unmodified asphalt binders were aged short-term and long-term using a Thin Film Oven Test (TFOT) and Pressurized Aging Vessel (PAV), respectively. Resultant aged binders were evaluated based on the mass change ratio and complex modulus aging index, CMAI (Equation 3.5). The mass

change ratio was determined for the unaged and TFOT samples as PAV cannot be used to obtain mass change. However, CMAI was determined for all the samples.

$$\text{CMAI} = \frac{\text{G*(aged)}}{\text{G*(unaged)}} \tag{3.5}$$

3.5.3.1 Thin Film Oven Test

For short-term aging, TFOT (Figure 3.11) was used instead of Rolling Thin Film Oven Test (RTFOT). The trials with RTFOT were failed as the CR particles hardly stayed in the bottles and spilled out. In addition, Subhy et al. (2018) used TFOT in their study and stated that as TFOT provides the same thickness for all samples (i.e., the same aging degree), it has an advantage over RTFOT when used for comparison purposes.

The procedure was carried out on ASTM D1754/D1754M "Standard Test Method for Effects of Heat and Air on Asphaltic Materials (Thin-Film Oven Test)". First, three flat-bottomed pans with 140 mm diameter and 9.5 mm depth were weighed, and each was filled with a hot sample of 50 ± 0.5 g around 135 °C for the base asphalt and 185 °C for the CRMA. The pans were allowed to cool at ambient temperature and weighed. Then, the pans were placed on the shelf in the preheated oven. After aging for 5 hours at 163 °C, the pans were allowed to cool at room temperature and weighed again to determine the mass loss. Next, the samples were heated back in the oven for 15 mins at 163°C and combined in a container. The container was maintained on a hot plate to prevent temperature drop, and the sample was stirred with a mixer for 10 mins before taking a sample for DSR and fluorescence microscopy.

Figure 3.12. TFOT oven.

3.5.3.2 Pressurized Aging Vessel (PAV)

PAV (Figure 3.12) was used to carry out the long-term aging of CRMA binders. The procedure was based on ASTM D6521 “Standard Practice for Accelerated Aging of Asphalt Binder Using a Pressurized Aging Vessel (PAV)”. First, the vessel, with the pan holder inside, was preheated to 100 °C. Then, the samples in the flat-bottomed pans, 140 mm in diameter and 9.5 mm in depth, were quickly placed in the pan holder. When the vessel temperature reached 100 °C back, a pressure of 2.1 Mpa was applied inside the vessel and the conditioning timing of 20 hours was started. After the conditioning time, the pressure was slowly released slowly. The pans were taken out of the vessel and maintained in an oven at 168 °C for 15 mins. Then, the samples were blended in a container and the container was placed in the preheated vacuum oven at 170 °C for another 15 mins. Next, the vacuuming was applied at 15 kPa for 30 mins. At the end of vacuuming, the containers were removed from the vacuum oven and the samples were stirred on a hot plate for 10 mins before the DSR and fluorescence microscopy samples were taken.

Figure 3.13. Vacuum oven (left) and PAV (right).

3.5.4 Fluorescence Microscopy (FM)

In this study, a fluorescence microscope (Zeiss LSM 510) equipped with a digital camera was utilized to investigate the effect of different CR modification (mixing time and mixing duration) levels of asphalt in terms of CR particle morphology and CR-asphalt interaction.

Samples were prepared by using the drop method. A small amount of the sample was dropped on a glass slide and covered with a cover glass. Then the sample was placed in an oven set to 135 °C for 3 mins to form a thin layer and allowed to cool at ambient temperature. Next, the gap between the glass slide and cover glass were sealed with duct-tape to prevent oxidation until the examination (Figure 3.13b).

(a) (b)

Figure 3.14. The fluorescence microscope used in this study, (b) a fluorescence microscope sample.

3.5.5 Methods Used for the Evaluation of Test Results

3.5.5.1 Analysis of Variance (ANOVA)

For the statistical analysis, analysis of variance (ANOVA) was utilized to determine whether the mixing time and mixing duration show a statistically significant difference in test results. This analysis was done for the penetration test, softening point test, viscosity test, resilience test, and true grade results. Since this study includes two factors (mixing time and mixing duration), two-way ANOVA without replication was used. The significance level (α) was chosen as 0.05. If a factor had P-value less than 0.05, it was accepted that the effect of the factor was statistically significant, otherwise not significant.

3.5.5.2 Master Curve

Master curve provides the viscoelastic properties (relaxation modulus, creep compliance, complex modulus, phase angle) of materials at a reference temperature over a broad range of time or frequencies. Thus, viscoelastic properties can be assumed at any temperature and over a broad frequency or time range (Papagiannakis and Masad, 2008; Booshehrian et al., 2013). In this study, master curves were used to evaluate the differentiations in the complex modulus (stiffness) and phase angles of CRMAs with changing modification levels. Master curves were constructed with the data obtained from the frequency sweep tests. The frequency sweep tests were performed at 21 frequency levels between 0.1 Hz and 10 Hz and 5 different temperature levels (40 °C, 52 °C, 64 °C, 76 °C, 88 °C). The reference temperature was taken as 64 °C. The master curves were established using Sigmoid fit in Equation 3.6 (MEPDG 2002, Rowe et al, 2009).

$$\log\left(G^{*}\right) = \delta + \frac{\alpha}{1+e^{\beta+\gamma(\log f_r)}} \tag{3.6}$$

Where G* is the complex modulus, δ is the minimum complex shear modulus, α is the difference between maximum and minimum complex modulus, and f_r is the reduced frequency (Hz). Moreover, β and γ are the shape parameters. While γ dominates on the steepness of the curve, β controls the horizontal turning point between the maximum and minimum complex modulus (Pellinen et al, 2004). Within this model, the upper part of the curve targets to reach to the maximum complex shear modulus.

CHAPTER 4

RESULTS AND DISCUSSION

4.1 Introduction

In this section, the results of the conventional tests, performance tests and 2D fluorescence microscope images will be analyzed. Eventually, it was aimed to analyze how mixing duration and mixing rate variables affect the intermediate and high temperature performance of the CRMA binders.

4.2 Evaluation of Conventional Test Results

4.2.1 Penetration Test

The penetration value of the base asphalt (B 70-100) is 72.33 as presented in Table 3.1 in the Materials and Method Section. Figure 4.1 demonstrates the penetration values of the samples prepared with different mixing rates and mixing durations determined in the design matrix. It is evident that crumb rubber modification reduced the base asphalt penetration value. According to ASTM D6114, it is required to have a minimum penetration of 25 and a maximum penetration of 75 for CRMA binders. Under all mixing duration and rate combinations analyzed in this study, all CRMA binders met the specification limits. Moreover, it can be highlighted that addition of CR decreases the penetration of the binder which leads to a more viscous resultant product. These results are in line with the phenomenon explained by Rahman (2004) and Jensen and Abdelrahman (2006) that is CR particles absorb the lightweight fractions of asphalt and leaving a denser liquid phase. Penetration values generally increases as the mixing time increases. In the same way, increasing mixing rate leads to rises of the penetration values. This can be a possible result of degradation of CR

particles with elevated mixing energy and duration. In addition, ANOVA output presented in Table B.4 has the p-values 0.014 and 0.000008 for the mixing rate and mixing duration, respectively. Since these values are smaller than the significance level ($\alpha = 0.05$), it can be said these two variables are statistically significant in terms of penetration. To summarize, it can be concluded that there is a trend between penetration and mixing duration. Typically, a higher penetration value indirectly indicates a lower stiffness modulus and hence, a higher fatigue resistance. Therefore, longer mixing duration or mixing rate could lead to a better fatigue resistance. However, this approach should be validated with further testing in the future studies.

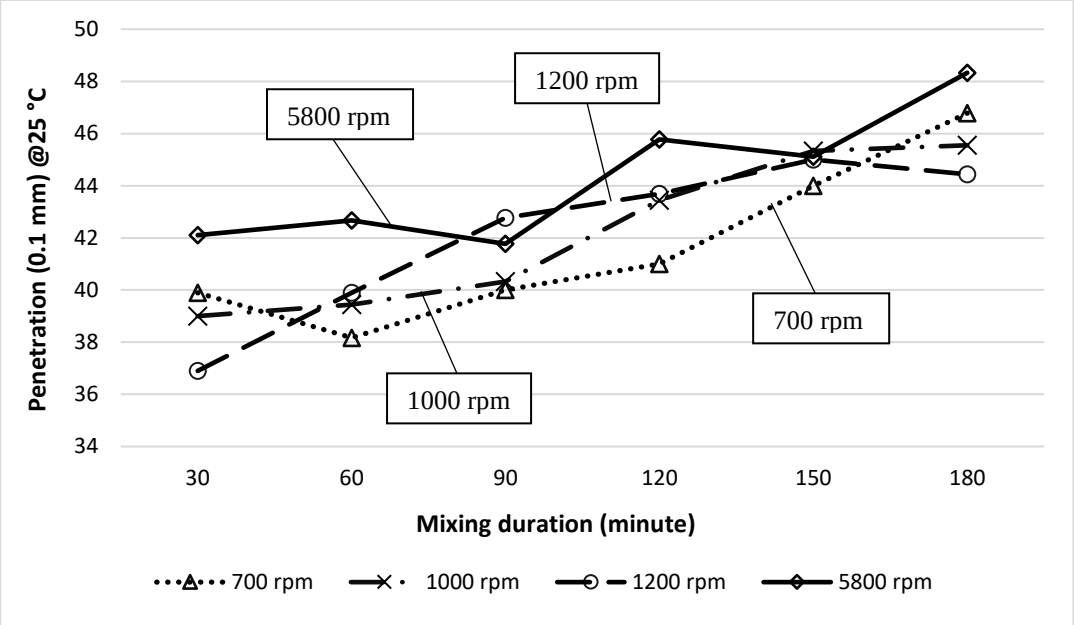

Figure 4.1. Penetration values for the design levels of mixing rate and mixing duration.

4.2.2 Softening Point

The softening point of the base asphalt is 46°C (Table 3.1). All the CRMAs presented in Figure 4.2 have higher softening point values than the base asphalt. Therefore, it can be inferred that CR modification enhances the temperature resistance of the asphalt which consequently provides a better rutting performance. It should be also noted that according to ASTM D6114, minimum softening point is expected as 52, 54 and 57 for cold, warm and hot regions, respectively. These limits were almost met for all CRMA binders, except for the binder with 700 rpm mixing rate and 30 minutes mixing duration. However, the softening point even for this binder was measured as 69.5. In terms of mixing rate and mixing duration, the softening point values at 5800 rpm (high shear mixing) are mostly lower than the values at low shear mixing rates up to 120 minutes, which is in line with penetration values. After 120 minutes the results don't follow a trend. However, the variation between the results for different mixing rates decreases after 120 minutes and follow a more stable state. When the overall results are considered, it can be anticipated that the lower softening point values are the possible results of the particle size decreasing due to higher mixing energy (5800 rpm). Moreover, the mixing duration doesn't have an exact correlation with the softening point results. However, the ANOVA output presented in Table B.5 suggests that the differences between the softening point values induced by the change in the mixing rate levels are not enough to make it a statistically significant variable with the p-value of 0.061 ($> \alpha = 0.05$). In the same manner, the mixing duration is also statistically insignificant with the p-value of 0.596 ($> \alpha = 0.05$) in terms of softening point.

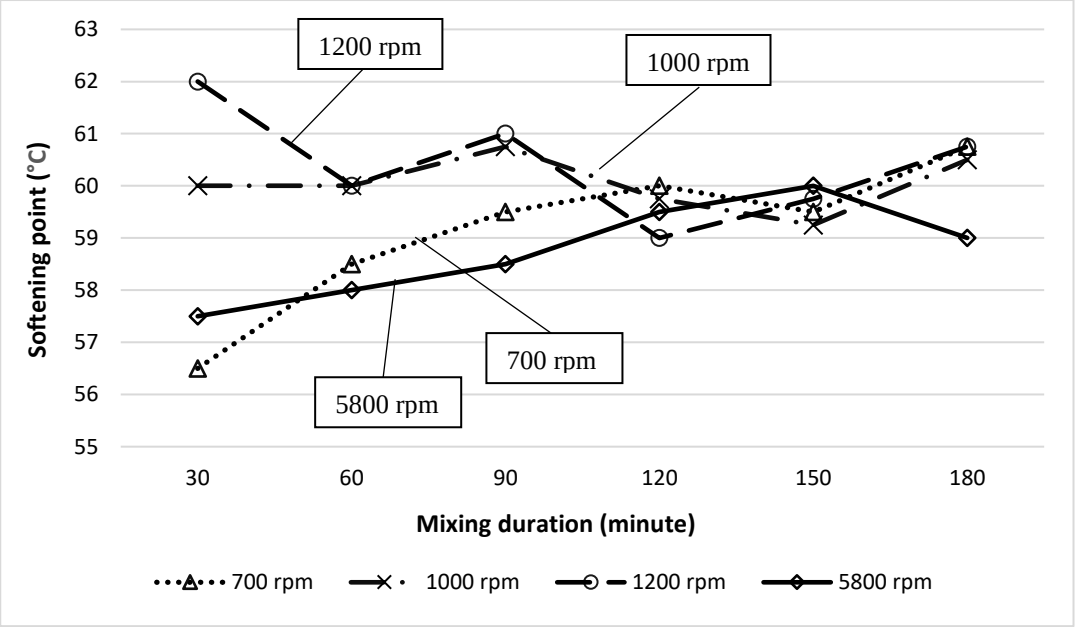

Figure 4.2. Softening point values for the design levels of mixing rate and mixing duration.

4.2.3 Resilience Test

The base asphalt has a resilience value of approximately 0 % (Fontes et al. 2006). However, rubber is a highly elastic material, and when the asphalt is modified with rubber, elastic properties of the asphalt is enhanced. Resilience is a significantly important parameter for CRMA binders and a measure of elasticity. Moreover, it gives an indication on the rutting and intermediate temperature fatigue-cracking susceptibility. According to ASTM D6114, the resilience is anticipated to be more than 25%, 20%, and 10% for hot, warm and cold regions, respectively. Figure 4.3 presents the change in resilience values of CRMA samples with regard to the different design levels of mixing time and mixing duration. The CRMA binders studied almost appropriate for all climatic regions, except for binders mixed for 30 minutes at a rate of 700 and 1000 rpm. It is revealed that 30 minutes interaction duration for the binder and CR was not enough for gaining adequate elasticity to be

used in road construction. On the other hand, it was observed that up to 90 minutes of mixing time, high shear mixing (5800 rpm) has the highest resilience while the lowest values are mainly obtained for 1000 rpm. While there is no trend among low shear mixing rates within the first 90 minutes, the resilience values are proportional with mixing rates between 90 minutes and 120 minutes. Increasing the mixing rate also increases the resilience of the CRMA. On the contrary, lower mixing rates provides higher resilience values after 120 minutes. In addition, the variation in the values decreases after 90 minutes and relatively a more stable trend is caught. Although the mixing duration mainly dominates the trend, the values don't differentiate by the change of mixing rate level. This fact is supported with the ANOVA output presented in Table B.6 that the p-values for the mixing rate and duration are 0.227 ($> \alpha = 0.05$) and 0.007 ($< \alpha = 0.05$), respectively. Therefore, mixing duration is a statistically significant variable while the mixing rate is insignificant in terms of resilience.

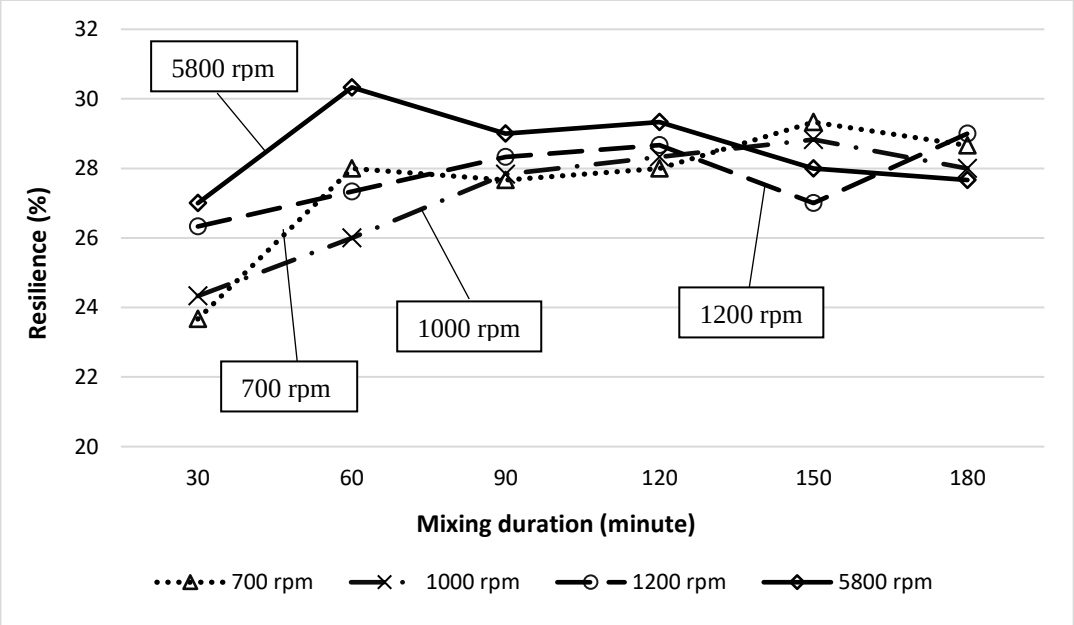

Figure 4.3. Resilience values for the design levels of mixing rate and mixing duration.

4.2.4 Viscosity Test

Viscosity is an important factor to consider while analyzing the CRMA as it governs the pumpability of asphalt binder and the workability and compaction properties of asphalt mixtures. Figure 4.4 demonstrates the Brookfield viscosity results for the base asphalt and CRMA samples prepared with the design mixing duration and mixing rate levels. It can be seen that modifying the base asphalt with CR increases the viscosity to around 10 times its original value. These results are in line with the findings in other studies such as Cong et al. (2013). As mentioned in Section **4.2.1**, this phenomenon is caused by CR particles that absorb the light weight fractions of asphalt and leave a dense; thus viscous, liquid phase. As the temperature increases, the difference between viscosities of CRMA binders decreases, whereas the difference is significant at lower temperatures. The viscosities at higher temperatures is essential for determining the pumping and mixing conditions, which are crucial for production, hauling and laying of asphalt mixtures. Thus, in order to compare the effect of mixing rates and durations at different levels, the viscosity results are given at a reference temperature of 175 °C in Figure 4.5. Figure 4.5 exhibits that increasing mixing rate decreases viscosity. It is the possible result of the process that CR particles degrade with increasing stirring energy, and the degradation accelerates with high shearing (5800 rpm). In terms of mixing duration, there is no trend for low shear mixing. However, the viscosity generally decreases with increasing mixing duration for high shear mixing (5800 rpm). However, this decrease is not in a substantial scale. These results are in accord with the ANOVA output shown in Table B.7 which represents the mixing rate as a highly significant variable with the p-values of 0.000002 ($< \alpha = 0.05$) and mixing duration insignificant with the p-value of 0.579 ($> \alpha = 0.05$) in terms of viscosity.

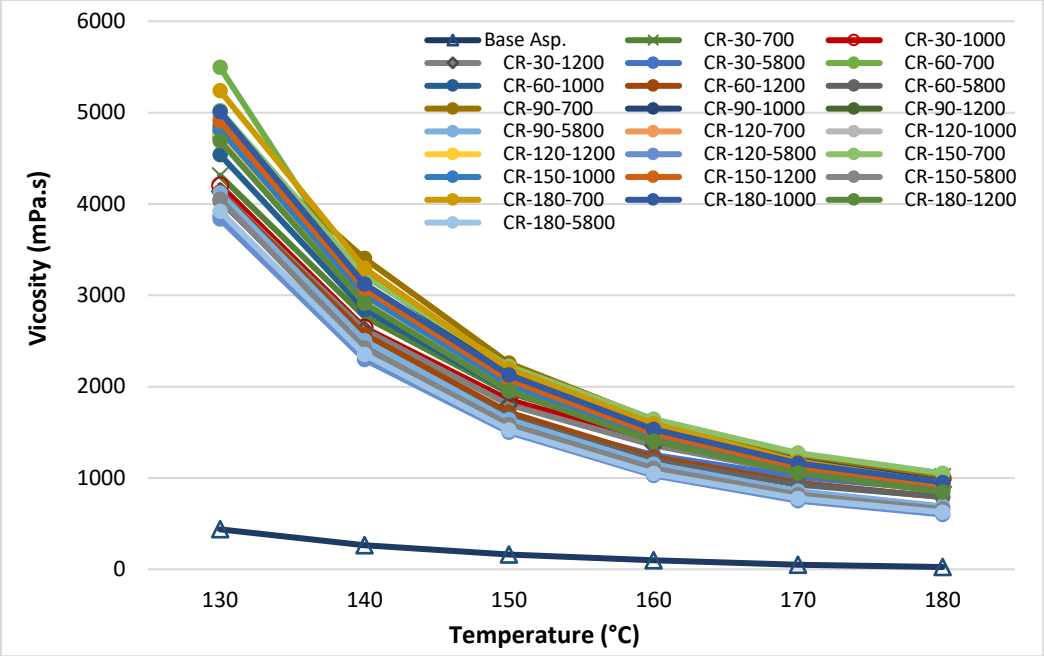

Figure 4.4. Brookfield viscosity values for the design levels of mixing rate and mixing duration.

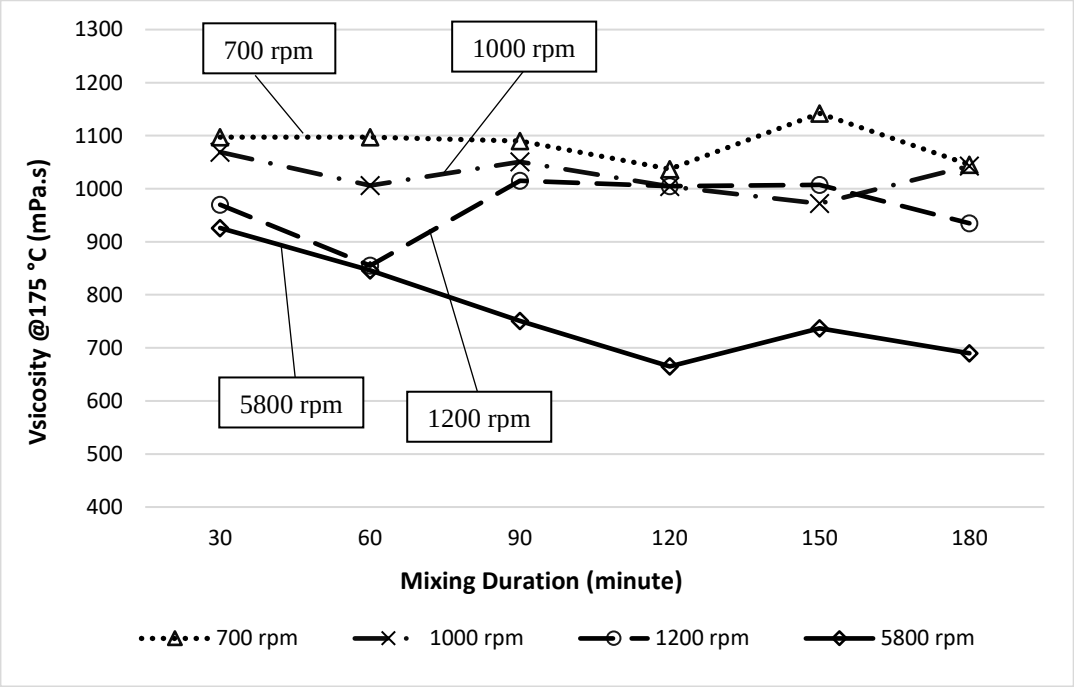

Figure 4.5. Viscosity values for the design levels of mixing rate and mixing duration at 175 °C

4.3 Evaluation of DSR Test Results

4.3.1 True Grade

High temperature true grade is defined as the maximum temperature providing the criteria of rutting resistance (G*/sinδ) given in Equation 3.2 and Equation 3.3 by of unaged and short-term aged asphalt. Intermediate temperature true grade defines the lowest temperature providing the criteria of fatigue cracking resistance (G*sinδ) given Equation 3.4 by long-term aged asphalt. Higher high temperature true grade can be obtained either for unaged or short-term aged asphalt as shown in the papers by Bennert (2013) and Ziari et al. (2016). In this study, higher values were obtained for the short-term (TFOT) samples. While determining the high temperature performance grade, AASHTO R29 instructs to accept the lower value. In this manner, TFOT true grades are used for comparison purposes. High temperature true grade of the base asphalt is determined to be 64.60 °C (Table 3.1). Figure 4.6 demonstrates the high temperature true grades for the CRMA binders prepared with different mixing durations and mixing rates. The values in Figure 4.6 show that CR addition increased high temperature true grade by increasing the complex shear modulus (G*) and decreasing the phase angle (δ) of the binders. In this regard, it can be assessed that CRMA has better rutting resistance than the unmodified asphalt. Therefore, it allows the binder to function in the regions with higher temperatures. In terms of mixing rate and duration, the samples prepared with high shear mixing (5800 rpm) has lower true grade than the one prepared with low shear mixing. It could be due to the degraded rubber particles. As the gradations gets finer, it slightly lowers the high true performance grade of the binder. This finding overlaps with the results of Plemons (2013). Furthermore, there is no trend for the lower shear mixing rates up to 120 minutes. After 120 minutes, the true grade decreases with the increasing mixing rates. However, the differences between the values of low shear

mixer rates are not significant while the difference between the low shear mixing and high shear mixing is explicit. The same findings are supported with the ANOVA output shown in Table B.8. The mixing rate with the p-value of 0.003 ($< \alpha = 0.05$) is found statistically significant; whereas the mixing duration with the p-value of 0.579 ($> \alpha = 0.05$) is not a statistically important variable in terms of high temperature true grade.

According to the findings up to this stage of study, it is revealed that the significance between mixing rates (700 rpm, 1000 rpm and 1200 rpm) is not significant based on the physical tests and high true temperature grades of the crumb rubber binders. Thus, the experimental matrix in terms of mixing rates is reduced to 1000 rpm and 5800 rpm. Furthermore, intermediate true grades were measured on the PAV samples prepared with low shear mixing of 1000 rpm and high shear mixing of 5800 rpm. Figure 4.7 exhibits intermediate true grade results. Intermediate true grade for the base asphalt was found as 21.30 °C (Table 3.1). As seen from Figure 4.7, CRMA samples has lower intermediate true grades. The lower temperatures provide the higher complex shear modulus (G*) and the lower phase angle (δ) values. Therefore, it can be inferred that CR modification slightly increase the fatigue cracking resistance of the asphalt. As for mixing rate and duration, the values for 5800 rpm mainly follow a lower trend compared to 1000 rpm with an exception of 90 minutes. After 120 minutes, the results for 1000 rpm reach a more stable state. However, no trend can be observed in terms of mixing duration overall. Based on the ANOVA output presented in Table B.9, the mixing rate has the p-value of 0.623 ($> \alpha = 0.05$). Therefore, the difference between the two levels of mixing rate is not enough to make it statistically significant. Moreover, the mixing duration is also found insignificant with the p-value of 0.881 ($> \alpha = 0.05$).

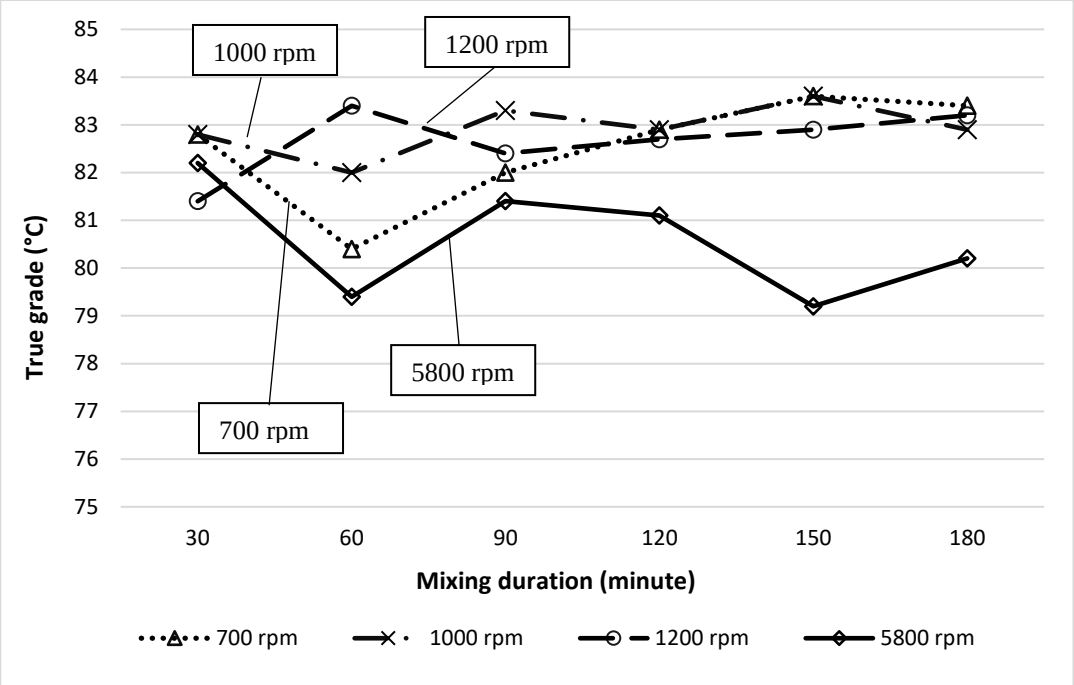

Figure 4.6. High temperature true grade values for CRMA binders with different mixing rates and mixing durations.

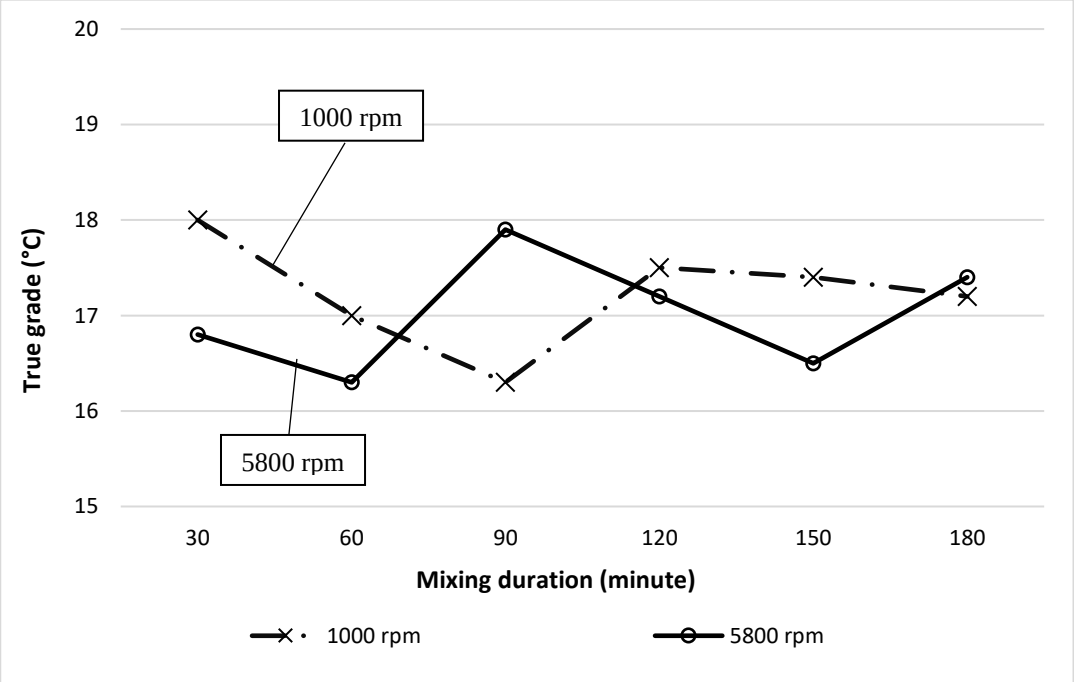

Figure 4.7. Intermediate temperature true grade values for the design levels of mixing duration and mixing rate of 1000 and 5800 rpm.

4.3.2 Complex Modulus Aging Index (CMAI)

In order to evaluate the aging performance of CRMA, and how the variables of mixing rate and duration affect this performance, CMAI was utilized. Each CMAI was determined using Equation 3.5. It is basically the ratio of the complex modulus of aged sample to unaged sample. The complex modulus values were obtained through the temperature sweep tests at 10 rad/s. Figure 4.8 presents the CMAI values for all CRMA combinations in terms of short-term aging (TFOT). It is observed that all CRMA samples have lower CMAI values than the base asphalt. This result is in line with the study finding by Wang et al. (2020) that is CR introduction decreases the oxidation products in the binder. Based on these results, it can be inferred that CR modification decreases the aging degree of asphalt during the hot mixture asphalt production and the road construction. In regard to mixing duration and mixing rate, variation in aging degree between the combinations at 40 °C mainly decreases as the temperature increases; therefore, the lowest variation happens at 88 °C. Figure 4.9 shows the CMAI results for different levels of mixing rate. The results show that increasing the mixing rate decreases the CMAI; thus, improves the aging resistance. However, the difference is not significant between 700 rpm and 1000 rpm. Furthermore, Figure 4.10 demonstrates the CMAI results obtained at different levels of mixing duration. Up to a point between 52 °C and 64 °C, increasing mixing duration decreases the CMAI with exception of 30 and 60 minutes. However, the difference for these durations is not much. After this point, a correlation between mixing duration and aging cannot be observed. For short-term aging, it can be concluded that adjusting both mixing duration and rate can improve the aging resistance of CRMA.

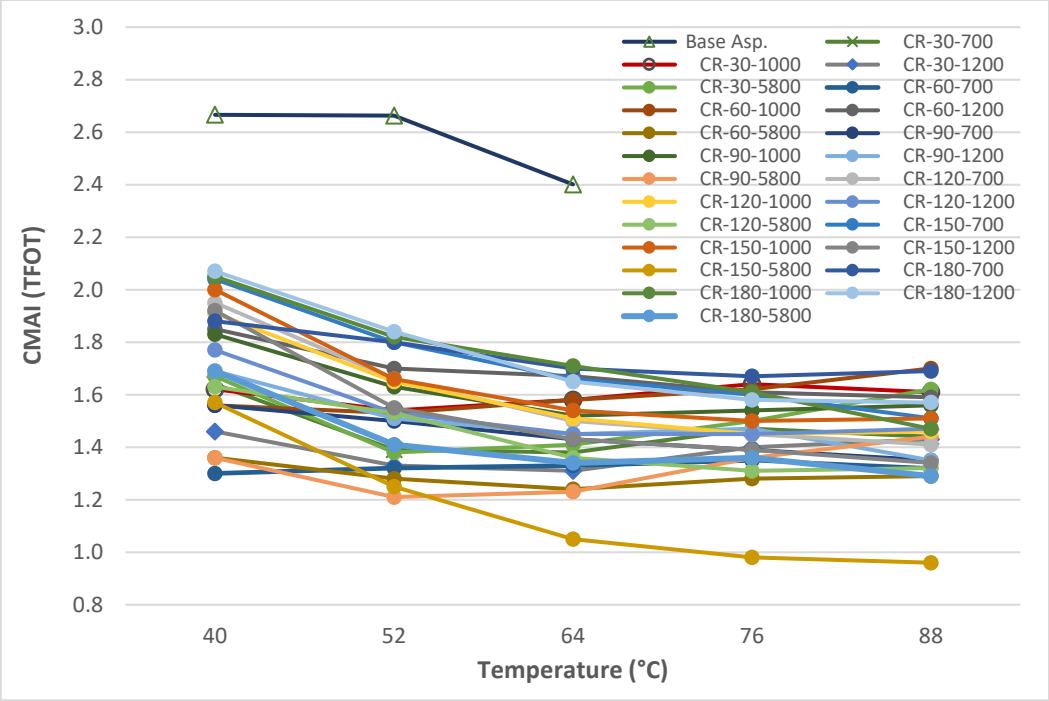

Figure 4.8.CMAI values for short-term aging for the design levels of mixing rate and mixing duration.

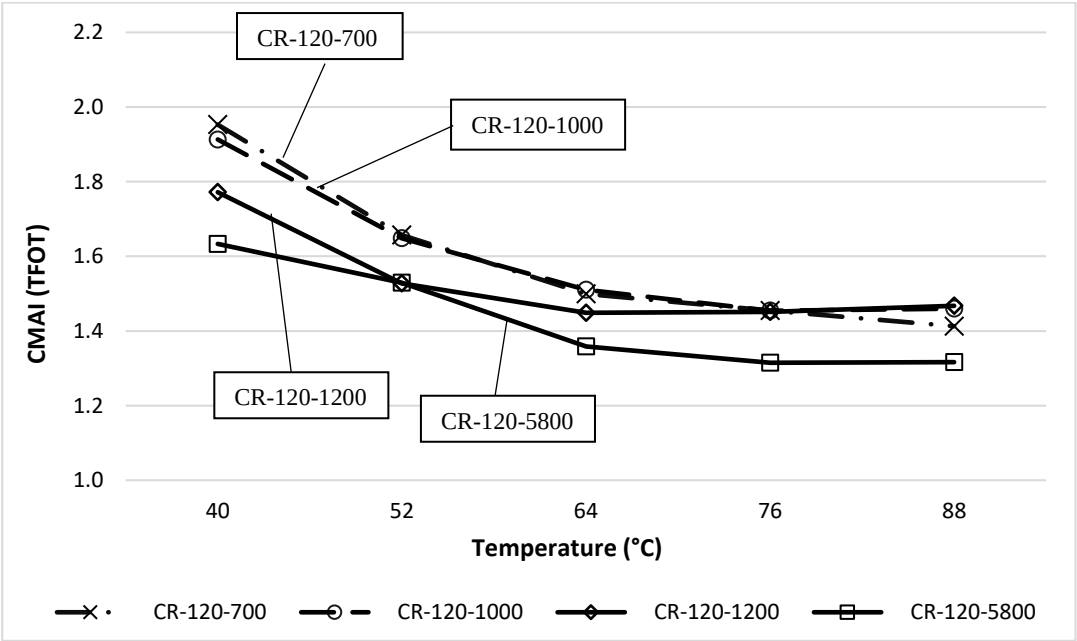

Figure 4.9. CMAI values for short-term aging at different mixing rates and fixed mixing duration of 120 minutes.

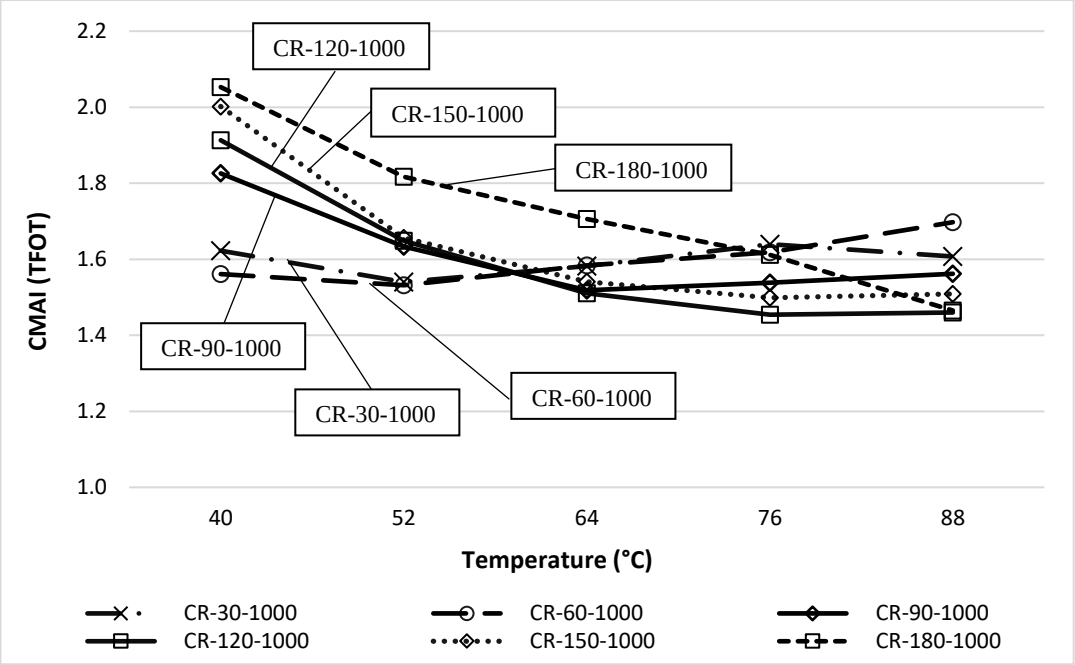

Figure 4.10. CMAI values for short-term aging at different mixing durations and fixed mixing rate of 1000 rpm.

As for the long-term aging, CMAI values are given in Figure 4.11. CMAI index for the base asphalt increased five times to its TFOT value while it is around three times for the CRMA samples. Therefore, CR modification keeps delaying the aging of the binder during its service life. Compared to TFOT CMAI values, PAV CMAI values show less variation and more stable. In regard to mixing time and duration, the high shearing (5800 rpm) decreases the aging phenomenon compared to low shearing (1000 rpm) as seen in Figure 4.12. Even more difference is observed at higher temperatures. As Figure 4.13 exhibits, the highest aging takes place for 120 minutes whereas the lowest is for 90 minutes. For the rest of mixing duration levels, a trend is not noted. These results indicate that there is no correlation between the mixing duration and aging degree as observed in the TFOT CMAI results.

All in all, mixing rate has an enhancing effect on the aging of modified samples while the effect of mixing duration mostly doesn't show an explicit correlation.

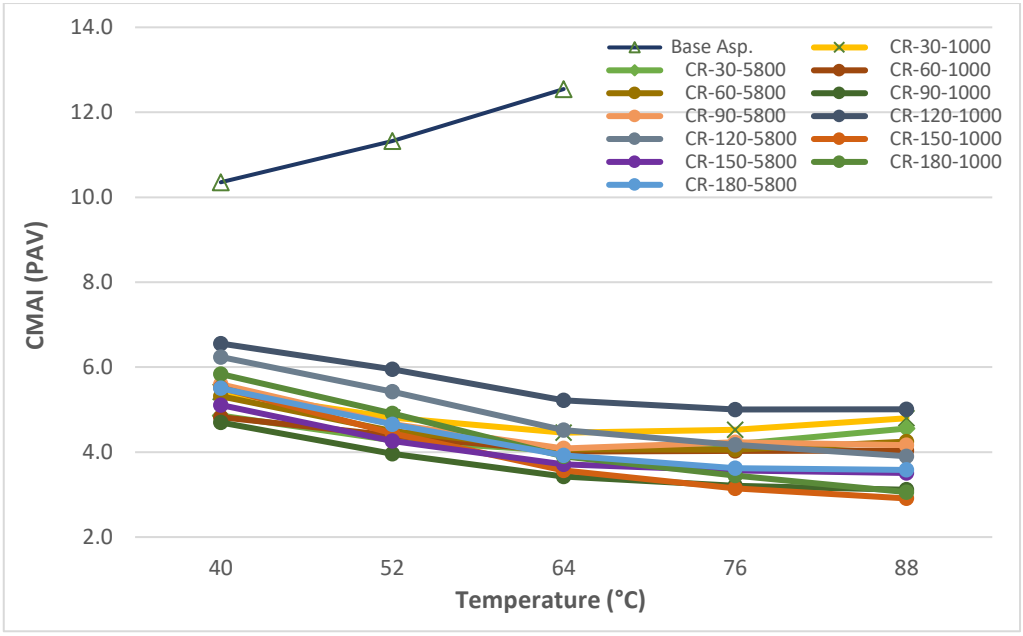

Figure 4.11.CMAI results for long-term aging at the design levels of mixing rate and mixing duration.

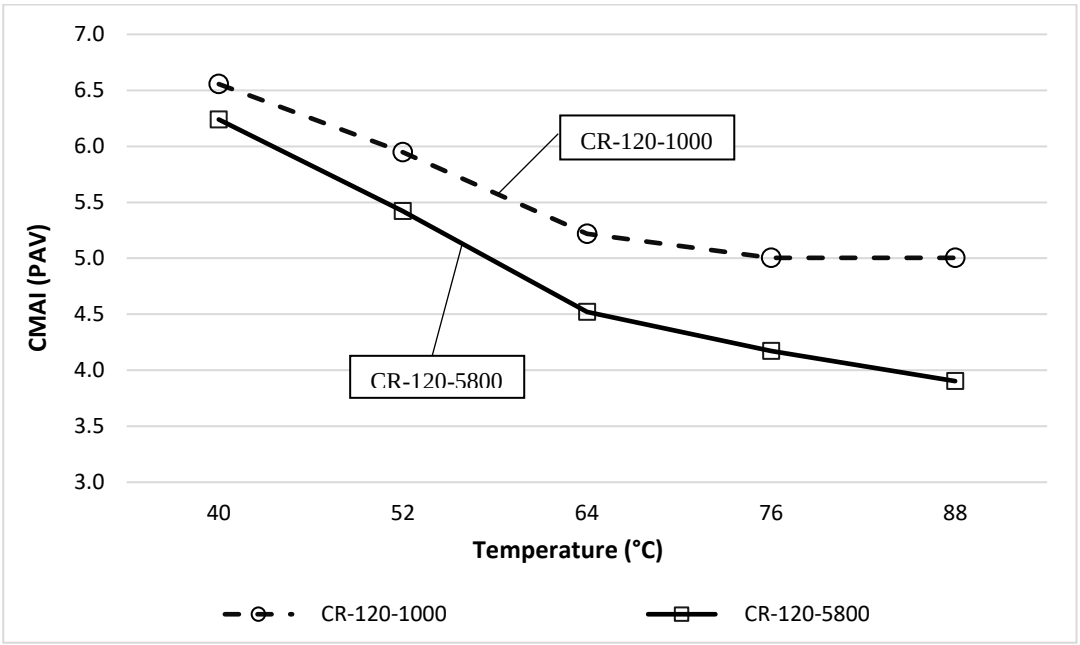

Figure 4.12. CMAI results for long-term aging at different mixing rates and fixed mixing duration of 120 minutes.

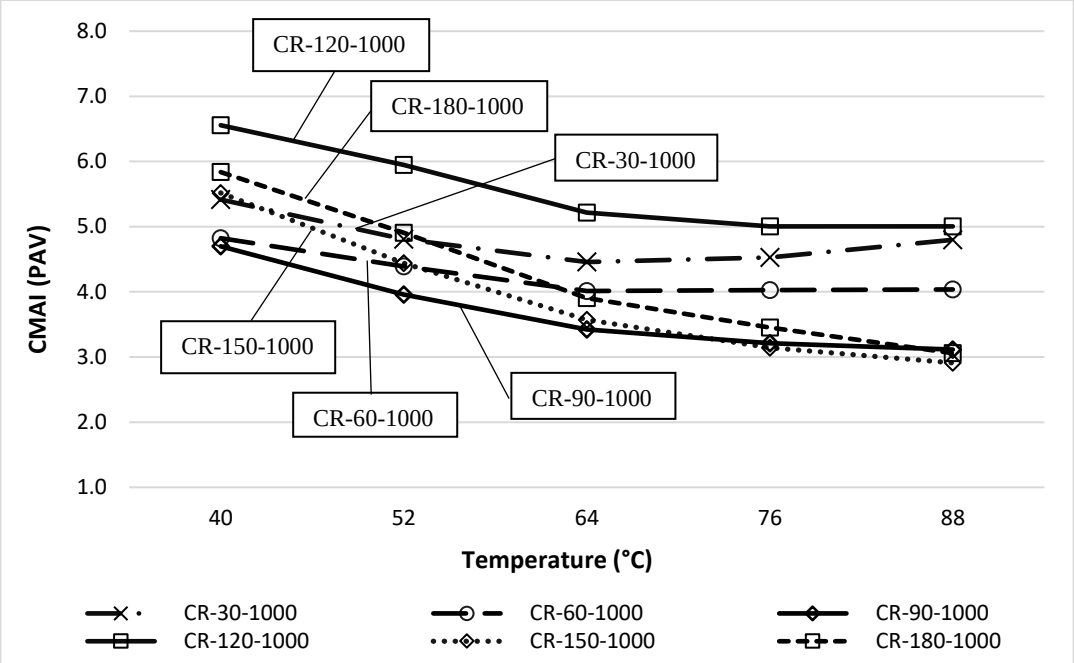

Figure 4.13. CMAI results for long-term aging at different mixing durations and fixed mixing rate of 1000 rpm.

4.3.3 Master Curves

Master curves were constructed to analyze the rheological behaviors of the binders in a wide range of frequencies and temperatures before and after laboratory short-term and long-term aging. From Figure 4.14 to 4.18 present master curves constructed with Sigmoid fit at a reference temperature of 64 °C. Figure 4.14 exhibits the comparison of CRMA binders at different mixing rates for each mixing duration. These curves suggest that there is only a slight difference between the complex modulus values of mixing rates at low frequencies (high temperature) for 30 minutes of duration. The highest value was obtained for 700 rpm whereas the lowest value belongs to 1200 and 5800 rpm. Therefore, increasing mixing rate slightly decreases stiffness of the binders. However, this slight difference is not apparent for the higher frequencies for 30 minutes and at any frequencies for the rest of mixing durations.

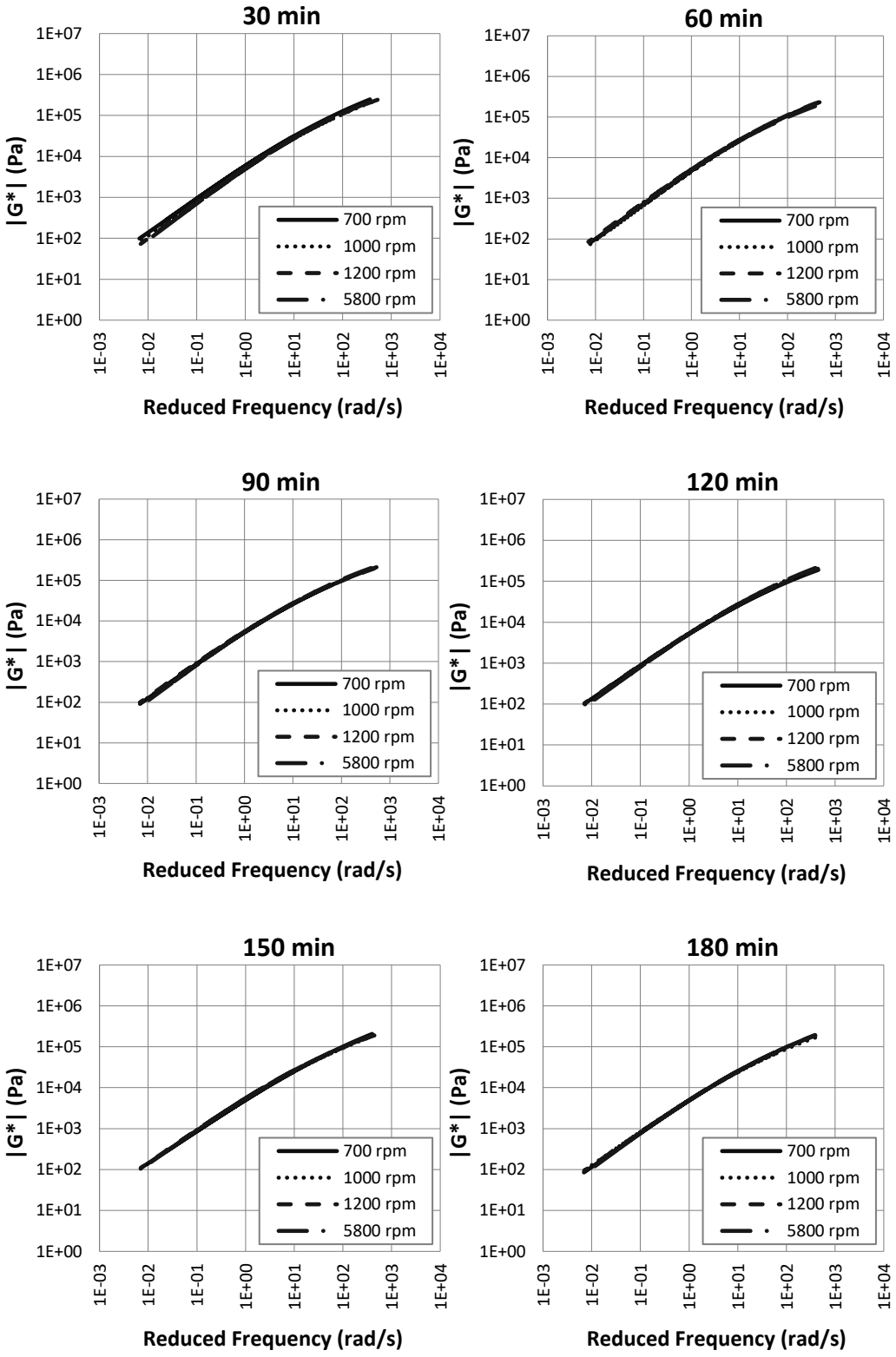

Figure 4.14. Master curves for unaged samples at the design levels of mixing rates for each mixing duration.

These results claim that, mixing rate doesn't have a significant effect on the rheological properties of the unaged CRMA binders in a broad range of temperature and frequencies.

Master curves constructed for short-term aged (TFOT) modified binders at different mixing rates for each mixing duration are demonstrated in Figure 4.15. Compared to unaged CRMA binders, some divergence appears between the curves of mixing rates mainly up to 90 minutes which is in line with the CMAI results in which mixing rate affected the aging degree. However, the difference between the curves for each mixing levels is still not in significant level and there is no a pattern. Based on the results, it can be assessed that mixing rate doesn't have a significant effect on the stiffness of CRMA binders investigated in a wide range of temperature and frequencies.

For long-term aged (PAV) modified binder, comparison is made between low-shearing (1000 rpm) and high shearing (5800 rpm). The relevant master curves plotted for these two shearing levels are presented in Figure 4.16. As observed in the unaged and TFOT samples, increasing the intensity of the mixing rate doesn't make a major influence on the rheological properties of the modified binders. However, some partial divergences are noted in small degrees as in the TFOT samples. Different from the TFOT, these divergences mainly appear at low frequencies (high temperatures) which totally fades at the duration of 180 minutes. In addition, the higher value shifts for the level of mixing rates at each temperature. Therefore, an explicit trend is not noted.

In order to investigate the rheological differences between the unaged, TFOT, and PAV samples of the modified binders in regard to low (1000 rpm) and high (5800 rpm) shearing rates, the master curve graphics in Figure 4.17 are constructed. From these graphics, it is observed that the curves for the PAV samples explicitly separates with higher complex modulus values from the ones for the unaged and TFOT samples at both shearing rate levels. In addition, the curves for the PAV samples follow a relatively straight line throughout the wide range of the frequencies.

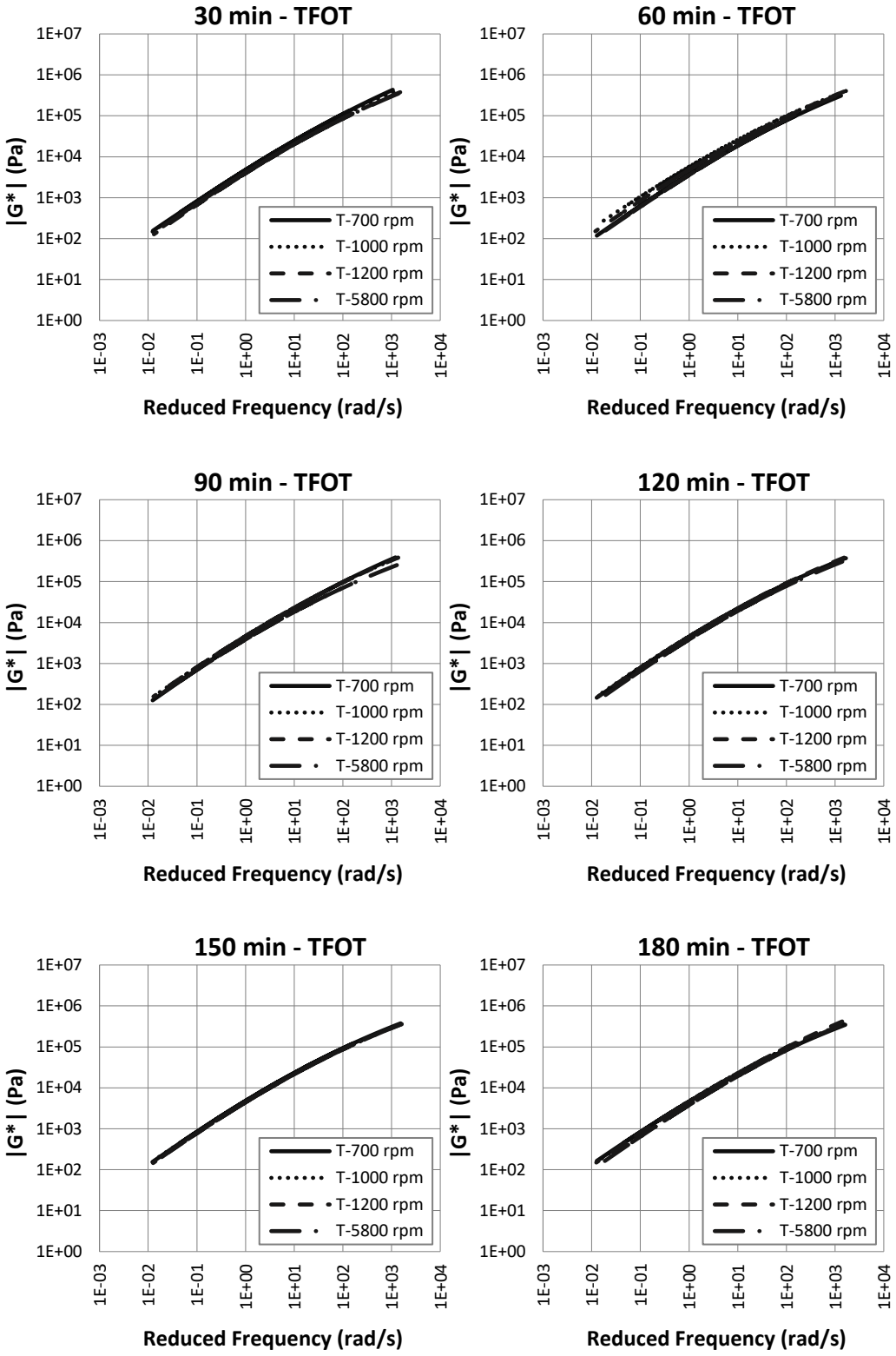

Figure 4.15. Master curves for TFOT samples at the design levels of mixing rates for each mixing duration.

Therefore, stiffness of the PAV samples is less dependent on the loading frequencies compared to the unaged and TFOT samples. On the other hand, a major difference between the complex modulus values for the unaged and PAV samples doesn't appear for the both low and high sharing levels. However, the curves for TFOT samples slightly diverge mainly with lower complex modulus values from the ones for the unaged samples at the different parts of frequencies for the high shearing rate. This result is accord with the findings that high shear mixing has lower CMAI values; thus, the lower degree of aging. In addition, the results are in line with the study by Subhy et al. (2018) in which the aged samples of the some CRMA binders prepared with high shear mixing has lower following master curves at some frequencies. The overall results suggest that rheological properties of CRMA samples are not significantly influenced in short-term aging. However, the major changes happen in the long-term aging duration.

Furthermore, the influence of the mixing duration on the rheological properties of the CRMA binder was analyzed through the master curves presented in Figure 4.18. For the unaged and TFOT, overlapping curves indicate that rheological properties of the CRMA binders are not significantly dependent on the mixing duration. In terms of PAV samples, the curves for mixing durations of 30 and 120 minutes slightly diverge from the rest of the curves with lower complex modulus values at low frequencies (high temperatures). And this divergence is more notable for 1000 rpm than 5800 rpm.

All in all, it can be concluded that both the variables of mixing duration and mixing rate don't influence the rheological properties of the CRMA binders when investigated in a wide range of temperature and loading frequency. Furthermore, the only major differentiation is observed for the long-term aging (PAV) samples. It can be assessed that CR modification of asphalt considerably lowers the effect of short-term aging.

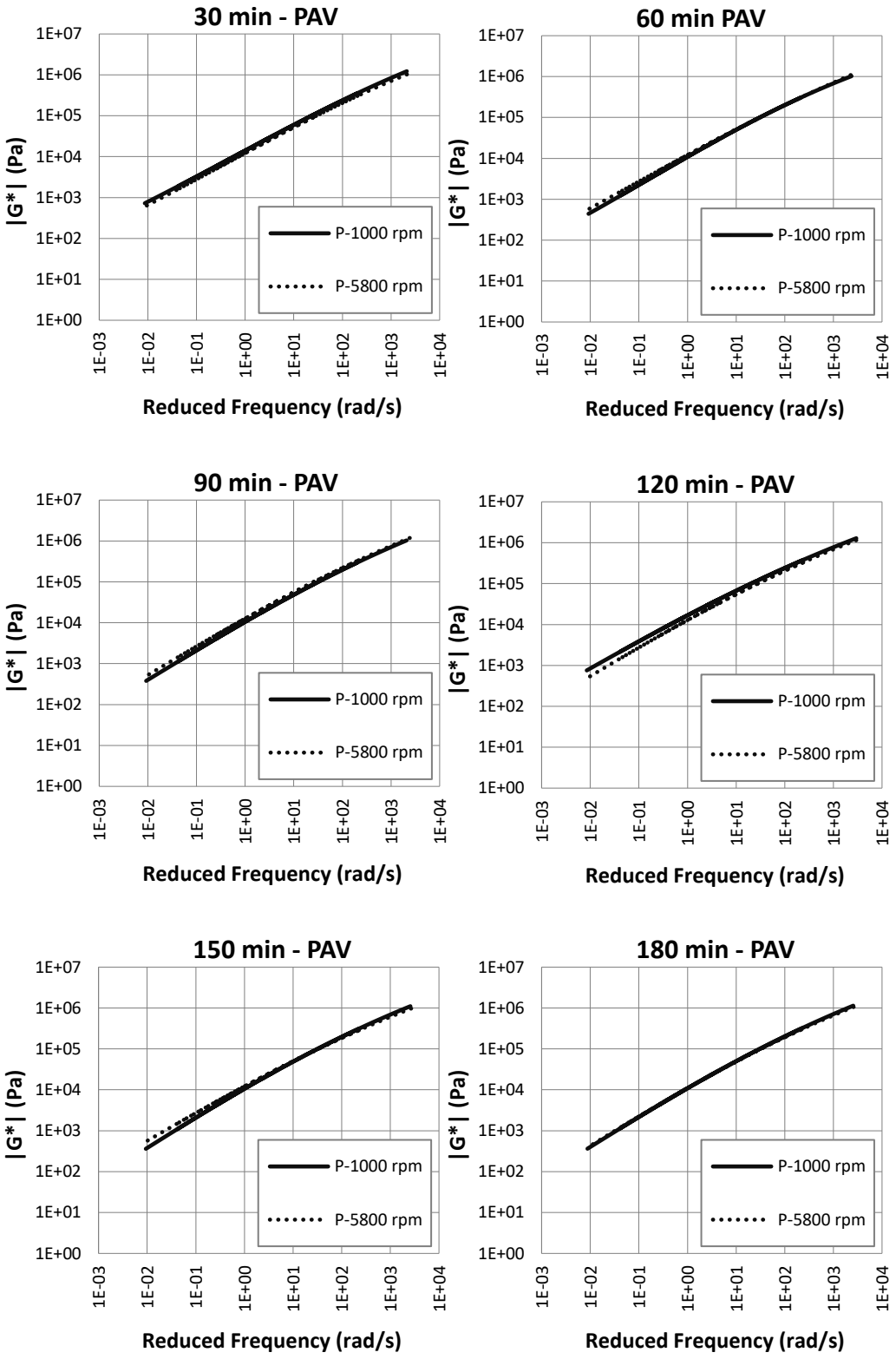

Figure 4.16. Master curves for the PAV samples at the mixing rates of 1000 and 5800 rpm for each mixing duration.

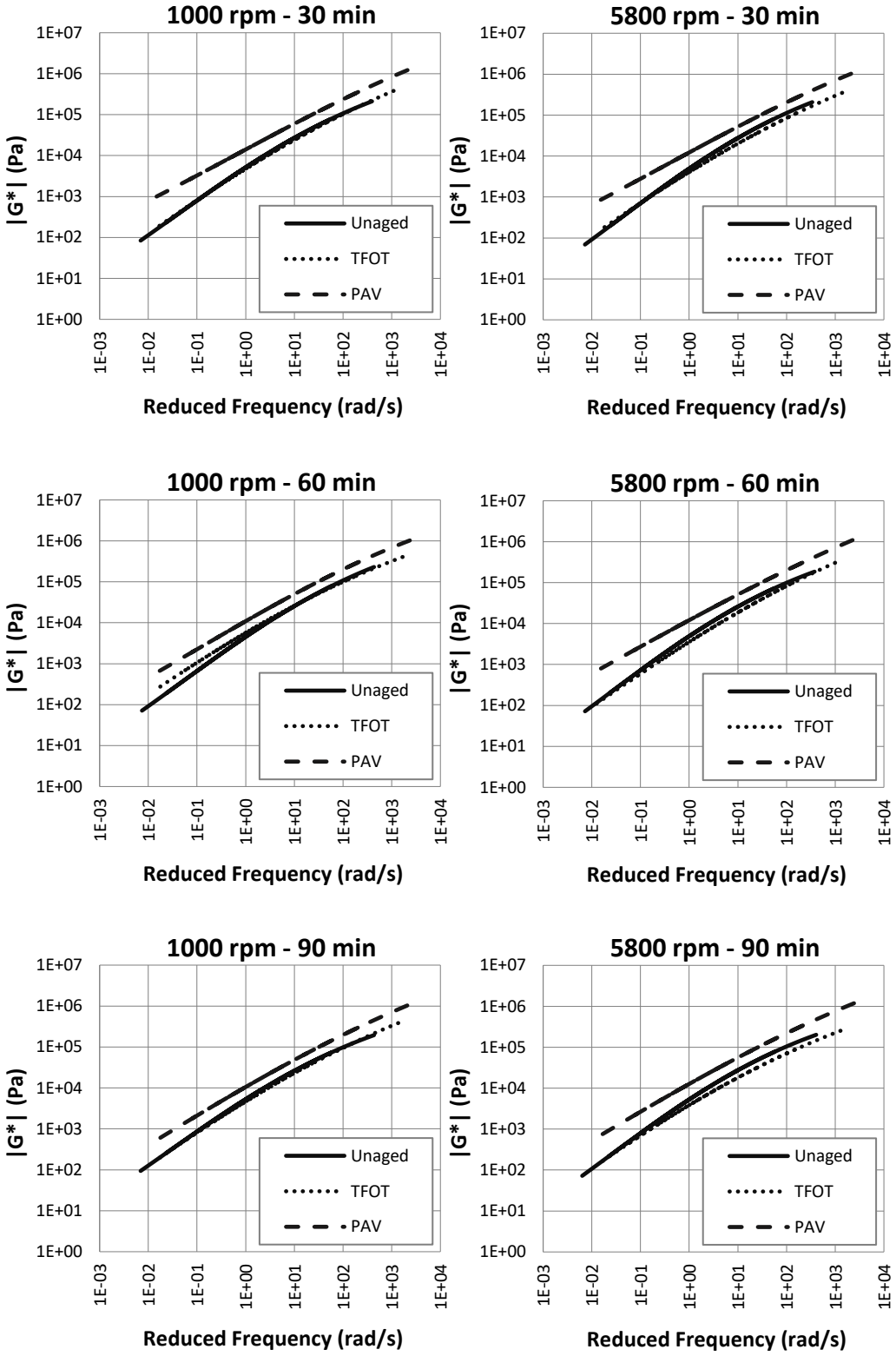

Figure 4.17 Master curves for the unaged and aged samples at the mixing rate of 1000 and 5800 rpm for each mixing duration

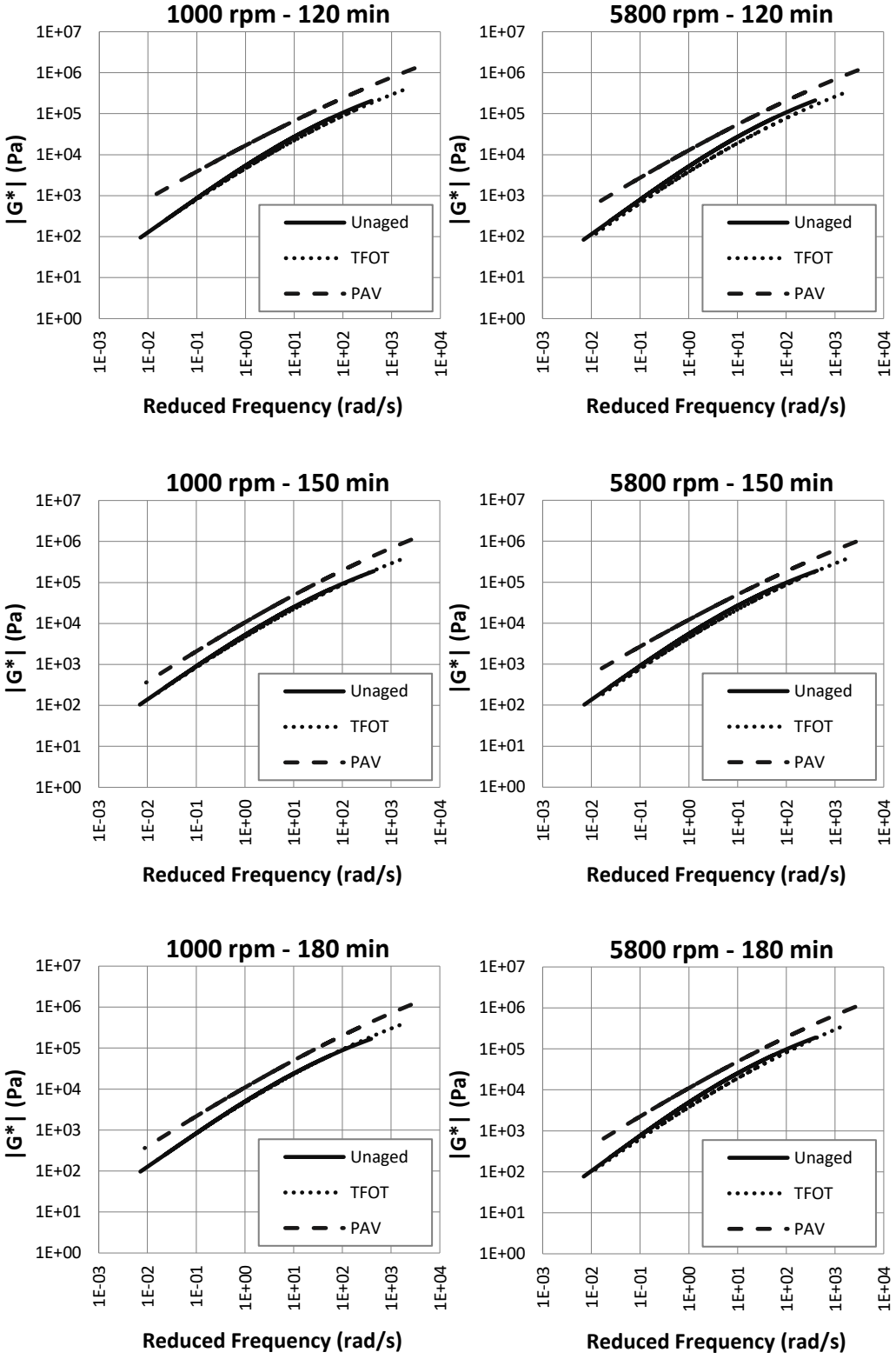

Figure 4.17. (Continued)

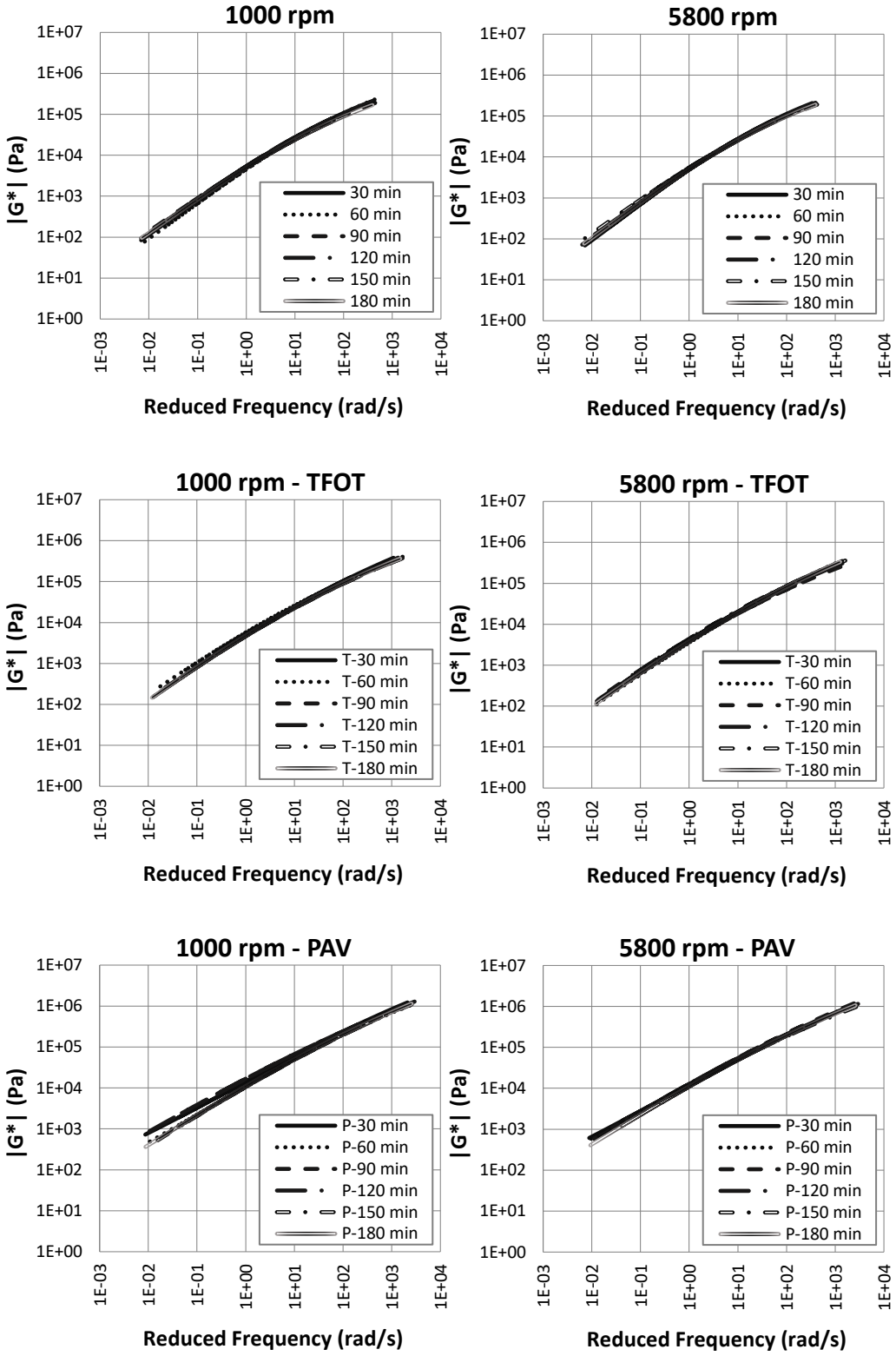

Figure 4.18. Master curves for the unaged and aged samples at the design levels of mixing duration for the mixing rate of 1000 and 5800 rpm.

4.4 Fluorescence Microscope Analysis

Fluorescence microscope was employed as a further evaluation method additional to conventional and advance performance tests. 2D images obtained through the fluorescence microscope are demonstrated from Figure 4.19 to 4.21. For each combination, the whole sample area was scanned by receiving around 80 fluorescence microscope images, and the images representing the common CR particle conditions for these combinations were chosen for the comparison purposes. Figure 4.19 shows the comparison of mixing rate levels and the aging affect. Maltenes (mainly aromatics) are the fractions that emit the most intensive fluorescence in the asphalt (Handle, 2016). It is observed the intensive fluorescence gathers around the CR particles which indicates the absorption of the light fraction of asphalt by CR particles. When the images for 1000 rpm and 5800 rpm are compared, smaller sized CR particles appears in the image for 5800 rpm. It shows high shearing changes the morphology of CR particles by reducing their sizes. As a result, it can shorten the minimum required time for the CR – asphalt interaction. Furthermore, the intensity of the fluorescence around the CR particles diminishes for the TFOT samples. It can be the possible result of oxidation during the aging process. However, it doesn't totally fade. It can be inferred that CR preserves some of the light fractions against the oxidation. Figure 4.20 and 4.21 show the fluorescence microscope images for each duration level at 1000 and 5800 rpm. There is no any significant difference observed throughout the mixing durations for both 1000 rpm and 5800 rpm in terms of fluorescence intensity around CR particles. The images suggest that increasing the mixing duration doesn't have a significant influence on the CR particles or the interaction between CR and asphalt.

When the utilizing of fluorescence microscopy on the assessment of the CRMA is considered, it can be noted that fluorescence microscopy is useful to monitor the changes in the CR morphology and the interaction between CR and asphalt. However, it doesn't present the total picture of the mixture as it only receives images from limited small areas. Therefore, it cannot be used to investigate the distribution

of the CR particles in the asphalt. Furthermore, the findings must be supported by chemical analysis to robust the analysis.

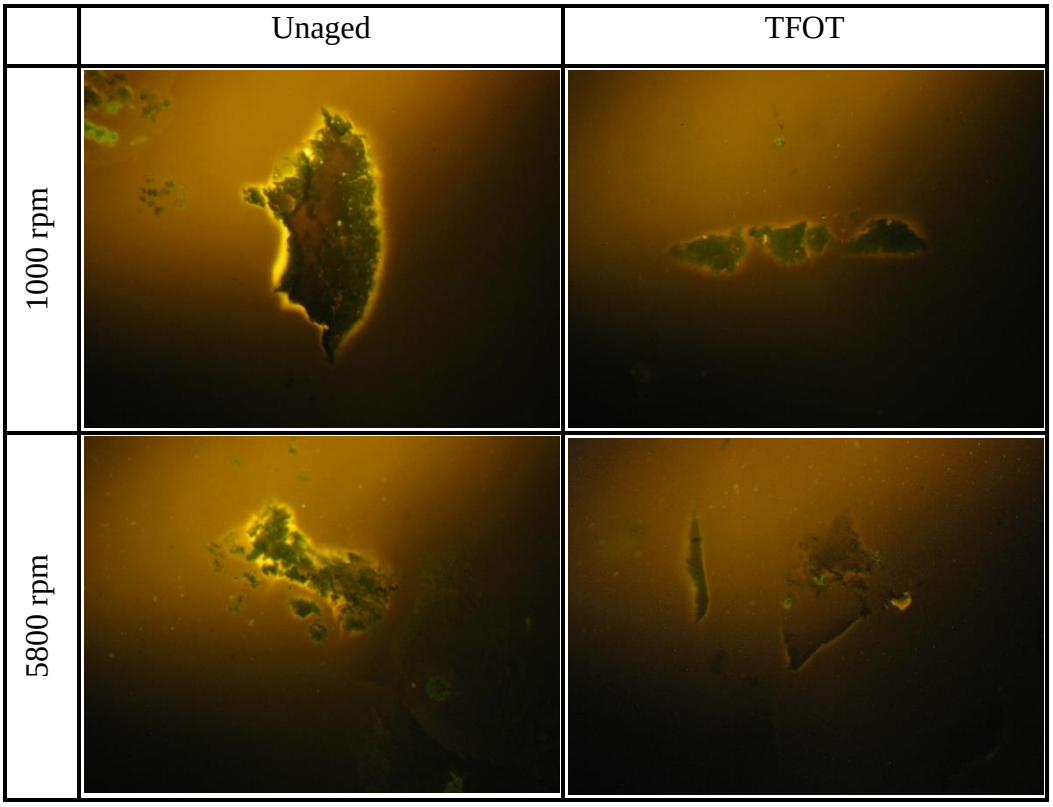

Figure 4.19. Fluorescence microscope images for the unaged and TFOT samples at mixing duration of 120 minutes and mixing rate of 1000 rpm and 5800 rpm.

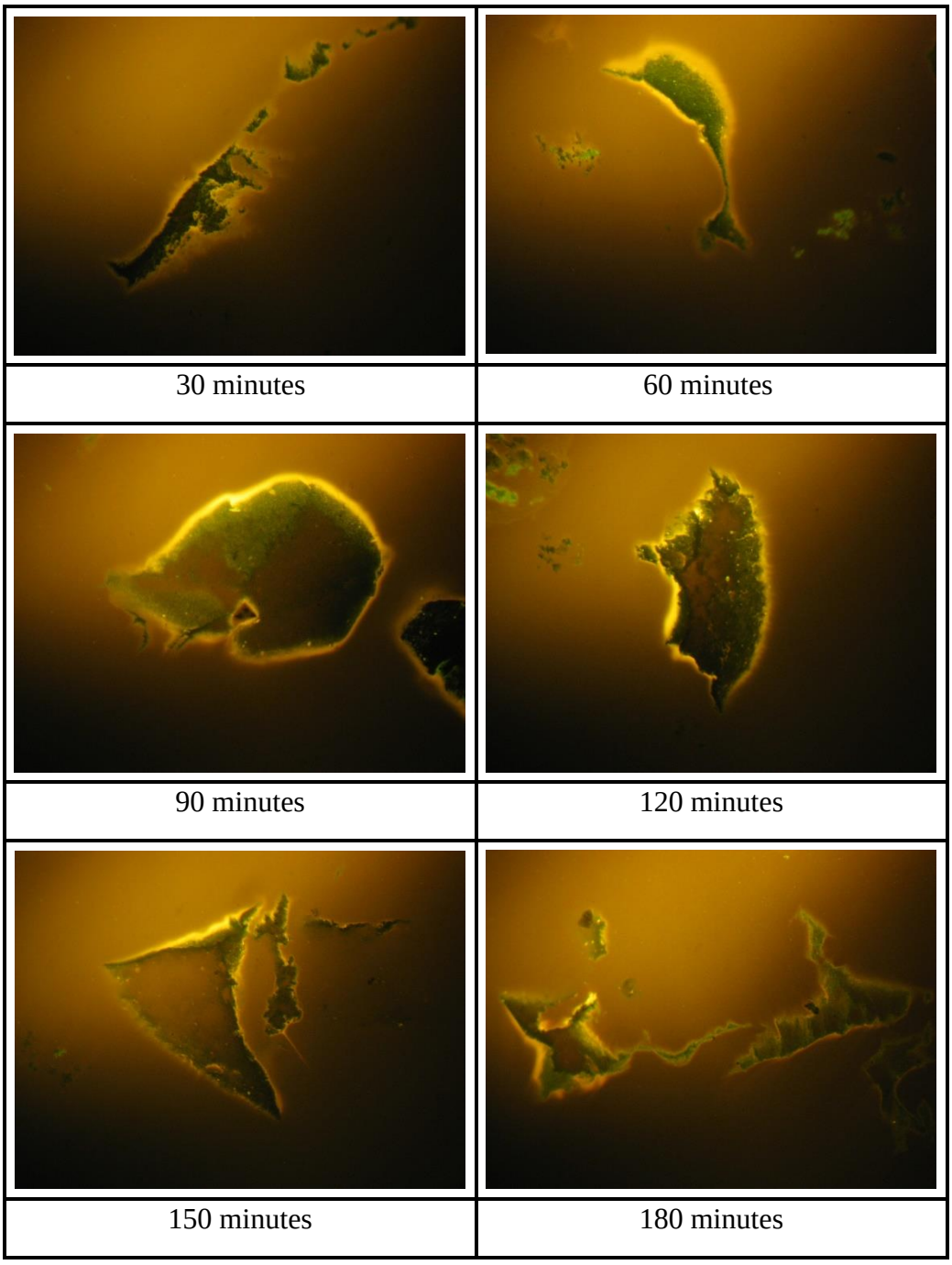

Figure 4.20. Fluorescence microscope images for each mixing duration level at mixing rate of 1000 rpm.

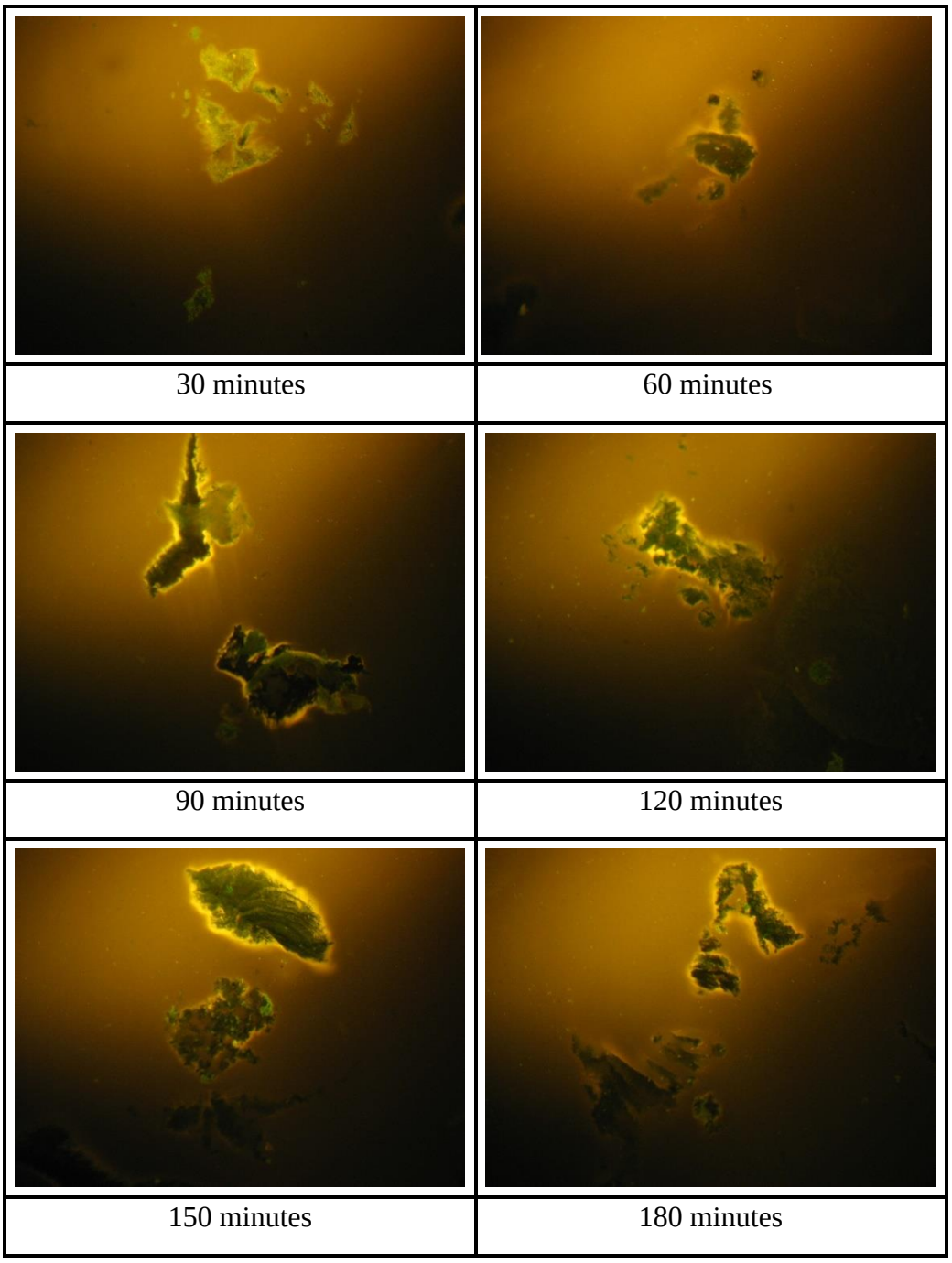

Figure 4.21. Fluorescence microscope images for each mixing duration level at mixing rate of 5800 rpm.

CHAPTER 5

CONCLUSIONS AND RECOMMENDATIONS

5.1 Introduction

In this section, the considerable findings of this study are summarized. The results are concluded in terms of engineering and general contribution. In addition, future studies are recommended to extend the insight about the effect of the mixing rate and duration on the performance of crumb rubber modified asphalt (CRMA).

5.2 Conclusions

Within the scope of this experimental study, two crumb rubber (CR) asphalt modification variables (mixing duration and mixing rate) were investigated to understand their effect on the intermediate and high temperature performance of the resultant product (CRMA). For this purpose, CRMA samples were prepared by using 6 mixing duration and 4 mixing rate levels. The rest of variables were kept fixed since the effect of these variables were mainly revealed by the previous studies. The constant variables were selected based on these previous studies. Furthermore, the physical and performance related properties of these samples were analyzed on unaged, short-term and long-term aged conditions. The findings are summarized as follows:

- Introducing CR into asphalt cement increased the softening point, resilience, viscosity, high temperature true grade of the asphalt while decreasing the penetration, intermediate temperature true grade, and complex modulus aging index (CMAI) values.
- Improved rheological properties (higher complex shear modulus (G*) and lower phase angel (δ)) were obtained for CRMA.

- Higher softening point, viscosity and high temperature true grade results of CRMA indicates that CRMA is less temperature susceptible; thus, better rutting-resistant ($G^*/\sin\delta$) compared to unmodified asphalt.
- Lower intermediate true grade results of CRMA suggest that CRMA slightly improved the fatigue-cracking resistance ($G^*\sin\delta$) compared to unmodified asphalt.
- Resilience results show that CR modification improved the elastic properties of the asphalt which is an important factor for rutting and fatigue-cracking resistance.
- CRMA has lower CMAI values than unmodified asphalt; therefore, modification of asphalt significantly improved the short-term and long-term aging resistance of the asphalt.
- Master curves revealed that the rheological properties of the CRMA don't substantially differ during short-term aging when investigated in a wide range of temperatures and loading frequencies. The major change was obtained for long-term aging.
- In terms of the intermediate and high temperature performance of CRMA, mixing duration was found significant only for the penetration and resilience test results. As for the resilience, the effect of the mixing duration was insignificant for the mixing duration levels except for 30 minutes. Resilience results for the 30 minutes of mixing duration were obtained low compared to the rest of mixing durations; thus, poorer elasticity of the binder. For this reason, the duration of 30 minutes is not sufficient for the mixing.
- Based on the same tests and analysis, mixing rate mainly effected the viscosity and high temperature true grade of CRMA. The main difference for the mixing rate levels was noted between the low shearing (700, 1000, 1200 rpm) and high shearing. A significant difference was not observed within the low shear mixing rate levels.

- The 2D images obtained through fluorescence microscopy revealed that high shear mixing can reduce the size of CR particles. In addition, CR particles help preserving some amount of the light fractions of asphalt against aging.
- Based on the finding of this study, it is not necessary to utilize extensive mixing durations and higher low shear mixing rate (in the case of high shear mixing is not applicable and not required) in the process of CRMA preparation. Therefore, energy consumption can be reduced.

5.3 Recommendations

The major findings of this study are presented in Section 5.2. However, the research can be detailed more by the future studies. In this study, the variables of the mixing rate and mixing duration are investigated in terms of intermediate and high temperature performance. However, the effect of these two variables on the low temperature performance of CRMA is also necessary to be investigated. Furthermore, fluorescence microscope imaged should be supported with chemical analysis in order to robust the assessment.

REFERENCES

Abdelrahman, M. A., & Carpenter, S. H. (1999). Mechanism of interaction of asphalt cement with crumb rubber modifier. Transportation Research Record, 1661(1), 106-113.

Abdelrahman, M. (2006). Controlling performance of crumb rubber–modified binders through addition of polymer modifiers. Transportation research record, 1962(1), 64-70.

Aflaki, S., & Memarzadeh, M. (2011). Using two-way ANOVA and hypothesis test in evaluating crumb rubber modification (CRM) agitation effects on rheological properties of bitumen. Construction and Building materials, 25(4), 2094-2106.

Airey, G. D., & Rahimzadeh, B. (2004). Combined bituminous binder and mixture linear rheological properties. Construction and Building Materials, 18(7), 535-548.

Akbas, A., & Yuhana, N. Y. (2021). Recycling of Rubber Wastes as Fuel and Its Additives. Recycling, 6(4), 78.

Ali, A. H., Mashaan, N. S., & Karim, M. R. (2013). Investigations of physical and rheological properties of aged rubberised bitumen. Advances in Materials Science and Engineering, 2013.

Amirkhanian, S. (2020). Utilization of scrap plastics in asphalt binders. In Eco-efficient pavement construction materials (pp. 13-32). Woodhead Publishing.

American Association of State Highway and Transportation Officials (AASHTO), "Design of New and Re-constructed Flexible Pavements", Mechanistic Empirical Design Guide (MEPDG) Part 3-Design Analysis, 2002, Chapter-3, pp 3.3

Artamendi, I., Khalid, H., Page, G. C., Redelius, P. G., Ebels, L. J., & Negulescu, I. (2006). Diffusion kinetics of bitumen into waste tyre rubber. Asphalt Paving Technology, 75, 133.

ASTM D5/D5M – 20. (2020). Standard Test Method for Penetration of Bituminous Materials. ASTM International, West Conshohocken, PA, 2020, DOI: 10.1520/D0005_D0005M-20, www.astm.org.

ASTM D8 – 22a. (2022). Standard Terminology Relating to Materials for Roads and Pavements. ASTM International, West Conshohocken, PA, 2020, DOI: 10.1520/D0008-22A, www.astm.org.

ASTM D36/D36M – 14. (2020). Standard Test Method for Softening Point of Bitumen (Ring-and-Ball Apparatus). ASTM International, West Conshohocken, PA, 2020, DOI: 10.1520/D0036_D0036M-14R20, www.astm.org.

ASTM D1754/D1754M-20. (2020). Standard Test Method for Effects of Heat and Air on Asphaltic Materials (Thin-Film Oven Test). ASTM International, West Conshohocken, PA, 2020, DOI: 10.1520/D1754_D1754M-20, www.astm.org.

ASTM D4402/D4402M – 15. (2022). Standard Test Method for Viscosity Determination of Asphalt at Elevated Temperatures Using a Rotational Viscometer. ASTM International, West Conshohocken, PA, 2020, DOI: 10.1520/D4402_D4402M-15R22, www.astm.org.

ASTM D5329-20. (2020). Standard Test Methods for Sealants and Fillers, Hot-Applied, for Joints and Cracks in Asphalt Pavements and Portland Cement Concrete Pavements. ASTM International, West Conshohocken, PA, 2020, DOI: 10.1520/D5329-20, www.astm.org.

ASTM D6114/D6114M-19. (2019). Standard Specification for Asphalt-Rubber Binder. ASTM International, West Conshohocken, PA, 2020, DOI: 10.1520/D6114_D6114M-19, www.astm.org.

ASTM D6521-22. (2022). Standard Practice for Accelerated Aging of Asphalt Binder Using a Pressurized Aging Vessel (PAV). ASTM International, West Conshohocken, PA, 2020, DOI: 10.1520/D6521-22, www.astm.org.

ASTM D7175-15. (2015). Standard Test Method for Determining the Rheological Properties of Asphalt Binder Using a Dynamic Shear Rheometer. ASTM International, West Conshohocken, PA, 2020, DOI: 10.1520/D7175-15, www.astm.org.

ASTM D7405-20. (2020). Standard Test Method for Multiple Stress Creep and Recovery (MSCR) of Asphalt Binder Using a Dynamic Shear Rheometer. ASTM International, West Conshohocken, PA, 2020, DOI: 10.1520/D7405-20, www.astm.org.

Bagnell, R. (2012). Fluorescence Microscopy. Retrieved November 10, 2022 from https://docplayer.net/23830484-Chapter-12-fluorescence-microscopy-c-robert-bagnell-jr-ph-d-2012.html

Bairgi, B., Hossain, Z., & Hendrix, R. D. (2015). Investigation of rheological properties of asphalt rubber toward sustainable use of scrap tires. In IFCEE 2015 (pp. 359-368).

Bennert, T. (2013). Grade determination of crumb rubber-modified performance graded asphalt binder (No. C-08-20). University Transportation Research Center.

Booshehrian, A., Mogawer, W. S., & Bonaquist, R. (2013). How to construct an asphalt binder master curve and assess the degree of blending between RAP and virgin binders. Journal of Materials in Civil Engineering, 25(12), 1813-1821.

CalRecycle. (2010). Technical Assistance and Training. A basic introduction to RAC Usage (RAC-101) https://calrecycle.ca.gov/tires/rac/techassist/

Caltrans. (2003). Asphalt rubber usage guide. s.l.: Sacramento, CA: State of California Department of Transportation, Materials Engineering and Testing Services.

Cao, R., & Bai, Q. (2008). Laboratory evaluation of performances of asphalt rubber and gap graded mixtures. In Plan, Build, And Manage Transportation Infrastructure in China (pp. 786-798).

Celauro, B., Celauro, C., Presti, D. L., & Bevilacqua, A. (2012). Definition of a laboratory optimization protocol for road bitumen improved with recycled tire rubber. Construction and Building Materials, 37, 562-572.

Cetin, A. (2013). Effects of crumb rubber size and concentration on performance of porous asphalt mixtures. International Journal of Polymer Science, 2013.

Chang, M., Zhang, Y., Pei, J., Zhang, J., Wang, M., & Ha, F. (2020). Low-Temperature Rheological Properties and Microscopic Characterization of Asphalt Rubbers Containing Heterogeneous Crumb Rubbers. Materials, 13(18), 4120.

Chavez, F., Marcobal, J., & Gallego, J. (2019). Laboratory evaluation of the mechanical properties of asphalt mixtures with rubber incorporated by the wet, dry, and semi-wet process. Construction and Building Materials, 205, 164-174.

Chen, Z., Wang, T., Pei, J., Amirkhanian, S., Xiao, F., Ye, Q., & Fan, Z. (2019a). Low temperature and fatigue characteristics of treated crumb rubber modified asphalt after a long term aging procedure. Journal of Cleaner Production, 234, 1262-1274.

Chen, T., Ma, T., Huang, X., Guan, Y., Zhang, Z., & Tang, F. (2019b). The performance of hot-recycling asphalt binder containing crumb rubber modified asphalt based on physiochemical and rheological measurements. Construction and Building Materials, 226, 83-93.

Chesner, W. H., Collins, R. J., MacKay, M. H., & Emery, J. (2002). User guidelines for waste and by-product materials in pavement construction (No. FHWA-RD-97-148, Guideline Manual, Rept No. 480017). Recycled Materials Resource Center.

Chiu, C. T., Hsu, T. H., & Yang, W. F. (2008). Life cycle assessment on using recycled materials for rehabilitating asphalt pavements. Resources, conservation and recycling, 52(3), 545-556.

Cong, P., Xun, P., Xing, M., & Chen, S. (2013). Investigation of asphalt binder containing various crumb rubbers and asphalts. Construction and Building Materials, 40, 632-641.

Dallas, P. (2020). Generation of Polymers and Nanomaterials at Liquid-Liquid Interfaces: Application to Crystalline, Light Emitting and Energy Materials. Elsevier.

de Almeida Júnior, A. F., Battistelle, R. A., Bezerra, B. S., & de Castro, R. (2012). Use of scrap tire rubber in place of SBS in modified asphalt as an environmentally correct alternative for Brazil. Journal of Cleaner Production, 33, 236-238.

Deshmukh, N. H., & Kshirsagar, D. Y. (2017). Utilization of rubber waste in construction of flexible pavement. International Journal for Advance Research and Development, 2(7), 70-77.

Ding, X., Ma, T., Zhang, W., & Zhang, D. (2017). Experimental study of stable crumb rubber asphalt and asphalt mixture. Construction and Building Materials, 157, 975-981.

Divya, P. S., Gideon, C. S., & Murali Krishnan, J. (2013). Influence of the type of binder and crumb rubber on the creep and recovery of crumb rubber modified bitumen. Journal of materials in civil engineering, 25(4), 438-449.

Duan, H., Zhu, C., Li, Y., Zhang, H., Zhang, S., Xiao, F., & Amirkhanian, S. (2021). Effect of crumb rubber percentages and bitumen sources on high-temperature rheological properties of less smell crumb rubber modified bitumen. Construction and Building Materials, 277, 122248.

EEA. (2003, March 31). Waste from vehicles (number and treatment of used tires). European Union. https://www.eea.europa.eu/data-and-maps/indicators/waste-from-road-vehicles/waste-from-road-vehicles-tyres-eu#:~:text=The%20EU%20landfill%20directive%20imposes,to%20the%20cheap%20landfilling%20activity

ETRMA (2021). End of Life Tyres Management – Europe – 2019. https://consorciocaucho.es/documentos/20210511_etrma_press-release_elt-2019.pdf

Fernández-Ruiz, R., Redrejo, M. J., Pérez-Aparicio, R., & Saiz-Rodríguez, L. (2020). Quantification of recycled rubber content of end-of-life tyres in asphalt bitumen by total-reflection X-ray fluorescence spectrometry. Spectrochimica Acta Part B: Atomic Spectroscopy, 166, 105803.

Fontes, L. P., Trichês, G., Pais, J. C., & Pereira, P. A. (2010). Evaluating permanent deformation in asphalt rubber mixtures. Construction and Building Materials, 24(7), 1193-1200.

FHWA (Federal Highway Administration). (1997). User guidelines for waste and byproduct materials in pavement construction.

Fini, E. H., Oldham, D. J., & Abu-Lebdeh, T. (2013). Synthesis and characterization of biomodified rubber asphalt: Sustainable waste management solution for scrap tire and swine manure. Journal of Environmental Engineering, 139(12), 1454-1461.

Fontes L., Pereira P., Pais J., Triches G. (2006). Behavior of Asphalt Rubber Mixtures with Different Crumb Rubber and Asphalt Biner Sources. Proceedings AR2006 International Conference on Asphalt Rubber, Palm Springs, California, 2006.

Gallego, J., Rodríguez-Alloza, A. M., & Giuliani, F. (2016). Black curves and creep behaviour of crumb rubber modified binders containing warm mix asphalt additives. Mechanics of Time-Dependent Materials, 20(3), 389-403.

Gao, Y., & Cao, R. (2010). Interaction theory of asphalt and rubber. Journal of Wuhan University of Technology-Mater. Sci. Ed., 25(5), 853-855.

Ghavibazoo, A., & Abdelrahman, M. (2013). Composition analysis of crumb rubber during interaction with asphalt and effect on properties of binder. International Journal of Pavement Engineering, 14(5), 517-530.

Ghavibazoo, A., & Abdelrahman, M. (2014). Effect of crumb rubber dissolution on low-temperature performance and aging of asphalt–rubber binder. Transportation Research Record, 2445(1), 47-55.

Ghavibazoo, A., Abdelrahman, M., & Ragab, M. (2013). Effect of Crumb Rubber Modifier Dissolution on Storage Stability of Crumb Rubber–Modified Asphalt. Transportation research record, 2370(1), 109-115.

Glover, C. J., Davison, R. R., Bullin, J. A., Estakhri, C. K., Williamson, S. A., Billiter, T. C., ... & Wattanachai, P. (2000). A comprehensive laboratory and field study of high-cure crumb-rubber modified asphalt materials (No. FHWA/TX-01/1460-1,).

Glover, C. J., Davison, R. R., Bullin, J. A., Estakhri, C. K., Williamson, S. A., Billiter, T. C., Chipps J. F., Chun, J. S., Juristyarini, P., Leicht, S. E., & Wattanachai, P. (2000). A comprehensive laboratory and field study of high-cure crumb-rubber modified asphalt materials (No. FHWA/TX-01/1460-1,).

Gopal, V.T., Sebaaly, P.E., Epps, J. (2002). Effect of Crumb Rubber Particle Size and Content on the Low Temperature Rheological Properties of Binders. Transportation Research Board, Annual Meeting, Washington D.C.

Gresham, R. M. (2008). Viscosity: A fluid's resistance to flow. Tribology & lubrication technology, 64(11), 55.

Green, E. L., & Tolonen, W. J. (1977). The chemical and physical properties of asphalt rubber mixtures. Part i. Basic material behavior (No. ADOT-RS-14 (162)-1).

González, V., Martínez-Boza, F. J., Gallegos, C., Pérez-Lepe, A., & Páez, A. (2012). A study into the processing of bitumen modified with tire crumb rubber and polymeric additives. Fuel processing technology, 95, 137-143.

Han, L., Zheng, M., & Wang, C. (2016). Current status and development of terminal blend tyre rubber modified asphalt. Construction and Building Materials, 128, 399-409.

Handle, F., Füssl, J., Neudl, S., Grossegger, D., Eberhardsteiner, L., Hofko, B., Hospodka, M., Blab, R., & Grothe, H. (2016). The bitumen microstructure: a fluorescent approach. Materials and Structures, 49(1), 167-180.

Hao, G., & Wang, Y. (2021). 3D reconstruction of polymer phase in polymer-modified asphalt using confocal fluorescence microscopy. Journal of Materials in Civil Engineering, 33(1), 04020400.

Hicks, R. G., Lundy, J. R., Leahy, R. B., Hanson, D., & Epps, J. A. (1995). Crumb rubber modifiers (CRM) in asphalt pavements: Summary of practices in Arizona, California, and Florida (No. FHWA-SA-95-056). United States. Federal Highway Administration. Office of Technology Applications.

Heitzman, M. (1992). Design and construction of asphalt paving materials with crumb rubber modifier. Transportation Research Record, 1339.

Hicks, R. G., & Epps, J. A. (2000). Quality control for asphalt rubber binders and mixes. Proceedings, Asphalt Rubber, 13-17.

Hrušková, L., Hájeková, E., & Daučík, P. (2016). Effects of mixing conditions on properties of asphalt modified by crumb rubber. Petroleum & Coal, 58(2).

Huang, J., Zhang, J., Ren, J., & Chen, H. (2021). Anti-rutting performance of the damping asphalt mixtures (DAMs) made with a high content of asphalt rubber (AR). Construction and Building Materials, 271, 121878.

Huff, B. J., & Vallerga, B. A. (1979). Characteristics and performance of asphalt-rubber material containing a blend of reclaim and crumb rubber. Transportation Research Record, 821, 29-36.

Jain, A. (2016). Compendium of Technologies for the Recovery of Materials/Energy from End of Life (EoL) Tyres Final Report. Nations, United Programme, Environment Environmental, International Centre, Technology.

Jensen, W., & Abdelrahman, M. (2006). Crumb rubber in performance graded asphalt binder. Rep. No. SPR-01 (05) P585, Univ. of Nebraska, Lincoln, NE.

Jeong, K. D., Lee, S. J., Amirkhanian, S. N., & Kim, K. W. (2010). Interaction effects of crumb rubber modified asphalt binders. Construction and Building Materials, 24(5), 824-831.

Kandhal, P. S. (1992). Waste materials in hot mix asphalt – An overview. NCAT Report 92-06.

Karger-Kocsis, J., Mészáros, L., & Bárány, T. (2013). Ground tyre rubber (GTR) in thermoplastics, thermosets, and rubbers. Journal of Materials Science, 48(1), 1-38.

Katman, H. Y., Ibrahim, M. R., Karim, M. R., Koting, S., & Mashaan, N. S. (2016). Effect of rubberized bitumen blending methods on permanent deformation of SMA rubberized asphalt mixtures. Advances in Materials Science and Engineering, 2016.

Kim, H. H., Mithil, M., Lee, M. S., & Lee, S. J. (2016). Identification of the microstructural components of crumb rubber modified asphalt binder (CRMA) and the feasibility of using environmental scanning electron microscopy (ESEM) coupled with energy dispersive X-Ray spectroscopy (EDX). International Journal of Highway Engineering, 18(6), 41-50.

Kim, H., & Lee, S. J. (2013). Laboratory investigation of different standards of phase separation in crumb rubber modified asphalt binders. Journal of materials in civil engineering, 25(12), 1975-1978.

Kök, B. V., & Çolak, H. (2011). Laboratory comparison of the crumb-rubber and SBS modified bitumen and hot mix asphalt. Construction and Building Materials, 25(8), 3204-3212.

Klingensmith, W., & Baranwal, K. (1998). Best Practices in Scrap Tires & Rubber Recycling. Recycling Technology Assistance Partnership, Clean Washington Center.

Lee, T. K., & Kim, B. S. (2008). Vibration analysis of automobile tire due to bump impact. Applied Acoustics, 69(6), 473-478.

Lee, S. J., Akisetty, C. K., & Amirkhanian, S. N. (2008). The effect of crumb rubber modifier (CRM) on the performance properties of rubberized binders in HMA pavements. Construction and Building Materials, 22(7), 1368-1376.

Li, H., Dong, B., Zhao, D., Guo, P., & Zhang, J. (2019). Physical, rheological and stability properties of desulfurized rubber asphalt and crumb rubber asphalt. Arabian Journal for Science and Engineering, 44(5), 5043-5056.

Li, Y., Lyu, Y., Xu, M., Fan, L., & Zhang, Y. (2019). Determination of construction temperatures of crumb rubber modified bitumen mixture based on CRMB mastic. Materials, 12(23), 3851.

Li, P., Jiang, X., Ding, Z., Zhao, J., & Shen, M. (2018). Analysis of viscosity and composition properties for crumb rubber modified asphalt. Construction and Building Materials, 169, 638-647.

Liang, M., Xin, X., Fan, W., Ren, S., Shi, J., & Luo, H. (2017). Thermo-stability and aging performance of modified asphalt with crumb rubber activated by microwave and TOR. Materials & Design, 127, 84-96.

Liang, M., Xin, X., Fan, W., Luo, H., Wang, X., & Xing, B. (2015a). Investigation of the rheological properties and storage stability of CR/SBS modified asphalt. Construction and Building Materials, 74, 235-240.

Liang, M., Xin, X., Fan, W., Sun, H., Yao, Y., & Xing, B. (2015b). Viscous properties, storage stability and their relationships with microstructure of tire scrap rubber modified asphalt. Construction and Building Materials, 74, 124-131.

Liao, M. C., & Lo, T. J. (2021). Material Characterization and Balanced Design of Asphalt–Rubber Binders. Journal of Materials in Civil Engineering, 33(1), 04020424.

Liu, H., Chen, Z., Wang, W., Wang, H., & Hao, P. (2014). Investigation of the rheological modification mechanism of crumb rubber modified asphalt (CRMA) containing TOR additive. Construction and Building Materials, 67, 225-233.

Liu, H., Fu, L., Jiao, Y., Tao, J., & Wang, X. (2017). Short-term aging effect on properties of sustainable pavement asphalts modified by waste rubber and diatomite. Sustainability, 9(6), 996.

Liu, H., Luo, G., Wang, X., & Jiao, Y. (2015, June). Effects of preparation process on performance of rubber modified asphalt. In IOP Conference Series: Materials Science and Engineering (Vol. 87, No. 1, p. 012008). IOP Publishing.

Liu, W., Yan, K., Ge, D., & Chen, M. (2018). Effect of APAO on the aging properties of waste tire rubber modified asphalt binder. Construction and Building Materials, 175, 333-341.

Lo Presti, D., & Airey, G. (2013). Tyre rubber-modified bitumens development: the effect of varying processing conditions. Road Materials and Pavement Design, 14(4), 888-900.

Lo Presti, D., Memon, N., Airey, G., & Grenfell, J. (2009). Comparison between bitumen modified with crumb tyre rubber and styrene butadiene styrene. MAIREPAV 6 Proc, 54-63.

Loderer, C., Partl, M. N., & Poulikakos, L. D. (2018). Effect of crumb rubber production technology on performance of modified bitumen. Construction and Building Materials, 191, 1159-1171.

Loeber, L., Muller, G., Morel, J., & Sutton, O. (1998). Bitumen in colloid science: a chemical, structural and rheological approach. Fuel, 77(13), 1443-1450.

López-Moro, F. J., Moro, M. C., Hernández-Olivares, F., Witoszek-Schultz, B., & Alonso-Fernández, M. (2013). Microscopic analysis of the interaction between crumb rubber and bitumen in asphalt mixtures using the dry process. Construction and Building Materials, 48, 691-699.

Lv, S., Tan, L., Peng, X., Hu, L., & Cabrera, M. B. (2021a). Experimental investigation on the performance of bone glue and crumb rubber compound modified asphalt. Construction and Building Materials, 305, 124734.

Lv, S., Yuan, J., Peng, X., Cabrera, M. B., Liu, H., Luo, X., & You, L. (2021b). Standardization to evaluate the lasting capacity of rubberized asphalt mixtures with different testing approaches. Construction and Building Materials, 269, 121341.

Ma, T., Wang, H., He, L., Zhao, Y., Huang, X., & Chen, J. (2017). Property characterization of asphalt binders and mixtures modified by different crumb rubbers. Journal of Materials in Civil Engineering, 29(7), 04017036.

Ma, Y., Hu, W., Polaczyk, P. A., Han, B., Xiao, R., Zhang, M., & Huang, B. (2020). Rheological and aging characteristics of the recycled asphalt binders with different rejuvenator incorporation methods. Journal of Cleaner Production, 262, 121249.

Mark, J. E., Erman, B., & Roland, M. (Eds.). (2013). The science and technology of rubber. Academic press.

Mashaan, N. S., & Karim, M. R. (2013). Investigating the rheological properties of crumb rubber modified bitumen and its correlation with temperature susceptibility. Materials Research, 16, 116-127.

Mashaan, N. S., Ali, A. H., Karim, M. R., & Abdelaziz, M. (2011). Effect of crumb rubber concentration on the physical and rheological properties of rubberised bitumen binders. International journal of the physical sciences, 6(4), 684-690.

Medina, J. G., Giancontieri, G., & Presti, D. L. (2020). Quality control of manufacturing and hot storage of crumb rubber modified binders. Construction and Building Materials, 233, 117351.

Mamlouk, M. S., & Zaniewski, J. P. (1999). Materials for civil and construction engineering.

Martinez Arguelles, G., Crispino, M., & Fuentes, L. G. (2012). Evaluation of an Alternative Gradation of Crumb Rubber on Binders and Asphalt Hot Mixes. In Proceedings of the Asphalt Rubber Conference (pp. 291-304).

Mturi, G. A., O'Connell, J., Zoorob, S. E., & De Beer, M. (2014). A study of crumb rubber modified bitumen used in South Africa. Road materials and pavement design, 15(4), 774-790.

Mukhtar, I. (2021, August 12). Kuwait struggling to get rid of world's biggest tire graveyard. Anadolu Agency. https://www.aa.com.tr/en/environment/kuwait-struggling-to-get-rid-of-world-s-biggest-tire-graveyard/2332769

Navarro, F. J., Partal, P., Martínez-Boza, F. J., & Gallegos, C. (2007). Influence of processing conditions on the rheological behavior of crumb tire rubber-modified bitumen. Journal of applied polymer science, 104(3), 1683-1691.

Navarro, F. M., & Gámez, M. C. R. (2012). Influence of crumb rubber on the indirect tensile strength and stiffness modulus of hot bituminous mixes. Journal of Materials in Civil Engineering, 24(6), 715-724.

Nejad, F. M., Aghajani, P., Modarres, A., & Firoozifar, H. (2012). Investigating the properties of crumb rubber modified bitumen using classic and SHRP testing methods. Construction and Building Materials, 26(1), 481-489.

Neto, S. A. D., Farias, M. M. D., Pais, J. C., & Pereira, P. A. (2006). Influence of crumb rubber gradation on asphalt-rubber properties. Asphalt Rubber Conference 1-14.

Neto, S. A. D., Farias, M. M., Pais, J. C., Pereira, P. A., & Sousa, J. B. (2006b). Influence of crumb rubber and digestion time on the asphalt rubber binders. Road materials and pavement design, 7(2), 131-148.

Oliver, J. W. (1981). Modification of paving asphalts by digestion with scrap rubber. Transportation Research Record, (821).

Oliver, J. W. H. (1982). Optimizing the improvements obtained by the digestion of comminuted scrap rubbers in paving asphalts (with discussion). In Association of Asphalt Paving Technologists Proceedings (Vol. 51).

Oliveira, J. R., Silva, H. M., Abreu, L. P., & Fernandes, S. R. (2013). Use of a warm mix asphalt additive to reduce the production temperatures and to improve the performance of asphalt rubber mixtures. Journal of Cleaner Production, 41, 15-22.

Ould-Henia, M., & Dumont, A. G. (2006, October). Assessment of the rheological properties of asphalt rubber binder and its residual phases. In Asphalt Rubber 2006 Conference, Palm Springs, California, USA.

Pais, J. C., Amorim, S. I., & Minhoto, M. J. (2013). Impact of traffic overload on road pavement performance. Journal of transportation Engineering, 139(9), 873-879.

Pan, J., Hossain, M. I., & Tarefder, R. A. (2017). Temperature and moisture impacts on asphalt before and after oxidative aging using molecular dynamics simulations. Journal of Nanomechanics and Micromechanics, 7(4), 04017018.

Papagiannakis, A. T., & Masad, E. A. (2008). Pavement design and materials. John Wiley & Sons.

Pellinen, T. K., Witczak, M. W., & Bonaquist, R. F. (2004). Asphalt mix master curve construction using sigmoidal fitting function with non-linear least squares optimization. In Recent advances in materials characterization and modeling of pavement systems (pp. 83-101).

Peralta, J., Silva, H. M., Machado, A. V., Pais, J., Pereira, P. A., & Sousa, J. B. (2010). Changes in rubber due to its interaction with bitumen when producing asphalt rubber. Road Materials and Pavement Design, 11(4), 1009-1031.

Pereira, P. A., Pais, J. C., Trichês, G., & Fontes, L. P. T. L. (2008). Laboratory optimization of continuous blend asphalt rubber. Proceedings of 3rd European pavement and asset management EPAM, 3, 1-12.

Picado-Santos, L. G., Capitão, S. D., & Neves, J. M. (2020). Crumb rubber asphalt mixtures: A literature review. Construction and Building Materials, 247, 118577.

Poovaneshvaran, S., Hasan, M. R. M., & Jaya, R. P. (2020). Impacts of recycled crumb rubber powder and natural rubber latex on the modified asphalt rheological behaviour, bonding, and resistance to shear. Construction and Building Materials, 234, 117357.

Presti, D. L. (2013). Recycled tyre rubber modified bitumens for road asphalt mixtures: A literature review. Construction and Building Materials, 49, 863-881.

Presti, D. L., Fecarotti, C., Clare, A. T., & Airey, G. (2014). Toward more realistic viscosity measurements of tyre rubber–bitumen blends. Construction and Building Materials, 67, 270-278.

Presti, D. L., Memon, N., Grenfell, J., & Airey, G. (2017). Alternative methodologies to evaluate storage stability of rubberised bitumens. Adv Mater Sci Eng, 2, 12.

Pure Energy Circle. (2021, October 6). Kuwait tire fire. https://www.pureenergycircle.com/news/kuwait-tire-fire

Radziszewski, P., Piłat, J., Sarnowski, M., Kowalski, K. J., Król, J. B., & Krupa, Z. (2012, October). Asphalt Rubber as Alternative of Polymer Modified Bitumen. In Asphalt Rubber 2012 Conference Roads of the Future, Munich, Germany (pp. 475-488).

RAF (Rubberized Asphalt Foundation). Glossary of Rubberized Asphalt Terms. Retrieved October 21, 2022 from https://www.ra-foundation.org/glossary/

Rahman, M. (2004). Characterisation of dry process crumb rubber modified asphalt mixtures (Doctoral dissertation, University of Nottingham).

Razmi, A., & Mirsayar, M. M. (2018). Fracture resistance of asphalt concrete modified with crumb rubber at low temperatures. International Journal of Pavement Research and Technology, 11(3), 265-273.

Read, J., & Whiteoak, D. (2003). The shell bitumen handbook. Thomas Telford.

Reschner, K. (2008). Scrap tire recycling. A summary of prevalent disposal and recycling methods. Entire-Engineering, Berlin, 1, 115-240.

Rise, G. (2021, January 15). Fluorescent Microscopy. Microbial Life - Educational Resources. https://serc.carleton.edu/microbelife/index.html

Rochlani, M., Leischner, S., Wareham, D., Caro, S., Falla, G. C., & Wellner, F. (2020). Investigating the performance-related properties of crumb rubber modified bitumen using rheology-based tests. International Journal of Pavement Engineering, 1-11.

Rodríguez-Alloza, A. M., Gallego, J., & Pérez, I. (2013). Study of the effect of four warm mix asphalt additives on bitumen modified with 15% crumb rubber. Construction and Building Materials, 43, 300-308.

Rowe, G., Baumgardner, G., & Sharrock, M. (2009). Functional forms for master curve analysis of bituminous materials. In Advanced testing and characterization of bituminous materials, two volume set (pp. 97-108). CRC Press.

Santagata, E., Dalmazzo, D., Lanotte, M., Zanetti, M. C., & Ruffino, B. (2012, October). Relationship between crumb rubber morphology and asphalt rubber viscosity. In Proceedings of the 5th asphalt rubber international conference, Munich, Germany (pp. 513-532).

Santagata, F. A., Canestrari, F., & Pasquini, E. (2007, September). Mechanical characterization of asphalt rubber-wet process. In Palermo: sn In: 4th International SIIV Congress.

Shafabakhsh, G. H., Sadeghnejad, M., & Sajed, Y. (2014). Case study of rutting performance of HMA modified with waste rubber powder. Case Studies in Construction Materials, 1, 69-76.

Shatanawi, K. M., Biro, S., Geiger, A., & Amirkhanian, S. N. (2012). Effects of furfural activated crumb rubber on the properties of rubberized asphalt. Construction and Building Materials, 28(1), 96-103.

Shatanawi, K., Biro, S., Thodesen, C., & Amirkhanian, S. (2009). Effects of water activation of crumb rubber on the properties of crumb rubber-modified binders. International Journal of Pavement Engineering, 10(4), 289-297.

Shen, Z. X. A. J. (2015). Multi-scale evaluation on the interaction between asphalt and crumb rubber. New Front, 2015, 10.

Shen, J., & Amirkhanian, S. (2005). The influence of crumb rubber modifier (CRM) microstructures on the high temperature properties of CRM binders. The International Journal of Pavement Engineering, 6(4), 265-271.

Sienkiewicz, M., Borzędowska-Labuda, K., Zalewski, S., & Janik, H. (2017). The effect of tyre rubber grinding method on the rubber-asphalt binder properties. Construction and Building Materials, 154, 144-154.

Singh, B., Kumar, L., Gupta, M., Chauhan, M., & Chauhan, G. S. (2013). Effect of activated crumb rubber on the properties of crumb rubber-modified bitumen. Journal of Applied Polymer Science, 129(5), 2821-2831.

Solaimanian, M., & Chen, X. (2019, January). Effect of aggregate gradation, aging, and compaction energy on swelling characteristics of rubber modified asphalts mixtures. In 7th International Materials Specialty Conference 2018, Held as Part of the Canadian Society for Civil Engineering Annual Conference 2018 (pp. 114-124). Canadian Society for Civil Engineering.

Southern, M. (2015). A perspective of bituminous binder specifications. In Advances in asphalt materials (pp. 1-27). Woodhead Publishing.

Specht, L., & Khatchatourian, O. (2014). Application of artificial intelligence to modelling asphalt–rubber viscosity. International Journal of Pavement Engineering, 15(9), 799-809.

Stangl, K., Jäger, A., & Lackner, R. (2007). The effect of styrene-butadiene-styrene modification on the characteristics and performance of bitumen. Monatshefte für Chemie-Chemical Monthly, 138(4), 301-307.

Subhy, A., Pires, G. M., Presti, D. L., & Airey, G. (2018). The effects of laboratory ageing on rheological and fracture characteristics of different rubberised bitumens. Construction and Building Materials, 180, 188-198.

Subhy, A., & Lo Presti, D. (2017). Fatigue and healing properties of low environmental impact rubberized bitumen for asphalt pavement. Coatings, 7(5), 66.

Subhy, A., Lo Presti, D., & Airey, G. (2016). Rubberised bitumen manufacturing assisted by rheological measurements. Road Materials and Pavement Design, 17(2), 290-310.

Subhy, A., Lo Presti, D., & Airey, G. (2015). An investigation on using pre-treated tyre rubber as a replacement of synthetic polymers for bitumen modification. Road Materials and Pavement Design, 16(sup1), 245-264.

Szerb, E. I., Nicotera, I., Teltayev, B., Vaiana, R., & Rossi, C. O. (2018). Highly stable surfactant-crumb rubber-modified bitumen: NMR and rheological investigation. Road Materials and Pavement Design, 19(5), 1192-1202.

Sun, D. Q., & Li, L. H. (2010). Factors affecting the viscosity of crumb rubber–modified asphalt. Petroleum Science and Technology, 28(15), 1555-1566.

Tan, Y., Guo, M., Cao, L., & Zhang, L. (2013). Performance optimization of composite modified asphalt sealant based on rheological behavior. Construction and Building Materials, 47, 799-805.

Tang, N., Huang, W., & Xiao, F. (2016). Chemical and rheological investigation of high-cured crumb rubber-modified asphalt. Construction and Building Materials, 123, 847-854.

The Magazine of Asphalt Institute. (2008, November 24). Terminal blended rubberized asphalt goes mainstream – Now PG graded. Asphalt Institute. http://asphaltmagazine.com/terminal-blended-rubberized-asphalt-goes-mainstream-now-pg-graded/

Thives, L. P., Pais, J. C., Pereira, P. A., Trichês, G., & Amorim, S. R. (2013). Assessment of the digestion time of asphalt rubber binder based on microscopy analysis. Construction and Building Materials, 47, 431-440.

Thodesen, C., Shatanawi, K., & Amirkhanian, S. (2009). Effect of crumb rubber characteristics on crumb rubber modified (CRM) binder viscosity. Construction and Building Materials, 23(1), 295-303.

Takallou, H. B., & Hicks, R. G. (1988). Development of improved mix and construction guidelines for rubber-modified asphalt pavements (No. 1171).

Takallou, M. B., & Takallou, H. B. (1991). Benefits of Recycling Waste Tires in Rubber Asphalt Paving. Transportation Research Record, 1310(6), 87-92.

Thodesen, C., Shatanawi, K., & Amirkhanian, S. (2009). Effect of crumb rubber characteristics on crumb rubber modified (CRM) binder viscosity. Construction and Building Materials, 23(1), 295-303.

Thives, L. P., Pais, J. C., Pereira, P. A., Trichês, G., & Amorim, S. R. (2013). Assessment of the digestion time of asphalt rubber binder based on microscopy analysis. Construction and Building Materials, 47, 431-440.

Thodesen, C., Shatanawi, K., & Amirkhanian, S. (2009). Effect of crumb rubber characteristics on crumb rubber modified (CRM) binder viscosity. Construction and Building Materials, 23(1), 295-303.

USTMA. (2020). 2019 U.S. Scrap Tire Management Summary. https://www.ustires.org/sites/default/files/2019%20USTMA%20Scrap%20Tire%20Management%20Summary%20Report.pdf

Venudharan, V., & Biligiri, K. P. (2017). Heuristic principles to predict the effect of crumb rubber gradation on asphalt binder rutting performance. Journal of Materials in Civil Engineering, 29(8), 04017050.

Walsh, I. D., & Widyatmoko, D. (2009). The effect of crumb rubber in hot bitumen. In 9th Annual international conference on sustainable aggregates, At Liverpool, UK. https://doi. org/10.13140/RG (Vol. 2, No. 3012.6168).

Wang, H., Dang, Z., Li, L., & You, Z. (2013a). Analysis on fatigue crack growth laws for crumb rubber modified (CRM) asphalt mixture. Construction and Building Materials, 47, 1342-1349.

Wang, H., Liu, X., Apostolidis, P., van de Ven, M., Erkens, S., & Skarpas, A. (2020). Effect of laboratory aging on chemistry and rheology of crumb rubber modified bitumen. Materials and Structures, 53(2), 1-15.

Wang, H., You, Z., Mills-Beale, J., & Hao, P. (2012). Laboratory evaluation on high temperature viscosity and low temperature stiffness of asphalt binder with high percent scrap tire rubber. Construction and building Materials, 26(1), 583-590.

Wang, J. G. (2015). Characterization of failure and permanent deformation behaviour of asphalt concrete. (Doctoral dissertation, Delft University of Technology).

Wang, Y., Zhu, J., Liu, L., & Sun, L. (2013b). Gradation evaluation of asphalt rubber mixture with warm-mix additive. Procedia-Social and Behavioral Sciences, 96, 31-38.

Way, G. B., Kaloush, K. E., & Biligiri, K. P. (2012). Asphalt-rubber standard practice guide. Rubber Pavements Association, Tempe.

Widyatmoko, I., Elliott, R., Grenfell, J., Airey, G., Collop, A., & Waite, S. (2009). Laboratory assessment of workability, performance and durability of rubberised asphalt mixtures. In Proceedings of the Asphalt Rubber 2009 Conference (pp. 317-327).

Williams, R. C., Peralta, J., & Puga, K. L. N. (2015). Development of non-petroleum-based binders for use in flexible pavements-phase II (No. IHRB Project TR-650). Iowa State University. Institute for Transportation.

Wulandari, P. S., & Tjandra, D. (2017). Use of crumb rubber as an additive in asphalt concrete mixture. Procedia engineering, 171, 1384-1389.

Xia, C., Lv, S., Cabrera, M. B., Wang, X., Zhang, C., & You, L. (2021). Unified characterizing fatigue performance of rubberized asphalt mixtures subjected to different loading modes. Journal of Cleaner Production, 279, 123740.

Xiang, L., Cheng, J., & Que, G. (2009). Microstructure and performance of crumb rubber modified asphalt. Construction and Building Materials, 23(12), 3586-3590.

Xiao, F., Amirkhanian, S. N., Shen, J., & Putman, B. (2009). Influences of crumb rubber size and type on reclaimed asphalt pavement (RAP) mixtures. Construction and Building Materials, 23(2), 1028-1034.

Xu, J., Li, R., Liu, T., Pei, J., Li, Y., & Luo, Q. (2020). Study on the Effect of Microwave Processing on Asphalt-Rubber. Materials, 13(2), 411.

Xu, M., Liu, J., Li, W., & Duan, W. (2015). Novel method to prepare activated crumb rubber used for synthesis of activated crumb rubber modified asphalt. Journal of Materials in Civil Engineering, 27(5), 04014173.

Xu, O., Rangaraju, P. R., Wang, S., & Xiao, F. (2017). Comparison of rheological properties and hot storage characteristics of asphalt binders modified with devulcanized ground tire rubber and other modifiers. Construction and Building Materials, 154, 841-848.

Yan, K., Xu, H., & You, L. (2015). Rheological properties of asphalts modified by waste tire rubber and reclaimed low density polyethylene. Construction and Building Materials, 83, 143-149.

Yu, G. X., Li, Z. M., Zhou, X. L., & Li, C. L. (2011). Crumb rubber–modified asphalt: microwave treatment effects. Petroleum Science and Technology, 29(4), 411-417.

Yu, H., Leng, Z., Zhang, Z., Li, D., & Zhang, J. (2020a). Selective absorption of swelling rubber in hot and warm asphalt binder fractions. Construction and Building Materials, 238, 117727.

Yu, H., Zhu, Z., Leng, Z., Wu, C., Zhang, Z., Wang, D., & Oeser, M. (2020b). Effect of mixing sequence on asphalt mixtures containing waste tire rubber and warm mix surfactants. Journal of Cleaner Production, 246, 119008.

Zadshir, M., Ploger, D., Yu, X., Sangiorgi, C., & Yin, H. (2020). Chemical, thermophysical, rheological, and microscopic characterisation of rubber modified asphalt binder exposed to UV radiation. Road Materials and Pavement Design, 21(sup1), S123-S139.

Zaman, A. A., Fricke, A. L., & Beatty, C. L. (1995). Rheological properties of rubber-modified asphalt. journal of transportation engineering, 121(6), 461-467.

Zhang, J., Sakhaeifar, M. S., & Little, D. N. (2022). Characterisation of rheological properties of sulfur-extended asphalt with/without crumb rubber. International Journal of Pavement Engineering, 23(5), 1491-1499.

Zhang, J., Li, H., Liu, P., Liang, M., Jiang, H., Yao, Z., & Airey, G. (2020). Experimental exploration of influence of recycled polymer components on rutting resistance and fatigue behavior of asphalt mixtures. Journal of Materials in Civil Engineering, 32(6), 04020129.

Zhang, L., Zhou, B., Duan, P., Wang, F., & Xu, Y. (2016). Hydrothermal conversion of scrap tire to liquid fuel. Chemical Engineering Journal, 285, 157-163.

Zhou, T., Kabir, S. F., Cao, L., Luan, H., Dong, Z., & Fini, E. H. (2020). Comparing effects of physisorption and chemisorption of bio-oil onto rubber particles in asphalt. Journal of Cleaner Production, 273, 123112.

Ziari, H., Goli, A., & Amini, A. (2016). Effect of crumb rubber modifier on the performance properties of rubberized binders. Journal of Materials in Civil Engineering, 28(12), 04016156.

APPENDICES

A. Literature-Related Data

Table A.1 CRMA preparation variables with different levels used in the literature

No	CR Content (%)	Mixing Parameters			Binder Type	CR Gradation		Articles
		Temperature (˚C)	Duration (min.)	Mixer rate and type		Size	% Passing	
1	19, 21, 25	180	45, 60, 90	250 to 300 rpm	50/70	no.10 no.16 no.30 no.50 no.200	100 99 96 14 4	Pereira et al. (2008)
2	18 + 10 Evotherm	180	60	200-400 rpm	70/100	no.8 no.10 no.30	100 96.7 6	Wang et al. (2013b)
3	15, 18, 20, 22, 25	1) 170 + 2) 180	1) 10 + 2) 50	1) manually + 2) High shear 6500 rpm	80/100	#20 #40 #80	-	Wang et al. (2013a).
4	18	-	-	-	70/100	(mm) 2 0.42 0.177	100 23.1 0	Santagata et al. (2007)
5	1, 2	135-150	-	Manually	60/70	#40 #80	-	Wulandari and Tjandra (2017)
6	9 - CR + 0-5 - SBS = CR/SBS	1) 170 + 2) 160	1) 30 + 2) 150	1) High Shear Mixer 4000 rpm 2) Stirrer 1200 rpm	80/100	#40	-	Liang et al. (2015a)
7	0, 5, 10, 15, 20, 25	185	120	800	60/80 80/100	Given as graphic	-	Cong et al. (2013)

Table A.1 (continued)

No	CR Content (%)	Mixing Parameters			Binder Type	CR Gradation		Articles
		Temp. (˚C)	Duration (min.)	Mixer rate and type		Size	% Passing	
8	5, 10, 15	180 180	60 (high shear) + 180 (maturation in oven)	High Mixer Anchor Stirrer	70/100	(mm) < 0.20 0.20 0.30 0.50 0.63 0.71 > 0.80	Fraction (wt %) I(SGP) ---------- 20.28 17.01 33.05 18.44 6.85 4.14 0.24	Sienkiewicz et al. (2017)
						(mm) < 0.20 0.20 0.30 0.50 0.63 0.71 > 0.80	Fraction (wt %) II(FDGP) ---------- 6.25 12.48 43.27 25.63 9.04 3.22 0.12	
9	1) 0, 5, 10, 15, 20, 25 2) 20 3) 20 4) 20	1) 180 2) 180 3)180 4)140, 150, 160, 170, 180, 195	1) 90 2) 90 3) 30, 60, 90, 120, 150 4) 90	-	70/100	1) #60 2) #20, #40, #60, #80 3) #60 4) #60	-	Li et al. (2018)
10	20 (Normal CR) 20 (Desulfurized CR)	180	-	-	70/100	#40	-	Ma et al. (2017)
11	1) 18 2) 18	1) 180 2) 210	120 ---------- optimised	High Shear 3500 rpm	50/70	#30	-	Lo and Airey (2013)

Table A.1 (continued)

No	CR Content (%)	Mixing Parameters			Binder Type	CR Gradation		Articles
		Temp. (°C)	Duration (min.)	Mixer rate and type		Size	% Passing	
12	18	180	140	RV(Brookfiel) (100 rpm)	S (Soft) 200 H (Hard) 40	Given as graphic	Given as graphic	Subhy et al. (2015)
13	-	25	1) 15 2) 20	1) Brookfield SC Series No.27 (10 rpm, 100 rpm) 2) Dual Helical Impeller (DHI) (10 rpm, 100 rpm)	40/60	#40	-	Presti et al. (2014)
14	1) 18,5 2) 16	-	-	-	1) VE 40/60 2) ME 40/60	-	-	Widyatmoko et al. (2019)
15	1) 18 2) 18 3) 15	1) 180, 210 2) 180, 210 3) 180	1) 120 2) 120 3) 180	High Shear	50/70 50/70 70/100	#30 #30 #40	-	Presti et al. (2017)
16	18	1) 160 2) 180 3) 200	1) 60, 140 2) 60, 140 3) 15(S), 25(H), 60, 140	Brookfield viscometer with a modified Dual Helical Impeller 100 rpm	H - 40 S -200	0.5 mm (nominal max. Size)	Gradation is given as graphic	Subhy et al. (2016)
17	18	180	120	High Shear Mixer (3000 rpm)	H - 40 S -200	-	-	Subhy et al. (2018)
18	15	180 180	10 (while feeding the oil extender (flux) first and rubber later) + 60 (mixing)	High Shear Laboratory Mill (2000 rpm) High Shear Laboratory Mill (1000 rpm)	40/60 (PG 64-16) (92.5%) + Flux (7.5%)	(mm) 1.0 0.6 0.5 0.3 0.25 0.212 0.15 0.125 0.075 0.063	100 62.9 40.4 8.0 6.2 4.6 3.0 2.4 0.6 0.2	Lo et al. (2009)

Table A.1 (continued)

No	CR Content (%)	Mixing Parameters			Binder Type	CR Gradation		Articles
		Temp. (°C)	Duration (min.)	Mixer rate and type		Size	% Passing	
19	15, 18, 21	-	-	-	70	0.4-0.8 mm	-	Zhang et al. (2020)
20	10 18	195	Until viscosity peak (values are given as table) (For storage up to 480 min)	Brookfield DV-II Pro Digital Viscometer Dual Helical Ribbon (50 rpm)	50/70	Fine: 125-250 µm Raw: 125-800 µm	-	Medina et al. (2020)
21	15, 20, 25	190-200	60	-	70	#20	-	Liu et al. (2014)
22	25- CR + 0.1 - Stabilizer	1) Pre-blending 160 + 2) Mixing 180 + 3) Adding Stabilizer/ Breeding 160	90 + 60 + 30	2) High speed sharing and stirring 7000 rpm 3) 3000 rpm	50/70	#40-#80	-	Xiang et al. (2009)
23	16, 17, 20	180	30, 45, 60, 90	-	30, 50	Ambient (0.05-1.2) Cryogenic (0.2-0.8)	Given as graphic (ADOT standard is used)	Thives et al. (2013)
24	5, 10, 15, 20	177	30	700	PG 64-22	4 Different sources given as graphic	given as graphic	Thodesen et al. (2009)
25	21	180	60	230	10/20, 40/50, 60/70, 120/150	#80-#30	-	Peralta et al. (2010)

Table A.1 (continued)

No	CR Content (%)	Mixing Parameters			Binder Type	CR Gradation		Articles
		Temp. (˚C)	Duration (min.)	Mixer rate and type		Size	% Passing	
26	8, 10, 12	-	-	-	50/70 (air blown) 70/100 (blended)	(μm) ---------- 600 425 250 150 75 Pan	(% retained) Fine -------- 0.48 3.46 50.02 40.95 4.17 0.92	Divya et al. (2013)
						(μm) ---------- 600 425 250 150 75 Pan	(% retained) Coarse --------- 0.2 1.77 34.76 54.82 6.26 2.19	
27	2.14, 3.30, 5, 6.70, 7.86	119.7, 132, 150, 168, 180.3	10.4, 30.5, 60, 89.5, 109.6	15000	100/120	#20-#30	-	Hrušková et al. (2016)
28	15, 18, 20, 23	-	-	-	50/60	#40	-	de Almeida Júnior et al. (2012)
29	25	200	120	High shear mixer 4500 Hz	Grade 90	#50-#100	-	Tan et al. (2013)
30	20	-	-	-	-	#40 #80-#100 (plant-produced RA)	-	Ding et al. (2017)
31	18	176	60	High shear mixer	60/80	(mm) 0.600 0.425 0.300 0.150 0.075	100.0 92.3 58.7 26.2 12.5	Yu et al. (2020b)
32	10	177	30	Open blade mixer 700 rpm	PG 64-22	(μm) #30 (600) #40 (425) #50 (300) #80 (180) #100 (150) 200 (75)	100.0 91.0 59.1 26.2 18.3 0.0	Kim et al. (2016)

Table A.1 (continued)

No	CR Content (%)	Mixing Parameters			Binder Type	CR Gradation		Articles
		Temp. (˚C)	Duration (min.)	Mixer rate and type		Size	% Passing	
33	10, 15, 20, 25	1) 150 2) 175 3) 200 4) 225	1) 130 2) 70 3) 55 4) 5	X-shaped mixer 500 rpm	70/100	2.26 1.18 0.60 0.30 0.15 0.075 <0.075	#15 | #30 --- 0. 00 0. 00 32.3 0.20 62.1 15.2 5.30 66.2 0.40 16.6 0.00 1.90 0.00 0.00	Sun and Li (2010)
						2.26 1.18 0.60 0.30 0.15 0.075 <0.075	#60 | #100 --- 0.00 0 .00 0. 00 0.00 5.40 0.00 71.5 0.00 22.5 45.1 0.60 50.7 0.00 4.20	
34	20	170-180	90	A blender-stirrer combination 2000 rpm	VG30, VG40	-	9 gradations from 4 tates are used (given as table)	Venudharan and Biligiri (2017)
35	21	170	15, 30, 45, 60, 120, 180, 240, 300	-	50/70	#4 #8 #10 #16 #30 #50 #200	CR-1 CR-2 --- 100 100 99.9 77.0 96.8 59.6 47.7 31.1 18.7 15.5 7.50 5.50 0.00 0.00	Neto et al. (2006)
						#4 #8 #10 #16 #30 #50 #200	CR-3 --- 100 66.7 44.1 31.0 15.6 6.20 0.00	

Table A.1 (continued)

No	CR Content (%)	Mixing Parameters			Binder Type	CR Gradation		Articles
		Temp. (˚C)	Duration (min.)	Mixer rate and type		Size	% Passing	
36	10	160, 200, 240	Various durations within 180 minutes	Three-blade stirrer 80 rpm	PG 64-22	#30	-	Abdelrahman (2006)
37	20	-	-	-	50/70	Given as graphic	given as graphic	Huang et al. (2021)
38	20	176	30, 60, 90	High shear mixer 6000 rpm	60/70	#40	-	Yu et al. (2020a)
39	20	170 + 180	Until all CR is poured + 90	100 rpm + 500 rpm	Grade 90	#40	-	Xu et al. (2020)
40	5, 10, 15, 20	180	60	Stirring 3000 rpm	20/40 60/70 PMB (60/70) (%5 SBS)	#30	-	Liao and Lo (2021)
41	1) 6 ,8 10, 12,…26 2) 20	180	120	45 min 7300 rpm + 75 min 6500 rpm	1) 60/70 2) %80 60/70+ %20VB (VB: Vacuum bitumen- %97 maltene)	0-1 mm (nominal size)	-	Nejad et al. (2012)
42	5, 10, 15, 22	180	30	High Shear Mixer with a square hole screen 6000 rpm	PG 64-22 (70/100)	(mm) 0.710 0.500 0.355 0.180 0.125 0.063	100 93 63 21 9 2	Wang et al. (2020)
43	4, 8, 12, 16, 20	160, 180	30, 60	Propeller mixer 200 rpm	80/100	#30 (0.6)	-	Mashaan and Karim (2013)

Table A.1 (continued)

No	CR Content (%)	Mixing Parameters			Binder Type	CR Gradation		Articles
		Temp. (˚C)	Duration (min.)	Mixer rate and type		Size	% Passing	
44	3, 6, 9, 12, 15	180	60	Mixer with a four-blade impeller 1000 rpm	160-220	-	-	Kök and Çolak (2011)
45	11	180	1) 30 2) 90	1) Stirrer low speed + 2) high speed mixing 1200 rpm	80/100	mean particle size: 0.37 mm	-	Singh et al. (2013)
46	18-24	190-210	-	High speed stirring	70/100	-	given as graphic	Mturi et al. (2014)
47	10	180	60	4000 rpm	50/70	(mm) 1 0.5 0.25 0.125 0.063	 100.0 94.1 23.7 3.70 0.40	Franesqui et al. (2019)
48	10	180	1) while CR being added (5 g/min) 2) 60	1) High shear mixing 16000 rpm 2) Mechanical stirrer 14000 rpm	50/70	0.4-0.8 mm	-	Szerb et al. (2018)
49	8, 10, 15	177	30	1000 rpm	PG 64-22	#20	-	Duan et al. (2021)

Table A.1 (continued)

No	CR Content (%)	Mixing Parameters			Binder Type	CR Gradation		Articles
		Temp. (˚C)	Duration (min.)	Mixer rate and type		Size	% Passing	
50	15, 20	175	1) 3 2) 3 min mixing for every 40 mins -140 mins in total. (Sample kept in oven when not being mixed)	1) Speed Mixer 500 rpm	70/100	<0.4 mm	-	Loderer et al. (2018)
51	12	180, 200, 210	60, 120, 180	Rotor-stator mixer 8200 rpm	80/100	<0.8 mm	-	González et al. (2012)
52	5, 10, 15, 20	177, 200, 223	5, 30, 60, 90, 120, 240, 480	700 rpm "This mixing speed matches the field practices used in South Carolina to produce field mixtures."	PG 64-22	#40 (0.425 mm)	given as graphic	Jeong et al. (2010)
53	12	177	30	Medium shear radial flow impeller 700 rpm	PG 64-22	8 30 40 80 200 >200	A (fine) / B (coarse) 100 / 100 78.5 / 26.5 57 / 9.7 24.5 / 3.6 10.5 / 1.5 0 / 0	Chen et al. (2019a)
						8 30 40 80 200 >200	C (coarse) 100 20.1 8.1 3.0 1.9 0	
54	16, 18, 20, 22	180	45	1000 rpm	PG 64-22 PG 64-16	#20	-	Tang et al. (2016)

Table A.1 (continued)

No	CR Content (%)	Mixing Parameters			Binder Type	CR Gradation		Articles
		Temp. (˚C)	Duration (min.)	Mixer rate and type		Size	% Passing	
55	20	170	60	Stirring (without any shearing)	PG 64-22	#30	-	Chen et al. (2019b)
56	1) 15 2) 15 (activated) 3) 25 (activated)	180	150	200 rpm	50/70	Source A < 0.4 mm Source B < 1 mm	-	Rochlani et al. (2020)
57	4, 8, 12, 16, 20	180	30, 60	Propeller blade mixer 200 rpm	80/100	#30 (0.6 mm)	-	Mashaan et al. (2011)
58	10, 15, 20	160, 190, 220	60, 120, 240, 480	High shear mixer 10 Hz (600 rpm), 30 Hz (1800 rpm), 50 Hz (3000 rpm)	PG 58-28	#40-#30	-	Ghavibazoo et al. (2013)
59	5, 10, 15	160	30	High shear mixer 1000 rpm	60/70	(mm) 1.18 0.425 0.15 0.075 Pan	100 50 9 1 0	Poovaneshvaran et al. (2020)
60	8, 16	180	60	Propeller mixer 200 rpm	80/100	#20 (0.850) #30 (0.600) #40 (0.425) #50 (0.300) #80 (0.180) #100 (0.150) #200 (0.075)	100 97.7 61.1 33.9 12.5 7.5 0.0	Ali et al. (2013)
61	15	177	60	impellor rotating 700 rpm	PG 64-22	-	given as graphic for 4 different sources	Shatanawi et al. (2019)
62	-	175	180	High speed mixer 1200	50/70	#40	-	Liang et al. (2017)

Table A.1 (continued)

No	CR Content (%)	Mixing Parameters			Binder Type	CR Gradation		Articles
		Temp. (˚C)	Duration (min.)	Mixer rate and type		Size	% Passing	
63	15, 20	185	1) 30 + 2) 30	1) 2000 + 2) 900	50/70	(mm) 2 1.5 1 0.50 0.250 0.125 0.063	 100 100 100 94.1 23.7 3.7 0.4	Gallego et al. (2016)
64	10, 15, 20	177	60	700 rpm	PG 64-22	#10 #16 #30 #50 #200	100 100 99 35 2	Kim and Lee (2013)
65	15	180	90	impellor rotating 750 rpm	70/80	#40-#80	given as graphic	Xu et al. (2013)
66	10, 15, 20	-	-	-	50/70	#4-#20 #20-#200 #4-#200	given as graphic	Cetin, A. (2013)
67	20	180	60	High shear mixer 8000 rpm	70/100	-	-	Yu et al. (2011)
68	17	180	90	-	50/70 35/50	(mm) 2.00 1.18 0.60 0.30 0.075 (mm) 2.00 1.18 0.60 0.30 0.075	Ambient 100 99 96 44 4 Cryogenic 100 99 90 20 3	Fontes et al. (2010)
69	21	180	60	Overhead stirrer 500 rpm	50/70	#30	-	Oliveira et al. (2013)
70	10, 20	160, 190, 220	120, 240, 480	60, 180, 300	PG 58-28	#30-#40	-	Ghavibazoo and Abdelrahman (2014)
71	-	190	60	1500 rpm	80/100	#40	-	Liu et al. (2018)
72	15	1) 180 2) 150, 160, 170, 180	1) 60 + 2) 45	1) Swelling + 2) Shearing (5000 rpm)	80/100	#30 #40 #50	69.8 33.5 20.8	Liu et al. (2015)

Table A.1 (continued)

No	CR Content (%)	Mixing Parameters			Binder Type	CR Gradation		Articles
		Temp. (˚C)	Duration (min.)	Mixer rate and type		Size	% Passing	
73	20	175	60	Stirring 1000 rpm	PG 64-22	#20 #40 #60	-	Gao and Cao (2010)
74	16.6, 20	190	60	600 rpm	50/70	Average size of 0.42 mm	-	Zadshir et al. (2020)
75	10, 20	180	45	High shear 5000 rpm	PG 58-22	#60	-	Chang et al. (2020)
76	9	170	180	Stirrer 1200 rpm	50/70 70/100	Mean diameters for 4 dif. CR --------- 0.15 0.18 0.25 0.42	-	Liang et al. (2015b)
77	10	170	45	900 rpm	PG 67-22	#30	-	Shen (2015)
78	10	-	30	-	PG 64-22	#14 #16 #20 #30 #40 #50 #80 #100	6 different gradations are given	Xiao et al. (2019)
79	10, 15, 20	160	60	-	PG 64-22	#30	-	Bairgi et al. (2015)
80	10, 15, 20, 25	45	177	-	PG 64-22	-	given as graphic	Wang et al. (2012)
81	6, 12, 18	160, 180, 200	30, 45, 60	High shear mixer 4000 rpm	PG 64-22	#50, #30, >#30	-	Specht and Khatchatourian (2014)
82	15	180	90	mechanical mixer with anchor shaped mixer 600-700 rpm	50/70	-	given as graphic	Santagata at al. (2012)

Table A.1 (continued)

No	CR Content (%)	Mixing Parameters			Binder Type	CR Gradation		Articles
		Temp. (˚C)	Duration (min.)	Mixer rate and type		Size	% Passing	
83	15, 18	-	1) 30 + 2) 30	1) Shearing 4000 rpm + 2) Maturation 200 rpm	50/70 70/100	0.5-1.5 mm 0-1 mm	-	Radziszewski et al. (2012)
84	15	177	60	Rotating impellor 700 rpm	PG 64-22	-	given as graphic	Shatanawi et al. (2012)
85	-	-	-	-	60/70	(mm) 2 1.18 0.6 0.3 0.075	100 82.5 60 22.5 2.5	Shafabakhsh et al. (2014)
86	18	180	140	High shear mixer	Straight run bit. 200	-	given as graphic	Subhy and Lo Presti (2017)
87	18 pre-treated with 160/200 bitumen (%60) and activated mineral binder stabilizer (%23)	-	-	-	CA24 (40/50)	(mm) 2 1.5 1 0.5 0.25 0.125 0.063	100 100 100 94.1 23.7 3.7 0.4	Chavez et al. (2019)
88	12	180	60	propeller mixer 200 rpm	80/100	#40	-	Katman et al. (2016)
89	20 + %3 sasobit	190	1) 30 + 2) 45	High shear mixer 1) 2000 rpm + 2) 1000 rpm	PG 64-22 (70/100)	#40	given as graphic	Razmi and Mirsayar (2018)
90	21	-	-	-	60/80	#40	-	Xia et al. (2021)
91	21	180	1) 20 + 2) 60	1) stirring manually + 2) 300 rpm	50/70	#40	-	Lv et al. (2021b)

Table A.1 (continued)

No	CR Content (%)	Mixing Parameters			Binder Type	CR Gradation		Articles
		Temp. (˚C)	Duration (min.)	Mixer rate and type		Size	% Passing	
92	16.7, 22.7, 28.2	-	1) 15 + 2) 30, 60, 120 ,180	1) 6000 rpm + 2) 1500 rpm	40/60 100/150	-	-	Walsh and Widyatmoko (2009)
93	15	170	1) 5 + 2) 60	1) Blending 3000 rpm + 2) Agitation 700 rpm	PG 58-28	#30	given as graphic	Solaimanian and Chen (2019).
94	10, 14, 18	155	25	700 rpm	60/70	#4 #8 #10 #16 #30 #50 #200	CR-1 CR-2 100 99.2 98.9 94.6 97.4 88.8 73.3 48.6 34.6 15.1 8.0 1.70 0.0 0.0	Martinez Arguelles et al. (2012)
95	8, 10, 12, 14	160	55	mechanical stirrer	70/100	-	-	Deshmukh and Kshirsagar (2017)
96	18	180	1) 45 + 2) 60	1) Shear homogenizer 5000 rpm + 2) The blended mix contained in homogenizer to allow to swell	80/100	(mm) 0.55 0.38 0.27 0.25 0.212 0.18 0.16 0.15 0.12	 69.8 33.5 20.8 13.8 5.3 5.1 3.9 3.0 0.0	Liu et al. (2017)
97	15	-	-	-	50/70	(mm) 2 0.5 0.25 0.063	 100 43 4 0.4	Navarro And Gámez (2012)
98	10, 15	177	45	2000 rpm	PG 64-22	#40	-	Xu et al. (2017)
99	5, 10, 15	180	1) 20 + 2) 90 + 3) 20	1) Shearing process 2000 rpm + 2) stirring 5000 rpm + 3) stirring (to excluding air after high speed shearing) <100 rpm	(50/70)	Mean particles size: 0.29 mm	-	Yan and You (2015)
100	10, 15, 20, 25	170-180	60	propeller mixer 4500 rpm	60/80	#40	-	Li et al. (2019)

B. Results of the Conventional Tests and True Grades

Table B.1 Conventional test results and true grades for unaged samples

Unaged						
Combination	**Penetration (25°C)**	**Softening Point (°C)**	**Resilience (%)**	**Viscosity**		**True Grade (°C)**
				135° C	**175 °C**	
Base Bitumen	72.33	46.00	-	337	35	64.60
CR-30-700	39.89	56.50	23.67	3510	1083	87.40
CR-30-1000	39.00	60.00	24.33	3350	1096	86.00
CR-30-1200	36.90	62.00	26.33	3330	970	85.30
CR-30-5800	42.11	57.50	27.00	3075	1006	84.60
CR-60-700	38.17	58.50	28.00	4200	1097	85.10
CR-60-1000	39.44	60.00	26.00	3656	1006	87.20
CR-60-1200	39.89	60.00	27.33	3320	855	86.20
CR-60-5800	42.67	58.00	30.33	3025	846	84.70
CR-90-700	40.00	59.50	27.67	4085	1090	86.40
CR-90-1000	40.33	60.75	27.83	3960	1051	86.60
CR-90-1200	42.77	61.00	28.33	3870	1015	87.30
CR-90-5800	41.77	58.50	29.00	3247	751	85.40
CR-120-700	41.00	60.00	28.00	3980	1037	86.40
CR-120-1000	43.44	59.75	28.33	3840	993	87.00
CR-120-1200	43.69	59.00	28.67	3851	1012	86.60
CR-120-5800	45.78	59.50	29.33	3011	665	86.80
CR-150-700	44.00	59.50	29.33	4068	1142	86.40
CR-150-1000	45.33	59.25	28.83	3740	988	86.90
CR-150-1200	45.00	59.75	27.00	3960	1012	86.90
CR-150-5800	45.11	60.00	28.00	3172	737	87.40
CR-180-700	46.78	60.75	28.66	4194	1045	85.70
CR-180-1000	45.55	60.50	28.00	4013	1043	86.70
CR-180-1200	44.44	60.75	29.00	3759	935	86.30
CR-180-5800	48.33	59.00	27.67	3078	690	85.40

Table B.2 True grade results for the aged samples

	TFOT	PAV
Combination	**True Grade (°C)**	**True Grade (°C)**
Base Bitumen	65.00	21.30
CR-30-700	82.80	-
CR-30-1000	82.80	18.00
CR-30-1200	81.40	-
CR-30-5800	82.20	16.80
CR-60-700	80.40	-
CR-60-1000	82.00	17.00
CR-60-1200	83.40	-
CR-60-5800	79.40	16.30
CR-90-700	82.00	-
CR-90-1000	83.30	16.30
CR-90-1200	82.40	-
CR-90-5800	81.40	17.90
CR-120-700	82.90	-
CR-120-1000	82.90	17.50
CR-120-1200	82.70	-
CR-120-5800	81.10	17.20
CR-150-700	83.60	
CR-150-1000	83.60	17.40
CR-150-1200	82.90	-
CR-150-5800	79.20	16.50
CR-180-700	83.40	-
CR-180-1000	82.90	17.20
CR-180-1200	83.20	-
CR-180-5800	80.20	17.50

Table B.3 Viscosity test results

	RPM	Viscosity (mPa.s)					
		130 °C	**140 °C**	**150 °C**	**160 °C**	**170 °C**	**180 °C**
Base Asp.	-	437.5	262.5	162.5	97.9	50.0	25.0
30 min	**700**	4310.4	2764.6	1931.3	1464.6	1181.3	1016.7
	1000	4204.2	2641.7	1856.3	1408.3	1154.2	993.3
	1200	4137.5	2622.9	1802.1	1358.3	1056.3	900.0
	5800	3870.8	2397.9	1664.6	1252.1	1009.9	869.1
60 min	**700**	5495.8	3068.8	2104.2	1543.8	1208.3	1008.3
	1000	4539.6	2843.8	1947.9	1433.3	1116.7	947.9
	1200	4133.3	2568.8	1716.7	1231.3	945.8	789.6
	5800	4035.4	2481.3	1658.3	1189.6	927.1	793.8
90 min	**700**	4795.0	3404.2	2256.3	1633.3	1229.2	995.8
	1000	4730.0	3233.3	2162.5	1554.2	1187.5	960.4
	1200	4852.1	3016.7	2058.3	1491.7	1135.4	922.9
	5800	4118.8	2504.2	1637.5	1150.0	856.3	689.6
120 min	**700**	4950.0	3095.8	2102.1	1497.9	1162.5	947.9
	1000	4768.8	2991.7	2029.2	1450.0	1104.2	895.8
	1200	4785.4	2997.9	2029.2	1477.1	1127.1	914.6
	5800	3833.3	2295.8	1500.0	1027.1	750.0	600.0
150 min	**700**	5022.9	3210.4	2222.9	1643.8	1272.9	1052.1
	1000	4812.5	3000.0	2022.9	1437.5	1081.3	881.3
	1200	4906.3	3068.8	2075.0	1483.3	1122.9	916.7
	5800	4052.1	2422.9	1583.3	1104.2	818.8	658.3
180 min	**700**	5239.6	3293.8	2195.8	1591.7	1183.3	939.6
	1000	5010.4	3122.9	2127.1	1531.3	1160.4	950.0
	1200	4689.6	2912.5	1952.1	1402.1	1056.3	845.8
	5800	3920.8	2354.2	1525.0	1050.0	775.0	625.0

Table B.4 ANOVA results for penetration test

Source of Variation	*SS*	*df*	*MS*	*F*	*P-value*	*F crit*
Mixing rate	25.18661	3	8.395538	4.9451	0.0139069	3.287382
Mixing duration	150.3614	5	30.07227	17.713	0.000008	2.901295
Error	25.46641	15	1.697761			
Total	201.0144	23				

Table B.5 ANOVA results for softening point test

Source of Variation	*SS*	*df*	*MS*	*F*	*P-value*	*F crit*
Mixing rate	10.85417	3	3.618056	3.037901	0.061744	3.287382
Mixing duration	4.489583	5	0.897917	0.753936	0.596196	2.901295
Error	17.86458	15	1.190972			
Total	33.20833	23				

Table B.6 ANOVA results for resilience test

Source of Variation	*SS*	*df*	*MS*	*F*	*P-value*	*F crit*
Mixing rate	5.7889	3	1.929633	1.619535	0.226818	3.287382
Mixing duration	29.6021	5	5.92043	4.96900	0.006988	2.901295
Error	17.8721	15	1.19147			
Total	53.2631	23				

Table B.7 ANOVA results for viscosity test @ 175 °C

Source of Variation	*SS*	*df*	*MS*	*F*	*P-value*	*F crit*
Mixing rate	336571.1	3	112190.4	28.11924	0.000002	3.287382
Mixing duration	22031.38	5	4406.275	1.104383	0.3986907	2.901295
Error	59847.13	15	3989.808			
Total	418449.6	23				

Table B.8 ANOVA results for true grade (high temperature)

Source of Variation	*SS*	*df*	*MS*	*F*	*P-value*	*F crit*
Mixing rate	20.65125	3	6.88375	7.245417	0.003133	3.287382
Mixing duration	3.707083	5	0.741417	0.78037	0.579145	2.901295
Error	14.25125	15	0.950083			
Total	38.60958	23				

Table B.9 ANOVA results for true grade (intermediate temperature)

Source of Variation	*SS*	*df*	*MS*	*F*	*P-value*	*F crit*
Mixing rate	0.140833	1	0.140833	0.273551	0.623301	6.607891
Mixing duration	0.8275	5	0.1655	0.321463	0.880743	5.050329
Error	2.574167	5	0.514833			
Total	3.5425	11				

C. Results of DSR Test

Table C.1 Complex modulus values after temperature sweep tests

Duration	**Sample**	**RPM**	**Complex Shear Modulus (Pa) (@10 rad/s)**				
			40 °C	**52 °C**	**64 °C**	**76 °C**	**88 °C**
30 min.	**Unaged**	**700**	97000.00	26700.00	8120.00	2700.00	976.50
		1000	86460.00	23790.00	7168.00	2386.00	862.20
		1200	102400.00	25860.00	7476.00	2343.00	822.30
		5800	82210.00	23030.00	6954.00	2268.00	795.60
	TFOT	**700**	159300.00	37210.00	11190.00	3975.00	1410.00
		1000	140300.00	36640.00	11340.00	3912.00	1386.00
		1200	149600.00	34320.00	9786.00	3285.00	1178.00
		5800	137400.00	31870.00	9833.00	3398.00	1288.00
	PAV	**1000**	468200.00	114400.00	31950.00	10800.00	4136.00
		5800	399600.00	98530.00	27980.00	9491.00	3626.00

Table C.1 (continued)

Duration	Sample	RPM	Complex Shear Modulus (Pa) (@10 rad/s)				
			40 °C	52 °C	64 °C	76 °C	88 °C
60 min.	Unaged	700	89700.00	23100.00	6860.00	2224.00	828.30
		1000	86250.00	21970.00	6454.00	2074.00	748.20
		1200	84130.00	23350.00	7181.00	2413.00	869.70
		5800	77530.00	22050.00	6827.00	2279.00	814.10
	TFOT	700	116400.00	30390.00	9140.00	3012.00	1097.00
		1000	134600.00	33650.00	10220.00	3356.00	1270.00
		1200	155500.00	39610.00	12000.00	3888.00	1383.00
		5800	105800.00	28180.00	8488.00	2921.00	1047.00
	PAV	1000	416000.00	96400.00	25900.00	8353.00	3021.00
		5800	412100.00	99090.00	27740.00	9246.00	3459.00
90 min.	Unaged	700	92140.00	23810.00	7261.00	2456.00	904.10
		1000	83140.00	23220.00	7238.00	2483.00	915.80
		1200	85800.00	23600.00	7600.00	2620.00	966.60
		5800	82010.00	24100.00	7363.00	2314.00	823.90
	TFOT	700	143300.00	35810.00	10350.00	3409.00	1225.00
		1000	151800.00	37930.00	10990.00	3820.00	1430.00
		1200	144700.00	35640.00	11040.00	3844.00	1305.00
		5800	111900.00	29180.00	9071.00	3158.00	1184.00
	PAV	1000	390600.00	91960.00	24780.00	7972.00	2852.00
		5800	459000.00	112300.00	30080.00	9797.00	3433.00
120 min	Unaged	700	80960.00	22430.00	7166.00	2503.00	938.60
		1000	81650.00	22850.00	7335.00	2552.00	942.50
		1200	83760.00	23220.00	7379.00	2580.00	972.40
		5800	75370.00	20880.00	6756.00	2357.00	868.80
	TFOT	700	158100.00	37170.00	10740.00	3641.00	1326.00
		1000	156200.00	37670.00	11080.00	3711.00	1376.00
		1200	148400.00	35470.00	10690.00	3743.00	1427.00
		5800	123100.00	31930.00	9177.00	3099.00	1144.00
	PAV	1000	535300.00	135900.00	38270.00	12770.00	4717.00
		5800	470300.00	113200.00	30550.00	9832.00	3391.00

Table C.1 (continued)

Duration	Sample	RPM	Complex Shear Modulus (Pa) (@10 rad/s)				
			40 °C	52 °C	64 °C	76 °C	88 °C
150 min	Unaged	700	77250.00	21490.00	6835.00	2435.00	931.00
		1000	78230.00	22170.00	7146.00	2543.00	961.80
		1200	81770.00	23170.00	7441.00	2624.00	991.80
		5800	78920.00	23060.00	7553.00	2661.00	999.10
	TFOT	700	157400.00	38760.00	11380.00	3887.00	1408.00
		1000	156600.00	36720.00	11010.00	3811.00	1451.00
		1200	157100.00	35830.00	10620.00	3652.00	1332.00
		5800	124100.00	28760.00	7941.00	2610.00	957.20
	PAV	1000	431600.00	98470.00	25520.00	7993.00	2799.00
		5800	403200.00	98350.00	28010.00	9498.00	3506.00
180 min	Unaged	700	76430.00	20490.00	6444.00	2252.00	839.60
		1000	75700.00	20740.00	6730.00	2407.00	917.30
		1200	75000.00	20570.00	6621.00	2340.00	881.90
		5800	76610.00	21160.00	6699.00	2309.00	836.40
	TFOT	700	143600.00	36850.00	10970.00	3762.00	1421.00
		1000	155400.00	37690.00	11480.00	3878.00	1344.00
		1200	154900.00	37910.00	10920.00	3688.00	1382.00
		5800	129400.00	29930.00	8965.00	3140.00	1075.00
	PAV	1000	441900.00	101800.00	26270.00	8307.00	2806.00
		5800	421500.00	98530.00	26300.00	8364.00	2995.00

Table C.2 Phase angle values after temperature sweep tests

Duration	Sample	RPM	Phase Angle (°) (@10 rad/s)				
			40 °C	52 °C	64 °C	76 °C	88 °C
30 min.	Unaged	700	52.36	57.40	65.14	71.77	74.11
		1000	53.57	57.83	66.09	72.61	75.16
		1200	53.94	59.41	68.44	75.66	79.44
		5800	52.81	58.44	68.11	75.63	79.12
	TFOT	700	52.56	54.69	59.94	66.66	71.02
		1000	51.90	54.05	59.84	66.87	71.33
		1200	53.52	55.63	61.24	67.81	72.18
		5800	52.40	54.36	59.72	66.51	70.76
	PAV	1000	48.64	51.84	54.53	57.78	60.52
		5800	48.59	52.23	55.53	60.08	65.45
60 min.	Unaged	700	53.88	59.06	67.63	74.10	76.40
		1000	54.35	59.59	68.20	74.86	77.31
		1200	52.83	57.26	65.61	72.51	75.66
		5800	53.11	58.29	66.48	74.02	77.58
	TFOT	700	53	55.41	60.92	67.21	70.86
		1000	52.16	54.22	59.49	65.74	69.19
		1200	52.55	54.21	59.21	65.75	70.45
		5800	53.42	55.87	61.09	67.43	71.66
	PAV	1000	49.55	53.43	56.74	61.25	67.94
		5800	48.92	52.38	54.99	58.63	65.09
90 min.	Unaged	700	52.74	55.29	61.10	67.77	71.04
		1000	53.71	57.25	64.02	70.69	73.71
		1200	53.87	56.68	63.54	70.32	73.75
		5800	54.71	57.47	65.36	73.43	78.01
	TFOT	700	53.37	55.25	60.47	67.38	72.89
		1000	52.55	54.13	58.90	65.42	70.80
		1200	52.86	54.57	59.73	66.65	71.54
		5800	52.45	53.81	58.47	64.71	68.73
	PAV	1000	49.36	53.33	56.62	60.37	65.10
		5800	53.88	59.06	67.63	74.10	76.40

Table C.2 (continued)

Duration	Sample	RPM	Phase Angle (°) (@10 rad/s)				
			40 °C	52 °C	64 °C	76 °C	88 °C
120 min.	Unaged	700	48.55	52.48	55.94	60.96	66.72
		1000	54.69	56.72	63.43	69.57	72.17
		1200	54.15	56.84	63.41	70.37	74.33
		5800	52.94	56.67	63.72	69.90	72.15
	TFOT	700	55.03	56.58	63.38	70.74	75.21
		1000	53.08	54.64	59.34	65.88	70.90
		1200	53.15	54.45	59.17	65.68	70.92
		5800	53.11	54.82	59.43	65.87	70.92
	PAV	1000	53.79	55.62	59.89	66.07	71.39
		5800	46.46	50.19	52.70	55.57	61.07
150 min.	Unaged	700	48.32	52.34	55.49	59.43	66.82
		1000	54.57	56.83	62.65	68.31	70.21
		1200	54.06	56.35	62.25	68.63	71.51
		5800	53.58	56.82	62.73	68.89	71.45
	TFOT	700	52.51	55.01	62.61	69.72	73.11
		1000	52.48	53.89	58.62	65.35	70.84
		1200	52.70	53.85	58.26	64.72	69.38
		5800	53.14	54.72	59.34	65.74	70.91
	PAV	1000	54.53	57.15	62.15	68.31	72.60
		5800	49.69	54.18	57.74	61.74	67.92
180 min.	Unaged	700	48.39	51.75	54.31	58.20	64.00
		1000	54.80	57.81	63.75	69.92	73.55
		1200	54.29	56.31	62.39	68.74	72.26
		5800	55.37	56.97	62.97	69.35	72.82
	TFOT	700	53.58	56.80	64.02	71.57	76.30
		1000	52.78	53.89	58.17	64.42	69.00
		1200	53.03	54.55	59.23	65.82	70.53
		5800	53.19	54.72	59.20	65.64	70.70
	PAV	1000	54.16	56.01	60.39	66.45	71.00
		5800	49.89	54.43	58.04	62.96	69.01

Table C.3 CMAI values for short-term and long-term samples

	Complex Modulus Aging Index (CMAI)									
	Short Term-Aged (TFOT) ($G^*_{(TFOT\text{-}aged)} / G^*_{(unaged)}$)					**Long Term-Aged (PAV) ($G^*_{(PAV\text{-}aged)} / G^*_{(unaged)}$)**				
	40°C	**52°C**	**64°C**	**76°C**	**88°C**	**40°C**	**52°C**	**64°C**	**76°C**	**88°C**
Base Asp.	2.67	2.66	2.40			10.35	11.32	12.55		
CR-30-700	1.64	1.39	1.38	1.47	1.44	-	-	-	-	-
CR-30-1000	1.62	1.54	1.58	1.64	1.61	5.42	4.81	4.46	4.53	4.80
CR-30-1200	1.46	1.27	1.18	1.15	1.13	-	-	-	-	-
CR-30-5800	1.67	1.38	1.41	1.50	1.62	4.86	4.28	4.02	4.18	4.56
CR-60-700	1.98	1.90	1.94	2.07	2.11	-	-	-	-	-
CR-60-1000	2.20	1.86	1.80	1.86	2.00	4.82	4.39	4.01	4.03	4.04
CR-60-1200	1.85	1.70	1.67	1.61	1.59	-	-	-	-	-
CR-60-5800	1.36	1.28	1.24	1.28	1.29	5.32	4.49	4.06	4.06	4.25
CR-90-700	1.52	1.33	1.19	1.10	1.05	-	-	-	-	-
CR-90-1000	1.83	1.63	1.52	1.54	1.56	4.70	3.96	3.42	3.21	3.11
CR-90-1200	1.69	1.51	1.45	1.47	1.35	-	-	-	-	-
CR-90-5800	1.36	1.21	1.23	1.36	1.44	5.60	4.66	4.09	4.23	4.17
CR-120-700	1.95	1.66	1.50	1.45	1.41	-	-	-	-	-
CR-120-1000	1.91	1.65	1.51	1.45	1.46	6.56	5.95	5.22	5.00	5.00
CR-120-1200	1.77	1.53	1.45	1.45	1.47	-	-	-	-	-
CR-120-5800	1.63	1.53	1.36	1.31	1.32	6.24	5.42	4.52	4.17	3.90
CR-150-700	2.04	1.80	1.66	1.60	1.51	-	-	-	-	-
CR-150-1000	2.00	1.66	1.54	1.50	1.51	5.52	4.44	3.57	3.14	2.91
CR-150-1200	1.92	1.55	1.43	1.39	1.34	-	-	-	-	-
CR-150-5800	1.57	1.25	1.05	0.98	0.96	5.11	4.26	3.71	3.57	3.51
CR-180-700	1.88	1.80	1.70	1.67	1.69	-	-	-	-	-
CR-180-1000	2.05	1.82	1.71	1.61	1.47	5.84	4.91	3.90	3.45	3.06
CR-180-1200	2.07	1.84	1.65	1.58	1.57	-	-	-	-	-
CR-180-5800	1.69	1.41	1.34	1.36	1.29	5.50	4.66	3.93	3.62	3.58